Characterization of the glycosylation of newborn and adult α_2-macroglobulin

Laura Calvert, BSc

A Thesis

Submitted to the School of Graduate Studies

in Partial Fulfillment of the Requirements

for the Degree

Master of Science

McMaster University

MASTER OF SCIENCE (2016) MCMASTER UNIVERSITY

(Medical Science) Hamilton, ON

TITLE: Characterization of the glycosylation of newborn and adult α_2-macroglobulin

AUTHOR: Laura Calvert

SUPERVISOR: Dr. Anthony Chan

NUMBER OF PAGES: CXI

Abstract

Introduction: Alpha-2-macroglobulin (α_2m) is a plasma glycoprotein serine protease inhibitor. Previous studies have shown that coagulation factor concentrations are highly variable with age and α_2m levels have been found to be twice as high in newborns compared to adults. This may contribute to a resistance towards thrombotic events observed in young populations. Protein glycosylation is known to affect protein activity and the glycosylation profile of adult α_2m has previously been analyzed. Information regarding glycosylation of α_2m in other age groups has yet to be elucidated. Therefore, the purpose of this study is to examine the differences in the glycosylation profiles between newborn and adult α_2m.

Methods: To evaluate glycan macroheterogeneity, plasma samples were enzymatically deglycosylated by PNGaseF, followed by SDS PAGE and western blotting (WB) to detect α_2m. To evaluate microheterogeneity, plasma samples were incubated with Neuraminidase (C*lostridium perfringens*) followed by native PAGE and WB to determine sialic acid content. To detect non-sialylated terminal galactose residues, plasma samples were incubated with immobilized RCA_{120}, and lectin-bound molecules were separated from unbound molecules. Additionally, the affinity of α_2m for ricin was evaluated by eluting bound proteins with increasing concentrations of galactose. All fractions were subjected to SDS-PAGE and WB to detect α_2m. 2D gel electrophoresis was completed to examine differences in pI and molecular weight of α_2m in both age groups. Purification by immunoprecipitation was also performed and eluted α_2m was analyzed by fluorescence-assisted carbohydrate electrophoresis (FACE) to determine the glycan fingerprint in the two populations.

Results: Deglycosylation of both newborn and adult α_2m with PNGaseF resulted in a change in migration and apparent molecular weight, however no statistically significant difference was found between newborn and adult. On native PAGE following treatment with neuraminidase, newborn α_2m exhibited a statistically significant change in migration compared to adult. Additionally, newborn α_2m exhibited a higher percentage of molecules bound to RCA_{120} than adult (no statistical difference) and elution of α_2m from RCA_{120} with a galactose step gradient produced similar profiles for newborn and adult molecules. 2D electrophoresis and WB revealed a difference in pI of α_2m in newborns as compared to adults. Finally, purified newborn and adult α_2m were analyzed by FACE and quantification of prominent fluorescent bands revealed a higher secondary:primary band ratio in newborns when compared to adults.

Conclusions: To our knowledge, this is the first study investigating glycosylation differences between newborn and adult α_2m molecules. The results from PNGaseF analyses indicate no significant difference in total N-glycan content. Neuraminidase results suggest significantly greater sialic acid presence on newborn α_2m, however there was no significant difference in galactose content. 2D electrophoresis revealed a difference in pI as well as the way in which newborn and adult α_2m degrade when exposed to experimental conditions. A_2m was successfully purified from both newborn and adult plasma, and FACE results indicate that the proportion of more branched glycans present in the two major fluorescent bands are of higher quantity in newborns than adults.

ACKNOWLEDGEMENTS

I would like to extend sincere thanks to Dr. Anthony Chan for allowing me the opportunity to carry out this research as a member of his team. I would also like to express my gratitude to Les Berry for his profound and continued involvement in my learning and development throughout the course of this project. Additionally, I am thankful for Dr. Howard Chan and Helen Atkinsons' continued input and support of this work. I would like to thank Drs. Joseph Macri and William Sheffield as well as Les Berry for agreeing to be on my committee as well as their mentorship and guidance as I progressed through the project. Finally, thanks must be extended to my incredibly supportive family for encouraging me throughout this journey.

TABLE OF CONTENTS

LIST OF FIGURES

LIST OF TABLES

LIST OF ABBREVIATIONS

ADP	Adenosine diphosphate
α_1AT	Alpha$_1$-antitrypsin
α_2m	Alpha$_2$-macroglobulin
APC	Activated Protein C
Arg	Arginine
AT	Antithrombin
AT+H	Antithrombin-heparin complex
Asn	Asparagine
β-ME	β-mercaptoethanol
Ca^{2+}	Calcium
CDG	Congenital Disorder of Glycosylation
ER	Endoplasmic Reticulum
FII	Factor II or prothrombin
FV	Factor V
FVII	Factor VII
FVIII	Factor VIII

FIX	Factor IX
FX	Factor X
FXI	Factor XI
FXII	Factor XII
FIIa	Activated factor II or thrombin
FVIIa	Activated factor VII
FIXa	Activated factor XI
FXa	Activated factor X
FXIa	Activated factor XI
FXIIa	Activated factor XII
GAG	Glycosaminoglycan
GluNAc	N-acetyl-D-glucosamine
GPCR	G-protein coupled receptor
GPI	Glycophosphatidylinositol
HCII	Heparin Cofactor II
LDL	Low Density Lipoprotein
NeuAc	N-acetylneuraminic Acid (Sialic Acid)
PAGE	Polyacrylamide gel electrophoresis

PAR1	Protease Activated Receptor 1
PBS	Phosphate Buffered Saline
PNGaseF	Peptide N Glycosidase F
RCA	Ricinus Communis Agglutinin
Rf	Relative front
SDS PAGE	Sodium dodecyl sulfate polyacrylamide gel electrophoresis
Ser	Serine
Thr	Threonine
TF	Tissue Factor
TFPI	Tissue Factor Pathway Inhibitor
VCN	Vibrio Cholera Neuraminidase
VTE	Venous Thromboembolism
vWF	Von Willebrand Factor

1 INTRODUCTION

1.1 The Cell Based Model of Coagulation

Hemostasis describes the physiological process of maintaining a balance between pro-coagulant and anti-coagulant activity[33]. This ensures blood remains in a fluid state and prevents excessive bleeding during injury[51]. When there is an imbalance in this system, pathological circumstances occur. These include bleeding disorders in the case of excess anti-coagulation or lack of pro-coagulant activity and thrombosis in the case of excessive pro-coagulation or lack of anti-coagulant activity[33]. Extensive research has been devoted towards blood coagulation both *in vivo* and *in vitro*. Coagulation is often studied in terms of a cascade of events, which includes activating a series of zymogens to their enzymatic form and converting pro-cofactors to cofactors[37,51]. This response begins promptly following vessel injury and is usually divided into two main independent pathways; the intrinsic/contact pathway and the extrinsic/tissue factor pathway[46]. These pathways converge into a single pathway and contribute towards fibrin clot formation[46]. Although the cascade model presents an excellent model of coagulation *in vitro*, it has been discovered that it may not be the most accurate representation of coagulation *in vivo*[37]. This is because of the lack of incorporation of cellular components in the cascade model, specifically the phospholipid membrane surface and the presence of calcium[37,38]. It is for this reason that more recent models of coagulation focus specifically on the cellular components of hemostasis and describe three main phases which lead to the formation of a clot; initiation, amplification and propagation[37,47,51].

The initiation phase (shown in Figure 1(A)) is triggered when FVIIa, activated from FVII, forms a complex with tissue factor (TF) exposed on the endothelial surface following vascular injury [37,47,51]. FVII circulates in the blood as a zymogen, with a small proportion circulating as FVIIa. Once activated, the TF-FVIIa complex proceeds to activate FIX to FIXa

and FX to FXa, which then are able to activate more FVII through feedback mechanisms. There have also been studies to investigate the presence of a serine protease, FVII activating protease, and its ability to aid in this process [37,48]. FXa then continues on to activate a small amount of FV to FVa (cofactor for Xa), which together form the prothrombinase complex and facilitate conversion of prothrombin to thrombin (Figure 1)[46,47]. The factors involved in this complex dissociate rapidly and are neutralized by the Tissue Factor Pathway Inhibitor (TFPI) and Antithrombin (AT), discussed below[46,47]. It is at this point in the cell based model that the amplification phase is required to facilitate adequate signaling for further activation of clotting.

During the amplification phase, shown in Figure 1 (B), the thrombin that was generated during the initiation phase is able to activate platelets[51]. Thrombin exerts its action on platelets through proteolytic cleavage of a G-protein coupled receptors (GPCR), known as Protease-Activated Receptor-1 (PAR1)[10]. Once PAR1 has been cleaved, it initiates a sequence of intracellular events within the platelet[10,51]. These events include shape change through cytoskeletal rearrangement, aggregation, secretion of granular components (adenosine diphosphate (ADP)) and an increase in cytosolic calcium (Ca^{2+})[10,51]. These changes cause an alteration in the cell surface phospholipid expression to render it more pro-coagulant[10,51]. Thrombin is also able to cleave Von Willebrand Factor (VWF) off FVIII (so that VWF can continue on in the platelet adhesion and aggregation process) as well as activate factors V, XI and VIII[51].

Propagation begins following the activation of a small number of platelets by thrombin generated during the initiation phase and is shown in Figure 1 (C)[51]. Further platelet recruitment occurs due to the release of granular components during the amplification process[51]. The activated platelet surface provides a favorable environment for clotting to occur, with a

negatively charged phospholipid surface due to the exposure of phosphatidylserine (PS)[37]. The activated platelets aggregate together with the help of interactions between clotting factors produced from previous phases and factors present on the platelet surface[51]. FIXa binds with FVIIIa and Ca^{2+} to produce the intrinsic tenase complex[51]. On the platelet surface, this complex is able to generate FXa that will remain localized to the platelet surface and thus not be inhibited by TFPI and AT[37,51]. The FXa generated binds to FVa and Ca^{2+} and cleaves prothrombin to thrombin[51]. This phase produces a surge of thrombin leading to the conversion of fibrinogen to fibrin[51]. Provided there are enough fibrin monomers present, polymerization will occur to form the insoluble fibrin matrix that creates a stable clot[51].

Initiation (A)

Amplification (B)

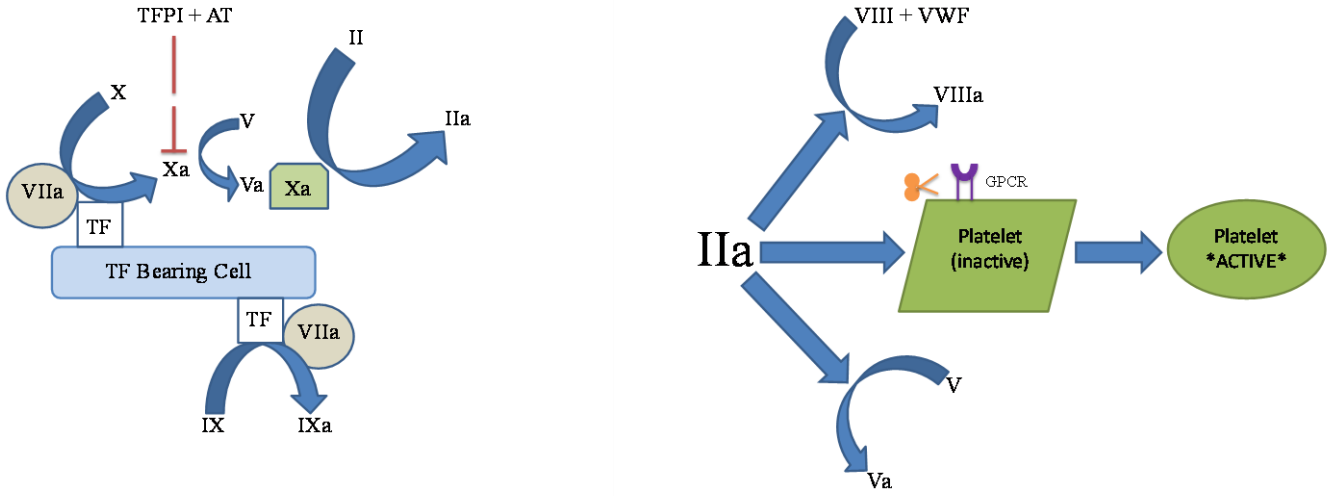

Propagation (C)

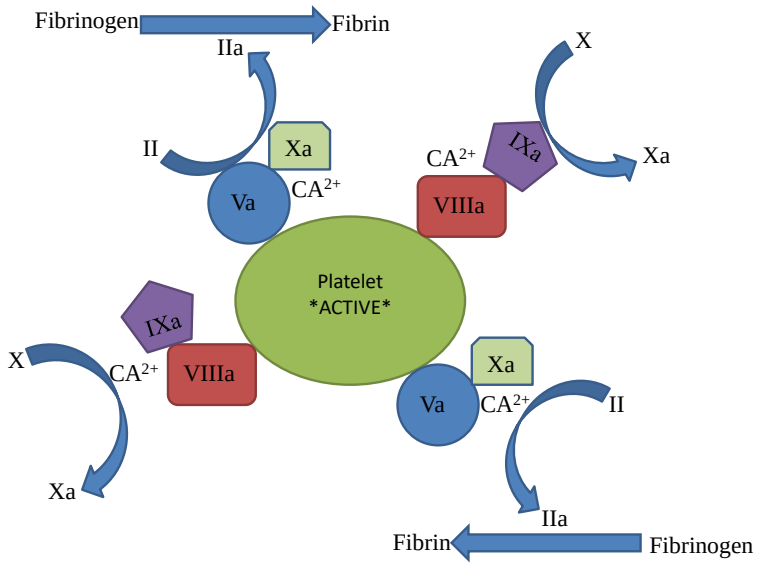

Figure 1: Cell based model of Coagulation. Initiation, amplification and propagation are depicted, as described in the text.

1.2 Natural Anticoagulants

In order to maintain hemostatic balance, it is crucial that there are highly specific mechanisms in place to regulate the coagulation system. There are many in vivo inhibitors of coagulation, the most prominent of which is AT[54]. In addition to AT, there are many less potent inhibitors of coagulation, including tissue factor pathway inhibitor (TFPI), α_1-antitrypsin (α_1AT), α_2-macroglobulin (α_2m) and heparin cofactor II (HCII) which will be discussed below. Deficiencies in these inhibitors often lead to pathological states and require treatment to maintain a homeostatic state in patients.

1.2.1. Antithrombin

AT is a 58 200Da glycoprotein that is a potent inhibitor of blood coagulation[32]. This serine protease inhibitor is present in plasma at concentrations of approximately 125ug/ml[32]. The AT polypeptide is synthesized in the liver with an accompanying signal peptide that is cleaved following transport through the endoplasmic reticulum, prior to secretion into the circulation[32].Once AT has been released into the circulation, its reactive site provides specificity towards serine protease inhibition[32]. In addition to the reactive site, AT also contains a binding site for its cofactor, heparin. Heparin binding to AT occurs through a distinct pentasaccharide sequence located on the heparin molecule and allows for a high affinity bond between the two molecules[18,32]. Once bound, the antithrombin-heparin (AT+H) complex undergoes a conformational change and exudes a much stronger level of inhibition towards many coagulation enzymes, including thrombin and FXa[18]. Enzyme inhibition occurs through covalent binding of a specific site on the reactive center loop of the inhibitor with the active site of the target enzyme[18]. Individuals that display low levels of AT are susceptible to thrombosis, particularly venous

thromboembolism (VTE)[32,44]. There are a few different forms of AT deficiency, including Type I quantitative and Type II qualitative, the latter of which is further divided into IIa (defective thrombin binding), IIb (defective heparin binding) and IIc (genetic pleiotropy)[44]. In addition to the increased risk of VTE, there is also an increased risk of arterial thrombosis, pregnancy complications and fetal loss[44].

1.2.2. Tissue Factor Pathway Inhibitor

TFPI is a serine protease inhibitor and anticoagulant whose ability to inhibit the TF-FVIIa complex, as well as FXa makes it an important natural anticoagulant. Inhibition of these factors can significantly reduce the amount of thrombin produced as a result of vascular injury. TPFI has two isoforms, TFPIα and TFPIβ, which differ in their splice sites[36]. Both isoforms contain 2 Kunitz-type inhibitory domains: K1 which binds FVIIa; and K2 which binds FXa[36,64,65]. The difference between the two is that TFPIα contains a unique 3rd inhibitory domain (K3) as well as a positively charged C-terminus and TFPIβ has a C-terminus that allows for interaction with glycosylphosphatidylinositol (GPI) anchors[36,65]. The mechanism of inhibition varies between the 2 isoforms. TFPIα is released by platelets and endothelial cells, at which time Protein S can bind to the K3 domain and increase its affinity for FXa[66]. TFPIβ is released by endothelial cells and is anchored to the cell surface which has been shown to produce a slightly better inhibition of FXa than is seen in soluble TFPIα[36]. Binding to FXa is the initial and rate limiting step in the inhibition of the TF-FVIIa-Xa complex[65]. Upon binding of the K2 domain of TFPI to the active site of FXa, the K1 domain binds the active site of FVIIa, thus inhibiting the entire complex[65]. Due to the fact that only the K1 and K2 domains are required for this interaction, both TFPIα and TFPIβ act through similar mechanisms[36,65]. Lastly, in addition to

both isoforms' ability to inhibit TF-FVIIa and FXa, TFPIα has recently been found to play a role in the inhibition of the prothrombinase complex, composed of FXa and FVa, early in the clotting process[64]. This occurs by binding of the basic C-terminal region of TFPIα to the acidic exosite B of FV[64]. Once thrombin proteolitically cleaves FV, the B domain is physically removed, thus preventing this interaction[64]. Therefore, inhibition of the prothrombinase complex can only occur when activation of FV is being completed by FXa, prior to thrombin-mediated FV activation[64].

In humans, complete deficiency of TFPI may be embryonically lethal, as clinical cases have not been described and this consequence has been shown in TFPI knockout mice[65]. Partial deficiency in TFPI has been shown to lead to many clinical phenotypes, including venous thrombosis, atherosclerosis, coronary heart disease and ischemic stroke[65].

1.2.3. α_1-antitrypsin

Alpha$_1$-antitrypsin (α_1AT), also known as α_1-proteinase inhibitor, is a 51,000Da glycoprotein and is another *in vivo* inhibitor of coagulation, as well as other protease-dependent processes[11]. Similar to AT, this molecule is synthesized in the liver hepatocytes and is found in high concentrations in plasma (1-2g/L)[49]. Unlike AT, α_1AT also has multiple targets throughout the body beyond the coagulation system[11]. However, within the coagulation system, α_1AT works as a serine protease inhibitor by targeting serine proteases such as thrombin, plasmin and FXa[49]. In addition to its anticoagulant activity, α_1AT is also thought to play a role during anti-inflammatory response as well as provide tissue protection[49].

Individuals with a deficiency in α_1AT have a risk of developing airway and liver diseases[12,16]. This is due to the effect of α_1AT on neutrophil elastase, the most common α_1AT protease target[16]. In the airway, α_1AT serves a protective function against neutrophil elastase in

the alveolar wall and thus, if levels of inhibitor are low, elastase is able to destroy the lung tissue and cause emphysema[16]. In the liver, the mechanism of disease progression is less well understood, however it is thought that abnormal processing of α_1AT may cause liver cirrhosis[12,16]. Due to the fact that the liver is responsible for the production and release of almost all coagulation factors and inhibitors, impaired hepatic cell function has the potential to have serious coagulation consequences[31]. As the state of disease progresses, clotting is more severely impaired until the patient reaches the end stage of disease where the risk of bleeding increases[31].

1.2.4. α_2-macroglobulin

Another *in vivo* inhibitor of blood coagulation is α_2m. In mammals, this protein is synthesized primarily in the liver and its structure consists of four 180kDa subunits that link together through disulfide linkages[4,52]. When α_2m inhibits plasma proteases, the mechanism is referred to as 'entrapment'[52]. To initiate binding of a protease to α_2m, cleavage must occur in a defined region, known as the 'bait region', of which there is one on each subunit[8]. Once this has occurred, α_2m undergoes a structural change that forces the protease into an internal pocket within the α_2m molecule[8]. This physical entrapment of the protease renders it unable to react with macromolecular substrates[8]. Due to the fact that α_2m does not react with the active site of the enzyme, the protease may still react with amide and ester bonds of small substrates which are not prohibited from diffusing into the internal pocket of α_2m due to steric hindrance[4]. These properties of α_2m make it unique, in that it is able to react with a broad spectrum of proteases and prevent them from carrying out their normal actions[8]. However, it also protects the enzyme so that other protease inhibitors cannot enter and react with their active site, thus rendering them inactive[8]. Once α_2m has carried out its inhibitory function, it is cleared within minutes by an α_2m

receptor[8]. The receptor is part of the low density lipoprotein receptor family and can be found on cells throughout the body including hepatocytes, adipocytes, monocytes, fibroblasts, macrophages and astrocytes[8]. This process of α_2m binding to its receptor is dependent on pH and calcium[21]. If conditions are favorable, α_2m will bind to its receptor, undergo endocytosis and be transported to endosomes and lysosomes for clearance[8].

Consequences of complete α_2m deficiency have not been well characterized. The limited number of studies conducted on α_2m deficient patients have found there to be no major clinical consequences associated with loss of this protein[9,55]. One study examined a 61-year-old male patient that presented with arterial thrombosis and low serum and plasma levels of α_2m[9]. Results of the study concluded that it was not the α_2m deficiency that had caused the adverse event, rather the presence of multiple risk factors including atherosclerosis, lack of exercise and smoking[9]. Other studies have implicated α_2m in some disease states, such as inflammatory disease[21]. Research by Panzironi et al. has shown that patients with systemic lupus erythematosus exhibit an abnormal pattern of glycosylation on their α_2m molecules[21,42]. These patients have been shown to have significantly elevated levels of mannose and galactose[21,42]. Although this alteration in glycosylation has not been extensively studied, the potential for use in differential diagnosis of disease provides value to the study of α_2m[21].

1.2.5. Heparin Cofactor II

HCII is a 56 500Da glycoprotein serine protease inhibitor which has a native conformation homologous to that of AT[5,14,61]. Synthesized in the liver, HCII is present in human plasma at a concentration of approximately 1µmol/L[24,59]. Upon release from the liver, HCII circulates in the blood in its native state. Upon cleavage of the reactive center bond of HCII,

located on amino acid residues 444 and 445, a conformational change occurs and traps thrombin in a covalent complex[59]. In the presence of specific glycosaminoglycans (GAGs), heparin, heparin sulfate and dermatan sulfate, the rate of thrombin inhibition increases by more than 1000-fold[24]. This is because, upon binding of HCII to cell surface GAGs, a conformational shift occurs which exposes the acidic N-terminus of HCII[5,29,59]. This domain is then able to directly bind to thrombin exosite I and thus increase the strength and rate of inhibiton[59,61]. The HCII-thrombin complex is then cleared from the circulation by an LDL receptor located on hepatocytes[30]. Studies evaluating the effect of HCII deficiency have failed to reveal any serious clinical phenotypes as a result of this condition. Research involving HCII knockout mice have found no difference in size, morphology or presence of thrombotic complications when compared to wildtype mice after 1 year[24].Though there have been limited studies evaluating the effect of homozygous HCII deficiency in humans, the research that has been conducted has not found there to be any detectable clinical phenotype associated with HCII deficient patients.

The above inhibitors of coagulation are all glycoproteins that are naturally present in the human body. The glycosylation of these proteins may have an impact on function and thus alterations could lead to disease states; whether it be alterations in sites of glycosylation or specific glycan residues that are affected.

1.2.6. Developmental Differences in Coagulation

There have been many differences described between the hemostatic systems of neonates, children and adults. Platelets have been noted as having an altered function in newborns compared to adults[56]. Although platelet count in healthy newborns is similar to that seen in adults, there seems to be a decrease in platelet size and response sensitivity[56]. The reduced

activity in newborn platelets may be due to altered expression of adhesion receptors and surface glycoproteins[56]. A study examined infants on days 1, 5, 30, 90 and 180 post-birth and compared values of the coagulation factors to adult reference ranges[2]. Results demonstrated that the Vitamin K-dependent coagulation factor concentrations were significantly lower in newborns as compared to adults[2]. Factor VII equilibrated to within adult reference range values by day 5, whereas Factors II, IX and X did not reach adult values until approximately 6 months of age[2]. At 6 months of age, the levels of all Vitamin-K dependent coagulation factors were within adult reference range, however they were found at the lower end of the range[2]. Further research in children found that these values remain low throughout childhood and in an age category of 11 to 16 years old, there remained a significant difference from adult values, with the childhood and adolescent values being reduced in comparison to adults[3]. Factor V and VIII displayed values at birth that were equal to adult values and VWF levels were elevated at birth, equilibrating to adult values by 6 months of age[2]. Research expanding the investigation into childhood and adolescence found that FV remained within a healthy adult range until 5 years of age, at which point levels declined and remained significantly different from adult values in the 11 to 16 year age group[3].

Inhibitors of coagulation also display different values in newborns and children in comparison to adults. AT levels are significantly reduced in the newborn, with adult values being achieved by roughly three months of age[2]. Similarly, Protein S takes around 3 months for values to reach adult levels and Protein C has a more extended period of equilibration, with levels remaining low through the teenage years [2,3]. α_2-antiplasmin levels were low at birth and rose to within the adult reference range by day 5 of life[2]. α_1AT displayed a different pattern of development, with levels being within adult reference rages at birth, dropping by 3 months of

age and rising again around 6 months[2]. Finally, α_2m levels were significantly higher than adult concentrations at birth[2]. It has been shown that newborns have approximately double the α_2m plasma concentration of adults[2]. Levels of this inhibitor continue to rise in the 6 months following birth and throughout childhood[2,3]. Studies have shown that in an 11 to 16 year old age population, α_2m plasma concentration remains significantly higher (approximately double) than adult reference values[3].

1.3 Glycosylation

Glycosylation is a post-translational modification that occurs with numerous proteins found within the human body. The addition of carbohydrate structures, also referred to as glycans, to proteins is classified based on the residue which attaches the carbohydrate to the protein backbone[40,45]. N-linked glycosylation occurs when glycans attach to nitrogen residues of asparagine (Asn) side chains, a process which begins in the endoplasmic reticulum[45]. With the help of Asn targeting enzymes, such as oligosaccaryltransferase, glycans are transferred from lipids to target Asn residues within a polypeptide containing the sequence Asn-X-Ser, where X can be any amino acid except proline[45]. Once the mannose-rich 14 sugar core structure has been added, glycosidase and glycosyltransferase enzymes take over to continue remodeling as the protein exits the ER and carries on to the Golgi apparatus, where this process will be completed[45]. Once in the Golgi, further cleavage allows for protein folding and final modifications to the glycan structures[45]. On the final product, N-linked glycans can be grouped into three categories; high-mannose type, hybrid type and complex type (Figure 2)[45].

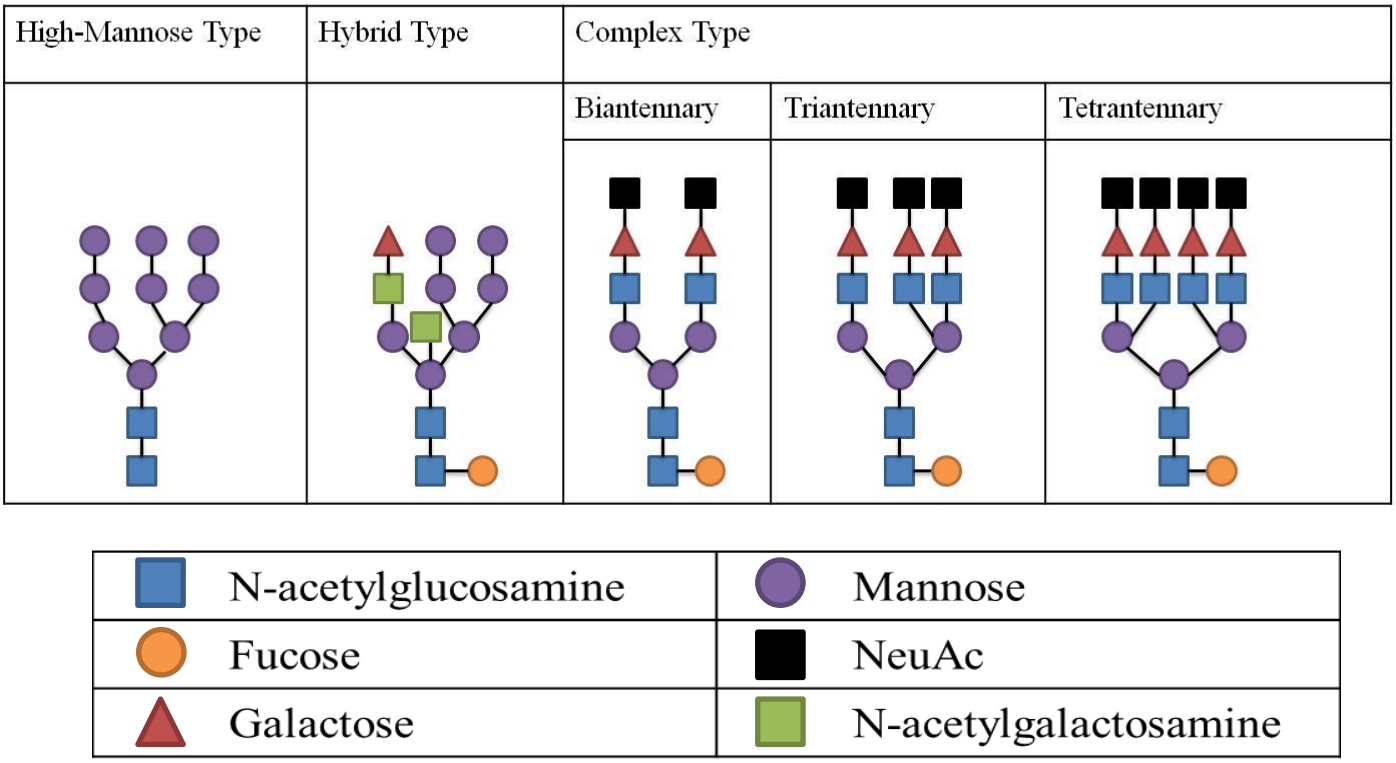

Figure 2: N-linked glycan structures commonly found on human glycoproteins. Figure adapted from Preston *et al*. (2013)[45].

O-linked glycosylation differs from N-linked in that it occurs on a serine or threonine residue and this process occurs strictly in the Golgi[45]. Another difference with O-linked glycosylation is that there is no addition of a core structure that requires modification prior to protein secretion; monosaccharides are added sequentially with similar glycosyltransferases that are employed in N-linked glycosylation[45]. The addition of sugar monomers one-by-one also results in a less complex final glycan structure than what is seen with N-linked glycans (Figure 3)[45].

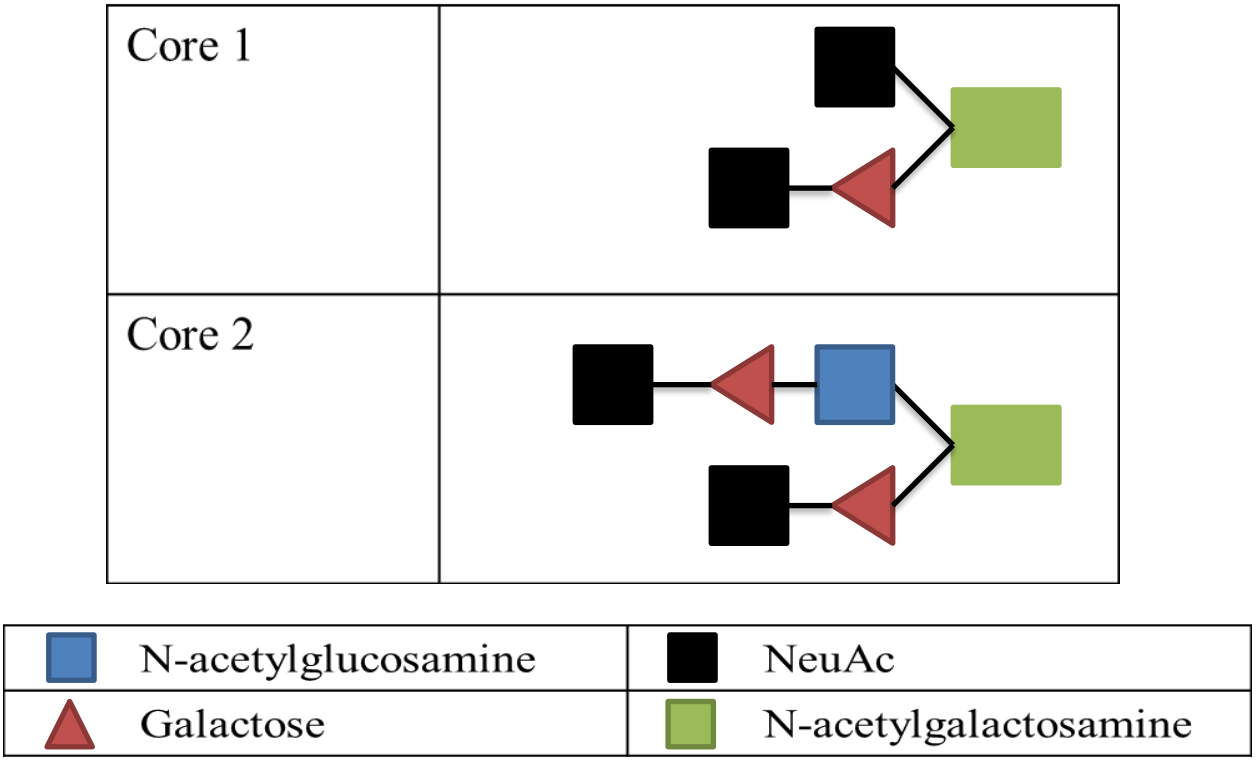

Figure 3: Common O-linked glycans found on human glycoproteins. Figure adapted from Preston *et al*. (2013)[45].

Although N and O-linked glycans are added through different mechanisms, it is possible for both types to be attached to a single protein. It is also common for glycoproteins to be heterogeneous, leading to the formation of multiple glycoforms. This heterogeneity may come in the form of macro-heterogeneity, meaning there is variation in which sites are glycosylated on the protein, or micro-heterogeneity, meaning there is variation in the glycan structure attached to each glycosylation site[28,58]. Following release into plasma from the ER, properly formed glycoproteins are able to exert many effects throughout the body[45]. Many of these glycoproteins are coagulation factors, such as TF, Factors V, VII – XIII, VWF, prothrombin and Protein C[45].

It has been found that abnormal glycosylation of glycoproteins plays a role in human disease states. Most glycosylation-associated coagulopathies have been found to be due to the addition of a site of glycosylation onto a glycoprotein[34,45]. This causes impaired function of the glycoprotein and may also result in bleeding tendencies, such as hemophilia B in the case of FIX[45]. It is also possible to see a reduction in the glycan profile, indicating a site of glycosylation has been removed due to genetic mutation[45]. If this occurs with Protein S, a cofactor for activated Protein C[34,45], the mutation results in enhanced clearance of Protein S, thus dramatically increasing the risk of VTE in these patients[45].

Lastly, there have been numerous congenital disorders of glycosylation (CDG) that have been identified to date. The known CDG's follow autosomal recessive inheritance and the extent of clinical phenotype associated with each is heavily dependent on the enzyme that is affected[27,63]. The most prevalent known CDG is a phosphomannomutase-2 deficiency, also referred to as CDG-Ia[27,63]. This enzyme plays a key role in the function of guanosine diphosphate (GDP) mannose enzyme, which is involved in the addition of mannose residues to glycans in the ER[27]. Children that possess this condition are frequently recognized shortly following birth due

to neurological and feeding complications[27]. As the children mature, renal, liver and cardiac consequences have also been reported[27]. The nervous system and liver are most commonly impacted by these disorders[27]. It is clear from the above information that glycosylation plays a critical role in proper protein function, and pathological situations may occur if something goes wrong or is incorrect in the glycosylation process. This makes it a vital process to study, as so many plasma proteins are glycoproteins, leaving a great deal of opportunity for mistakes to occur through the lengthy process of glycosylation.

1.3.1. Glycosylation differences in adult and newborn/child proteins

There have been previous findings of coagulation proteins that displayed differences in glycosylation pattern between newborns/adolescents and adults. One of these proteins is Protein C (PC), a critical component of the anticoagulant system[7]. Protein C is a Vitamin K-dependent coagulation factor that must be activated to activated Protein C (APC) to carry out its function[22,23,50]. Once active, it inhibits coagulation factors Va and VIIIa and thus acts as a regulator of thrombin generation [7,22,23]. Research has shown that there is variation in the glycosylation profile of protein C that is dependent on age[7]. In adults, PC contains four sites of N-linked glycosylation located on asparagine residues 97, 248, 313 and 329[7,23]. There are two major isoforms in adult plasma, one of which is fully glycosylated (alpha-PC) and another which lacks an N-glycan at Asn^{329} and thus contains only three sites of glycosylation (beta-PC)[7,23]. This indicates macroheterogeneity in PC glycosylation[7,23]. In newborns, there is a lower total concentration of PC in plasma; however a significantly higher proportion of the total PC consists of the alpha-PC glycoform in comparison to adults[7].

Another coagulation molecule that has been found to have variation in glycosylation due to age is plasminogen[17]. This molecule plays an important role in the fibrinolytic system which is responsible for clot lysis[43]. A reduced propensity for fibrinolysis in infants may be attributable to an altered glycan profile on newborn plasminogen in comparison to adults[17]. Both age groups have two known glycoforms, however newborn plasminogen was found to contain an increased amount of sialic acid and mannose residues (indicative of N-linked glycosylation)[17]. The alteration in glycan residues has been found to account for the reduced activation and cell binding potential of newborn plasminogen[17].

1.3.2. Glycosylation of α_2-macroglobulin

One of the previously discussed anticoagulants, adult α_2m is heavily glycosylated with 8 potential sites of N-linked glycosylation. Five of these potential sites of glycosylation occur in the amino terminal half of the molecule and three occur on the carboxy-terminal end of the peptide[34,53]. These sites of glycosylation occur at asparagine residues 55, 70, 247, 396, 410, 869, 991 and 1424[34]. Based on the primary sequence of human α_2m, 2 of the potential sites of N-linked glycosylation contain the favorable Asn-X-Ser sequence while the remaining 6 potential sites contain a less favourable sequence of Asn-X-Thr[53]. Detailed information has been obtained regarding the specific sites of glycosylation in adult α_2m, including the presence of heterogeneous carbohydrate structures. A study by Sottrup-Jensen *et al.* found the smallest glycan present on α_2m to contain 3 mannose and 2 GluNAc residues. Galactose, mannose, fucose, GluNAc and NeuAc were attached to the mannose/GluNAc base in variable amounts as well as on more complex glycan structures containing higher proportions of mannose and

GluNAc[53]. Although this information has been essential in determining glycosylation of adult α_2m, α_2m glycosylation in the newborn has yet to be characterized.

1.4 Overall Aim

The overall purpose of this research is to characterize the glycosylation of newborn and adult α_2m.

1.5 Hypothesis

There will be differences in the glycosylation profiles between adult and newborn α_2m.

1.6 Rationale

As discussed above, AT is the main inhibitor of blood coagulation in healthy adults. If there is a deficiency in this glycoprotein in adults, multiple clinical scenarios are possible, including an increased risk for thrombosis[44]. It has been shown that children, particularly newborns, possess low plasma concentrations of AT, whereas the concentration of α_2m is substantially elevated in this population[38]. Levels of α_2m are higher than that of adults beginning at birth, and rise to approximately twice the adult levels by 6 months of age[1]. It is not until the late teenage years that these values equilibrate to normal adult reference ranges[3]. It has also been shown that AT deficient children are able to inhibit thrombin more effectively than AT deficient adults, with no elevation in inhibition following the addition of heparin[44]. This indicates that it may in fact be α_2m that is responsible for compensating, since if it were HCII that was compensating for the reduction in AT, addition of heparin would increase thrombin inhibition[44]. Since α_2m is a significant inhibitor of coagulation in newborns, further functional effects from age-dependent variation in glycosylation may accentuate the relative increase in concentration of α_2m seen in this population. The fact that there are 32 potential sites of glycosylation on adult α_2m indicates there may be multiple opportunities for variation to occur, which is seen in the

form of microheterogeneity in adult α_2m, as previously discussed. Due to the amount of previous evidence that suggest age-dependent glycosylation differences occur with coagulation proteins, it is possible that these differences are also occurring on α_2m.

1.7 Specific Objectives

1) To evaluate α_2m glycoforms in newborn and adult plasma without purification.
2) To purify α_2m from both newborn and adult plasmas using immunoprecipitation.
3) To examine the different glycoforms of purified newborn versus adult α_2m and compare features of the glycan structures on newborn versus adult α_2m.

2 EXPERIMENTAL PROCEDURES

2.1 Materials

2.1.1 General Reagents

Acrylamide, sodium chloride, tris (tris(hydroxymethyl)aminomethane), thiourea, CHAPS ($C_{32}H_{58}N_2O_7S$), dithiothreitol, iodoacetaminde, MOPS ($C_7H_{15}NO_4S$) and glycine were obtained from Bioshop (Burlington, ON). Sodium dodecyl sulfate (SDS), sodium acetate trihydrate ($CH_3COONa{\cdot}3H2O$), potassium chloride (KCl), potassium dihydrogen orthophosphate monobasic (KH_2PO_4), ethylene diamine tetraacetic acid (Na_2EDTA), 2-mercaptoethanol (2-ME), sodium azide (NaN_3), dimethyl sulfoxide (DMSO), tri-sodium citrate ($Na_3C_6H_5O_7$) and calcium chloride dehydrate ($CaCl_2$) were purchased from BDH Inc. (Toronto, ON). Hydrochloric acid (HCl), sulfuric acid (H_2SO_4), HPLC grade methanol, dimethylformamide (DMF), glycerol and acetic acid were purchased from Caledon Laboratories Inc. (Georgetown, ON). Sodium phosphate monobasic monohydrate ($NaH_2PO_4{\cdot}H_2O$), sodium phosphate dibasic heptahydrate ($Na_2HPO_4{\cdot}7H_2O$) and sodium phosphate dibasic anhydrous (Na_2HPO_4) were purchased from EM Science (Darmstadt, Germany). Urea was purchased from Fisher Scientific (Markham, ON). HEPES, Bovine Serum Albumin, IGEPAL CA-630 (octylphenyl-polyethylene glycol), ANDS (7-amino-1,3-naphthalenedisulfonic acid monopotassium salt monohydrate), sodium cyanoborohydride ($NaBH_3CN$), ethanolamine and galactose were purchased from Sigma (St. Louis, MO). Ethanol was purchased from Commercial Alcohols Inc. (Brampton, ON). Disuccinimidyl suberate was purchased from Thermo Fisher Scientific (Waltham, MA).

2.1.2. Antibodies

Goat anti-human α_2m, affinity purified IgG primary antibody was obtained from Affinity Biologicals (Ancaster, ON). Anti-goat IgG peroxidase conjugated secondary antibody produced in rabbit was obtained from Sigma (St. Louis, MO).

2.1.3. Enzymes

Peptide N Glycosidase F (PNGaseF) was obtained from MP Biomedicals (Solon, OH). α2-3,6,8 Neuraminidase from *Clostridium Perfringens* was purchased from New England Biolabs (Whitby, ON).

2.1.4. Proteins

α_2m from human plasma was obtained from Sigma (St. Louis, MO).

2.1.6 Lectins

Agarose-bound Ricinus Communis Agglutinin I (RCA_{120}) was obtained from Sigma (St. Louis, MO) and Vector Laboratories (Burlington, ON).

2.2 Methods

2.2.1 Cleavage of N-linked glycans through treatment with Peptide N Glycosidase F

To evaluate cleavage of N-linked glycans in newborn and adult plasma, 1.0 μL newborn plasma (20X dilution) and adult plasma (10X dilution) were prepared and denatured with 10 μL 50mM phosphate/0.2% SDS/0.1M β-mercaptoethanol. Following denaturation, 1 μL 20% NP-40 was added followed by incubation with PNGaseF (9U/ml) for 16 hr at 37^0C with gentle shaking. Following incubation, 5.5 μL 4X SDS reducing sample buffer was added to all tubes, for a total of 27.5 μL, and mixed well at room temperature. Samples were then centrifuged for 20 seconds and 10 μL of each was electrophoresed on 5% denaturing SDS gel for 45 minutes at 200V.

Following electrophoresis, the gel was subjected to western blotting. The gel was submerged in transfer buffer for three 5 minute washes and transferred to a nitrocellulose membrane at 100 V constant voltage for 1 hour. Following transfer, the gel was blocked overnight at 4^0C in 25 ml of PBS (20mM Na_2HPO_4, 150mM NaCl) containing 2% BSA. Following multiple washes in PBS-Tween (0.1%v/v Tween-20 in PBS) solution, the membrane was incubated with primary antibody (0.57ug/mL) for 2 hours and was washed 6 times for 5 minutes with PBS-Tween solution prior to being incubated in secondary antibody (1:15,000 dilution) for 1 hour. Following antibody incubation, the membrane was developed using ECL Prime Western Blotting Detection Reagents (GE Healthcare) as per the manufacturer's instructions and imaged using a Bio-Rad Chemi-Doc XRS+ imaging system to detect α_2m in each sample. Migration of molecular weight standards was used to create a standard curve for calculation of the molecular weight of treated and untreated α_2m in all samples.

2.2.2 Hydrolysis of α (2-3, 6, 8) linked N-acetylneuraminic acid by Neuraminidase from *Clostridium Perfringens*

Newborn and adult plasmas were diluted 20X and 10X, respectively in 1X reaction buffer (50mM sodium citrate, pH 6.0). In 0.5ml Eppendorf tubes, 1 µL of newborn and adult plasma were mixed with 1 µL 10X reaction buffer and 1 µL Neuraminidase or ddH_2O. Samples were then incubated for 24 hours at 37^0C with vigorous shaking. Following incubation, 10 µL non-denaturing sample buffer was added to each tube and samples were electrophoresed on a 4% non-denaturing gel at 200V for 45 minutes. Following electrophoresis, samples were subjected to western blotting to detect α_2m, as described above. Relative front (Rf) values were obtained

using Image Lab 4.1 software to compare change in migration on non-denaturing PAGE with and without exposure to Neuraminidase.

2.2.3. Detection of terminal galactose content in newborn and adult plasma α_2m using agarose-bound Ricinus Communis (RCA_{120})

Agarose-bound RCA_{120} was re-suspended and washed with 0.15M NaCl, followed by centrifugation at 16873 xg for 5 minutes to remove any non-specifically bound molecules. Following the NaCl washes, 100 µL HBS (0.02M HEPES + 0.15M NaCl, pH 7.4) was added and beads were split into two separate tubes; 1 µL newborn plasma diluted 1/20 in HBS was added to one tube and 1 µL adult plasma diluted 1/10 in HBS was added to the other. Samples were incubated at room temperature with gentle mixing for 30 minutes. Following incubation, samples were centrifuged at 16873 xg for 5 minutes and 20 µL of the supernatant was removed to represent the fraction of α_2m which had not bound to the beads (unbound fraction). The beads were then washed three times with 50 µL HBS and the supernatant was removed following centrifugation of each wash. Following the HBS washes, 20 µL HBS was added to the beads followed by 6 µL 4X SDS sample buffer. 6 µL 4X SDS sample buffer was also added to the unbound fractions and 15 µL of 4X SDS sample buffer was added to all HBS wash samples. Samples were electrophoresed on a 5% denaturing SDS gel for 45 minutes at 200V. Following SDS-PAGE, gels were transferred to a nitrocellulose membrane and subjected to western blotting, as described above. To quantify the α_2m present in the samples, standards ranging from 10-100ng were prepared from purified α_2m and electrophoresed with the samples. Optimization of the standard curve was done to ensure the samples remained within the linear range of

detection for each experiment. The quantities of RCA_{120} bound and unbound fractions were calculated based upon the standard curve.

2.2.4. Determining the strength of RCA_{120} binding with D- (+)-Galactose

The RCA_{120}-binding protocol was carried out as described above. To obtain information regarding the strength of binding of α_2m to RCA_{120}, a galactose step gradient was used to elute α_2m from RCA_{120}. Following 30 minute incubation of newborn and adult plasma with agarose-bound RCA_{120}, the unbound fraction was removed and samples were washed twice with 50 µL HBS, followed by one wash with 50 µL 1M NaCl. Optimal galactose concentrations to elute α_2m from RCA_{120} were found to be between 100 µM to 1M. Galactose was prepared in fresh HBS (0.02M HEPES + 0.15M NaCl, pH 7.4) immediately prior to the experiment. The order of galactose elution steps was as follows; 0.1 mM, 1 mM, 5 mM, 10 mM, 20 mM, 200 mM (washed three times at this concentration), 1000 mM. After each wash, samples were centrifuged at 16873 xg for 5 minutes and the supernatant was removed using a gel loading pipette tip in order to leave the bead pellet containing the bound α_2m unaltered. Following the elution steps, 15 µL 4X SDS reducing sample buffer was added to all samples and 6 µL SDS reducing sample buffer was added to the bound and unbound fractions. Samples were then electrophoresed on 5% denaturing gels along with standards ranging from 0.5ng – 10ng purified α_2m. These standard quantities had been previously optimized to ensure samples fell within the linear range of detection. Following SDS-PAGE, gels were transferred to a nitrocellulose membrane and western blotting was carried out, as described above. The quantity of α_2m in each subsample was calculated based on the standard curve. Statistical analysis was conducted using a repeated measures two-way ANOVA.

2.2.5. 2D gel of commercial α_2m, newborn and adult α_2m in plasma

20 ng α_2m was solubilized for 1 hour with 0.625 µL IPG buffer (GE Healthcare) and 123.4 µL rehydration buffer (8M Urea, 2M Thiourea, 4% CHAPS, 60mM DTT). Following solubilization, samples were transferred to the IPG strip holder, a 7 cm Immobiline DryStrip (pH 4-7, GE Healthcare) was added and covered with 0.5 mL Dry Strip Cover Fluid (GE Healthcare). Passive rehydration of the IPG strip took place on an IPGphor isoelectric focusing system (GE Healthcare) at 20^0C and 30V for 12 hr. This was followed by 150V for 1hr, 500V for 1hr, 2500V – 8000V for 1hr and then 8000V until 15 000 Vhrs was reached. IPG strip was then equilibrated for 15 minutes in 2 equilibration solutions. Solution A contained equilibration buffer (50mM Tris-Cl, 6M Urea, 30% v/v glycerol, 2% w/v SDS and trace bromophenol blue) + 0.1% w/v DTT and Solution B contained equilibration buffer + 0.25% w/v iodoacetamide. The IPG strip was then transferred to a NuPAGE 4-12% Bis-Tris Zoom gel (Life Technologies) and covered with 0.5% w/v agarose to ensure it remained in place. The gel was electrophoresed for 10 minutes at 100V followed by 70 minutes at 200V. The gel was then removed and silver staining was completed using the ProteoSilver Silver Stain Kit (Sigma), as per the manufacturer's instructions.

To detect the pattern of newborn and adult α_2m on 2D electrophoresis, the experiment was repeated with plasma samples. Newborn plasma was diluted 1/40 and adult plasma was diluted 1/20. 1µL of each was added to 123.4µl rehydration buffer and 0.625µl IPG buffer. Samples were solubilized at room temperature for 1 hour with gentle vortexing every 15 minutes. Both newborn and adult samples were then transferred to a 7 cm IPG strip (pH 4-7) and run on the isoelectric focuser as above. IEF was followed by gel equilibration, electrophoresis, western blotting and immunostaining, as described above.

2.2.6. Testing the effect of 2D buffers on newborn and adult α_2m

To test for deleterious effects that may be occurring with newborn and adult plasma as a result of exposure to 2D buffers, experimental settings were replicated and samples were electrophoresed on 1-dimensional SDS-PAGE followed by western blotting. Newborn and adult plasmas were diluted 1/40 and 1/20, respectively. To evaluate the banding pattern in standard 1D electrophoretic conditions, 1 µl of each newborn and adult plasmas were added to 74 µl phosphate buffer and 25 µl SDS sample buffer (Condition A). In Condition B, 1 µL each of newborn and adult plasmas were added to 74 µL phosphate buffer + 25 µL SDS sample buffer and samples were boiled for 5 minutes. In condition C, 1 µl each of newborn and adult plasmas were added to 74 µl SDS sample buffer and 25 µL SDS sample buffer. In this condition, the SDS sample buffer was prepared with 60 mM DTT in lieu of the β-mercaptoethanol normally added. In condition D, 1 µL each of newborn and adult plasmas were added to 87.76 µl rehydration buffer and 10% glycerol. In condition E, 1 µl each of newborn and adult plasmas were added to 79 µl rehydration buffer and left on the bench to sit for 18 hours (approximate running time of IEF). Following the 18hour incubation period, 20 µl equilibration buffer (+0.1% w/v DTT) was added. In condition F, 1 µl each of newborn and adult plasmas were added to 79 µl rehydration buffer and 20 µl equilibration buffer (+0.1% w/v DTT). In condition G, 1 µl each of newborn and adult plasmas were added to 79 µl rehydration buffer and 20ul equilibration buffer (0.25% w/v iodoacetamide). In condition H, 1 µl each of newborn and adult plasmas were added to 79ul rehydration buffer and 0.4 µl IPG buffer and incubated at room temperature for 18 hours. Following the 18 hour incubation period, 20 µl equilibration buffer (+0.1% w/v DTT) was

added. All samples were thoroughly mixed by vortexing and 15 µL each were loaded onto 4-15% gradient gels. Gels were electrophoresed at 200V for 45 minutes followed by western blotting.

2.2.7. Pre-clearing newborn and adult plasma with Protein G to remove human IgG

Two Eppendorf tubes were identically prepared containing 1 mL each of 50% agarose-bound Protein G beads (Pierce). Beads were washed with 1 mL coupling buffer (20mM sodium phosphate, 150mM NaCl pH 7.4) per tube, followed by 1 mL HBS. Beads were centrifuged after each wash at 5000xg for 2 minutes. Adult plasma was thawed at 37^0C for 5 minutes and 500 µL was added to each Eppendorf tube of the washed Protein G beads as well as 250 µL HBS. The tubes were then incubated at 4^0C on a rotator for 1 hour before being centrifuged at 5,000xg for 2 minutes and the supernatant was removed and labelled pre-cleared plasma 1&2. 10 µL of each pre-cleared plasma sample was removed for gel analysis. To ensure all IgG was effectively removed, this pre-clearance step was repeated a second time with fresh protein G beads, and supernatant labelled pre-cleared plasma 3&4. 10 µL of pre-cleared plasma samples 3&4 were taken for gel analysis and the remainder was stored at -80^0C.

To test for IgG removal, unprocessed plasma and the four pre-cleared plasma samples were electrophoresed on a 4-15% gradient gel followed by western blotting for the detection of IgG. The plasma sample was prepared by adding 1 µL plasma (thawed at 37^0C for 5 minutes) to 29 µL HBS and 10 µL 4X SDS reducing sample buffer. To prepare the pre-cleared plasma samples, 10 µL of each pre-cleared plasma sample was added to 20 µL HBS and 10 µL 4X SDS reducing sample buffer. Following preparation, samples were centrifuged for 20 seconds and 4 µL of each was loaded onto the gel. Electrophoresis occurred for 45 minutes at 200V. Following

electrophoresis, the gel was transferred to a nitrocellulose membrane as described above. The gel was blocked overnight at 4^0C in 25 mL of PBS containing 2% BSA. The membrane was then washed 6 times in PBS-Tween (0.1%v/v Tween-20) and incubated with Goat anti-human IgG for 1 hour. Following incubating with the antibody, the membrane was washed 6 times with PBS-Tween and developed using ECL Prime Western Blotting Detection Reagents, as per the manufacturer's instructions.

This experiment was repeated identically for both newborn and adult plasmas.

2.2.8. Binding and cross-linking of α_2m antibody to Protein G beads

500 µL of 50% Protein G beads were placed in a 1.5 ml Eppendorf tube and centrifuged at 5000 xg for 5 minutes to remove the supernatant. Protein G beads were then washed three times in 1 mL coupling buffer. Antibody solution was prepared by adding 220 µL antibody (goat anti-human α_2m) to 100 µL 10X coupling buffer (200mM sodium phosphate, 1.5M NaCl pH 7.4) and 430 µL ddH_2O. The antibody solution was mixed well, added to the washed Protein G beads and mixed on a rotator for 1 hour at room temperature. Following incubation, the beads were centrifuged at 5000xg for 5 minutes and the supernatant was removed and retained. The antibody-bound beads were then washed once with 750 µL coupling buffer and twice with 1 mL coupling buffer. After each wash, the beads were centrifuged and supernatant removed, as above. A 2.5 mM solution of disuccinimidyl suberate (Thermo Fisher Scientific) was prepared by dissolving 1 mg DSS in 1086 µL DMF. A cross-linking solution was then prepared by adding 225 µL 2.5 mM DSS to 125 µL 10X coupling buffer and 700 µL ddH_2O and added to the antibody-bound beads, followed by mixing on a rotator for 1 hour at room temperature.

Following incubation, beads were centrifuged and supernatant retained, as above. 1 mL 0.1M ethanolamine pH 8.2 was added to the sample and mixed for 10 minutes at room temperature on a rotator. Following incubation, beads were washed twice with 1 mL 100mM Glycine-Cl and three times with 1 mL HBS. After each wash, the samples were centrifuged and supernatant was retained, as above.

In order to ensure that the antibody was effectively bound and cross-linked to the Protein G beads, samples of the various supernatant fractions from the above procedure were electrophoresed on SDS-PAGE followed by silver staining. To prepare an antibody control sample, 1 µL of anti-α_2m antibody was added to 10 µL coupling buffer and 4 µL SDS reducing sample buffer. To check for antibody present in the supernatant following the initial antibody binding step, 4 µL of the supernatant was added to 7 µL coupling buffer and 4 µL SDS reducing sample buffer. To check for the presence of antibody in the coupling buffer washes, 8 µL from each wash was added to 3 µL coupling buffer and 4 µL SDS reducing sample buffer. To check for free antibody following cross-linking, 2 µL supernatant was added to 9 µL coupling buffer and 4 µL SDS reducing sample buffer. To check for free antibody following blocking with 0.1 M ethanolamine, 2 µL supernatant was added to 9 µL coupling buffer and 4 µL SDS reducing sample buffer. Finally, to check for antibody in the glycine-Cl elution steps, 4 µL of each elution sample was added to 7 µL HBS and 4 µL SDS reducing sample buffer. All samples were mixed well, loaded on a 4-15% gradient gel and electrophoresed for 45 minutes at 200V. Following electrophoresis, silver staining was completed based on protocol outlined in ProteoSilver Silver Stain Kit.

Four identical tubes of antibody-bound beads were prepared as described above for use in immunoprecipitating α_2m from adult plasma, and an additional four tubes were prepared for immunoprecipitating α_2m from newborn plasma.

2.2.9. Immunoprecipitation of α_2m from newborn and adult plasma

To purify α_2m from plasma, 325 µL of pre-cleared plasma and 525 µl HBS was added to each of the four antibody-linked Protein G bead tubes, produced as described in 2.2.8. Plasma was incubated with the beads overnight (approximately 16 hours) at 4^0C on a rotator. Following incubation, beads were centrifuged at 5000 xg for 5 minutes and supernatant was retained to check for any free α_2m. The plasma-bound antibody-linked beads were then washed three times with 1 mL HBS. The bead samples were then subjected to 6 elution steps with 175 µL 100 mM Glycine-Cl pH 2.8. Following each wash and elution, the bead sample was centrifuged and supernatants were retained and stored at 4^0C for further analysis. Once all elution steps were complete, the beads were washed an additional three times with 1 mL HBS and stored at 4^0C in HBS (or 0.02% sodium azide for long-term storage).

To investigate the success of purification, 16 µL of each elution fraction was taken for further analysis. To determine the success of binding α_2m to the antibody-linked beads, 2 µL of the post-binding supernatant was added to 9 µL HBS and 4 µL SDS reducing sample buffer. To check for α_2m in the HBS washes, 2 µL of each wash was added to 9 µL HBS and 4uL 4X SDS reducing sample buffer. 15 µL of each sample was loaded onto 4-15% gradient gels and electrophoresed at 200V for 45 minutes followed by silver staining. To detect the purity of α_2m eluted from the beads, 5 µL of elution fractions 1-4 was added to 6 µL HBS and 4 µL 4X SDS

reducing sample buffer. 15 µL of each sample was loaded onto 4-15% gradient gels and electrophoresed at 200V for 45 minutes followed by silver staining. Finally, to quantify the amount of α_2m captured in elution fractions 1-4 from each tube, western blots were carried out. A portion of each elution fraction was electrophoresed on a 4-15% gradient gel, along with a standard curve of commercially obtained purified α_2m, followed by western blotting and immunostaining, as described above. Samples were quantified based on the standard curve and adjusted for the volume of the elution fraction that was loaded, to determine the total quantity of α_2m in each elution fraction.

A_2m was purified from both newborn and adult plasmas as described above.

2.2.10. Buffer exchange and concentration of purified α_2m from newborn and adult plasma

Immediately following purification of newborn or adult plasma, elution samples were subjected to buffer exchange in Amicon Ultra-0.5mL filter devices (EMD Millipore, maximum capacity 0.5 mL). Elution #1-4 from each antibody-bound Protein G tube (4 elutions from both newborn and adult x 4 tubes = 16 total) were carefully transferred into Amicon filter devices, labeled 1-16. 300 µL 50 mM phosphate buffer was added to each device and they were centrifuged at 3000 rpm for 10 minutes. Following centrifugation, the devices were removed and the filtrate from each device was measured to ensure the volume in the device was reduced to approximately 50-70 µL. The devices were then removed from the filtrate collection tubes and vortexed for 10 seconds (with cap on). After vortexing, the devices were placed in fresh filtrate collection tubes and 400 µL 50mM phosphate buffer was added. Following phosphate buffer

addition, the devices were centrifuged again for 10 minutes at 3000 rpm. Following centrifugation, the devices were removed and the filtrate from each device was measured to ensure the volume in the device was reduced to approximately 50-70 µL. The devices were then removed from the filtrate collection tubes and vortexed for 10 seconds (with cap on). Following this vortex step, the devices were left on the bench for 5 minutes to allow all fluid to settle. Once settled, gel loading pipette tips were used to transfer the buffer exchanged samples from their individual devices and pool them in a 1.5 mL Eppendorf tube. A 10 µL sample was taken of the final buffer exchanged product and the remaining volume (~750 µL) was transferred into an Amicon Ultra-2 Centrifugal Unit (maximum capacity 2 mL). This device was centrifuged at 3000 rpm for 10 minutes and vortexed, as above. Once the fluid had settled at the bottom, the resultant buffer exchanged/concentrated product was removed from the 2 mL device and prepared for PNGaseF removal of glycans and FACE as outlined below.

2.2.11. Fluorescence-assisted carbohydrate electrophoresis (FACE) of newborn and adult α_2m, fetuin and AT

Following immunoprecipitation and buffer exchange/concentration of adult α_2m from plasma, the 65 µL sample was prepared for FACE. Two 50 µg AT samples were also prepared in a total volume of 65uL with 50mM phosphate buffer. The AT and adult α_2m samples were then denatured with 65 µL 50 mM phosphate/0.2%SDS/0.1M 2-ME and left at room temperature for 10 minutes. Following denaturation, 8 µL 20% NP-40 was added to all samples prior to the addition of 4 µL (9U/ml) PNGaseF (or 4 µL phosphate buffer for the AT sample not being exposed to PNGaseF). Samples were then incubated for 16 hours at 37^0C with shaking.

Following incubation, 5 µL was removed from each sample and 1.5 µL 4X SDS reducing sample buffer was added and mixed well at room temperature. Samples were then centrifuged for 20 seconds and electrophoresed on 4-15% gradient gel for 45 minutes at 200V. Following electrophoresis, the gel was subjected to Silver staining to verify that cleavage of N-linked glycans occurred effectively. The remainder of the experiment required only samples that had been treated with PNGaseF.

Proteins in samples that had been treated with PNGaseF were cold precipitated by adding 3 volumes of 100% ethanol (450 µl), mixed well, and placed at -20^{0}C for 30 minutes. Once removed from the freezer, samples were centrifuged at 8000xg for 10 minutes and supernatants which contained released glycans were removed into fresh tubes over ice. The glycan samples were then dried in a Speed Vac Concentrator (SAVANT SVC 200H) for approximately 3.5 hours until a translucent pellet was obtained at the bottom of the tube. Once dried, the adult α_2m and AT samples were stored at -20^{0}C.

Following immunoprecipitation and buffer exchange/concentration of newborn α_2m from plasma, the 65 µL sample was prepared for FACE. Two 25 µg AT samples and two 20 µg Fetuin samples were also prepared to be included on the FACE gels as standards. The samples were all prepared in a total volume of 65 µL with 50mM phosphate buffer. The samples were then denatured with 65 µL 50 mM phosphate/0.2%SDS/0.1M 2-ME and left at room temperature for 10 minutes. Following denaturation, 8 µL 20% NP-40 was added to all samples prior to the addition of 4 µL (9U/ml) PNGaseF (or 4 µL phosphate buffer for the AT sample not being exposed to PNGaseF). Samples were then incubated for 16 hours at 37^{0}C with shaking. Following incubation, 5 µL was removed from each sample and 1.5 µL 4X SDS reducing

sample buffer was added and mixed well at room temperature. Samples were then centrifuged for 20 seconds and electrophoresed on 4-15% gradient gel for 45 minutes at 200V. Following electrophoresis, the gel was subjected to Silver staining to verify that cleavage of N-linked glycans occurred effectively. The remainder of the experiment required only samples that had been treated with PNGaseF.

Following incubation, samples were cold precipitated by adding 3 volumes of 100% ethanol (450 µl), mixed well and placed at -20^{0}C for 30 minutes. Once removed from the freezer, samples were centrifuged at 8000xg for 10 minutes and supernatants were removed into fresh tubes over ice. The glycan samples were then dried in the Speed Vac Concentrator (SAVANT SVC 200H) for approximately 4 hours until a translucent pellet was obtained at the bottom of the tube. Once dried, the newborn α_2m, AT and fetuin samples were stored at -20^{0}C for 24 hours.

Once all samples had been stored at -20^{0}C for at least 24 hours, 5 µL 0.15M ANDS in 15% (v/v) acetic acid and 5 µL 1.0M sodium cyanoborohydride in DMSO was added to the dried samples followed by incubation for 16 hours at 37^{0}C with gentle shaking. Following incubation, samples were prepared for loading onto a gel by adding 10 µL ddH_2O and 20 µL 2X native sample buffer. 5 µL of each sample was electrophoresed on a 20% non-denaturing gel at 20 mA constant current with stirring. The running apparatus was placed on ice for the duration of electrophoresis. Following electrophoresis, the gel was placed directly into tris-glycine running buffer and visualized on the ChemiDoc.

2.2.12. Checking for bias in the immunoprecipitation and FACE protocols by re-purifying commercial α_2m

The binding and cross-linking of antibody to beads, immunoprecipitation and buffer exchange processes all occurred as described above. However, in lieu of adult or cord pre-cleared plasma being mixed with the antibody-bound beads, 2 mL of commercial α_2m (1mg/ml) was mixed with the beads. Therefore, in each antibody-bound tube, 500 µl of commercial α_2m was added and 325 µl HBS. All other washing/elution/buffer exchange steps proceeded exactly as described above.

Some changes were required in the final FACE preparations. The buffer exchanged and concentrated product had a volume of 100uL. To provide a comparison to a commercial sample which had not been taken through the purification protocol, 100 µg α_2m was prepared as well as two 50 µg AT samples and two 50 µg Fetuin samples, all in 50 mM phosphate buffer. The samples were then denatured with 100 µL 50mM phosphate/0.2%SDS/0.1M 2-ME and left at room temperature for 10 minutes. Following denaturation, 10 µL 20% NP-40 was added to all samples prior to the addition of 6 µL (9U/ml) PNGaseF (or 4 µL phosphate buffer for the AT sample not being exposed to PNGaseF). Samples were then incubated for 16 hours at 37^0C with shaking. The remainder of the FACE protocol was carried out as described above.

3 RESULTS

3.1 Determination of molecular weight change of Newborn and Adult α_2m following removal of N-linked glycans

PNGaseF was used to cleave N-linked glycans from newborn and adult α_2m in plasma. Following overnight incubation with PNGaseF, samples were denatured with SDS sample buffer and electrophoresed on 5% denaturing SDS-PAGE with western blotting. Results are shown in Figure 4. It was previously determined that α_2m required denaturation for full deglycosylation. In the newborn plasma lanes, there is an obvious change in migration that happens in the (+) sample that was exposed to PNGaseF. The loss of molecular weight that accompanies N-linked glycan removal would reduce the overall weight of each α_2m monomer, thus allowing it to migrate further into the gel. Similarly, in the adult plasma lanes, PNGaseF treatment produces the same trend on SDS-PAGE. These results show that PNGaseF is able to successfully cleave N-linked glycans from α_2m in both newborn and adult plasma. Previous research found smaller molecular weight bands associated with α_2m on SDS-PAGE to be related to boiling during sample preparation. For this reason, samples were not heated during this experiment and instead were left at room temperature following addition of the 50mM phosphate/0.2% SDS/0.1M 2-ME solution. With this modification, the smaller molecular weight bands seen on SDS-PAGE were no longer present, indicating that there is degradation of the α_2m protein when is it subjected to boiling during denaturation. Based on an n=3, these results show that, although there was a slight trend towards a greater change in molecular weight seen in newborn α_2m (16.1 ± 0.42kDa) than that seen with adult α_2m (14.5 ± 0.99kDa), this difference was statistically insignificant (p=0.28). This suggests that there is no significant macroheterogeneity in terms of total molecular weight

of N-linked glycans present on newborn and adult α_2m. It cannot be concluded from this experiment whether there are similarities in glycans at the sites of glycosylation or the linkages.

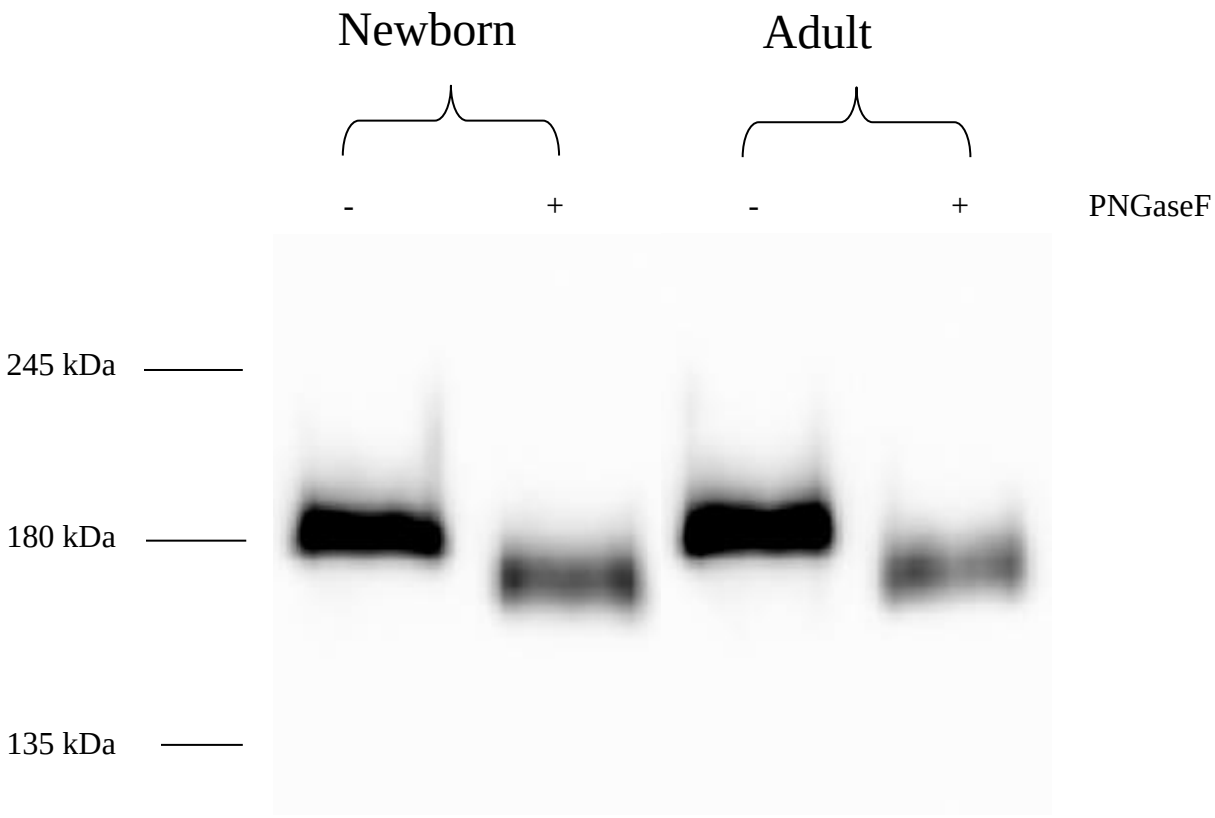

Figure 4: Cleavage of N-linked glycans from newborn and adult α_2m. Newborn and adult plasma was diluted and denatured by SDS and β-ME. SDS was neutralized by NP-40 and samples were incubated with PNGaseF (9U/ml) for 16 hours at 37^0C. SDS-PAGE and western blotting were used to detect α_2m in each sample. Migration of molecular weight standards was used to create a standard curve for calculation of the molecular weight change associated with PNGaseF treatment. Shown is a representative western blot.

3.2 Hydrolysis of α (2-3,6,8) sialic acid with Neuraminidase

Neuraminidase cloned from *Clostridium Perfringens* was used to cleave sialic acid from newborn and adult α_2m in plasma.

Results are shown in Table 1 and Figure 5. In the (+) and (-) newborn samples, it is clear that following incubation of plasma samples with Neuraminidase, there is a change in migration seen on native PAGE. The newborn sample that was exposed to Neuraminidase (+) does not migrate as far into the gel as the unexposed newborn sample (-). This indicates a loss of negative charge associated with sialic acid, as α_2m is not being drawn as readily towards the bottom of the gel. In adult plasma, treatment with Neuraminidase produced a similar change in migration on native PAGE. Data was compiled through comparison of Rf values obtained from the western blot (Table 1) and analyzed using a paired, two-tailed t test. Results revealed a significant difference in the change in migration seen in newborn α_2m compared to adult α_2m ($p = 0.028$, $n=5$).

Experiment Number	Newborn change in Relative Front	Adult change in Relative Front
1	0.078	0.069
2	0.032	0.028
3	0.057	0.049
4	0.065	0.052
5	0.063	0.062

Table 1: Change in relative front values obtained for newborn and adult α_2m in plasma following treatment with Neuraminidase.

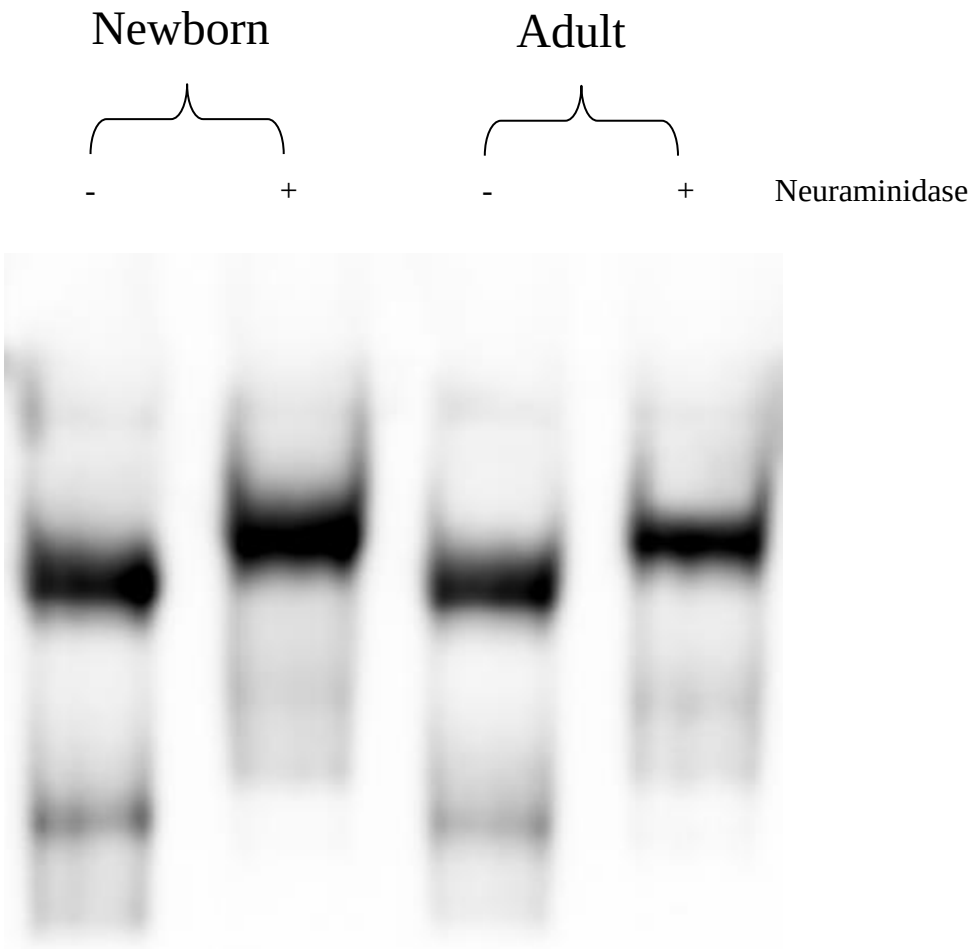

Figure 5: Newborn and adult α_2m in plasma with and without treatment with Neuraminidase. Plasma samples were diluted and incubated with Neuraminidase from *Clostridium Perfringens* (5000U/ml) for 24 hours at 37^0C. Following incubation, samples were electrophoresed on native PAGE followed by western blotting for detection of α_2m in plasma. Change in migration was calculated based on the relative front obtained with densitometry analysis. Shown is a representative western blot.

3.3 Evaluation of lectin binding with Agarose-bound RCA_{120}

Agarose-bound Ricinus Communis was selected for this experiment due to its high affinity for terminal galactose residues. Binding affinity for RCA_{120} can be used to evaluate the amount of unsialylated termini (i.e. galactose termini) on glycans bound to α_2m molecules. Following incubation of newborn and adult plasma with RCA_{120}, supernatant (unbound fraction) was removed, and multiple washes with HBS were performed to separate all remaining unbound α_2m from the beads. These HBS fractions were collected and electrophoresed on separate 5% denaturing gels to ensure no α_2m signal was present. These results are shown in Figure 6 (B). The bound and unbound fractions were electrophoresed, alongside purified α_2m standards and plasma from each age group that had not been exposed to the RCA_{120}. Results are shown in Figure 6 (A). 'Total' samples represent a newborn/adult plasma and HBS buffer. These samples had no exposure to RCA_{120} and thus represents the total amount of protein in the bound and unbound lanes. 'Bound' samples represent newborn/adult plasma that remained bound to RCA_{120} following the various mixing and washing steps. 'Unbound' samples represent the supernatant that was removed following 30 minute incubation of newborn/adult plasma with RCA_{120}. That is, whatever α_2m that did not directly bind to RCA_{120} through the incubation process and was free in solution would be captured in this fraction. There are 6 standards present on the gel that ensure all samples fall within the linear range of detection after western blotting. From these results, it is clear that the majority of α_2m in both newborn and adult plasma bound to RCA_{120} during the incubation. Using the densitometry analysis, a standard curve was created and the equation of the line was used to quantify the amount of α_2m in the 'total' and 'bound' lanes (figure 6 (C)). Those quantities were then converted to a percentage of α_2m bound in both newborn and adult plasma (figure 6 (D)). Upon analysis of this data, it was determined that although newborn plasma

exhibited a higher percentage (62.1% ± 9.7) of α_2m bound to RCA_{120} than α_2m in adult plasma (50.4% ± 2.8), this difference was not statistically significant (p=0.404, n=3).

Once this information was established regarding the binding tendency of α_2m to RCA_{120}, the strength of binding was evaluated. This was accomplished by washing the bound beads containing α_2m with various concentrations of galactose, as described in the methods section. All washes were then electrophoresed on 5% denaturing gels, followed by western blotting to detect α_2m. Figure 7 shows representative western blots from one experiment. In Figure 8, the final graph of quantified data is shown. This data was obtained from plotting the standard curve from each gel and using the equation of the line to quantify the amount of α_2m in each individual sample. A two-way ANOVA with repeated measures was then completed for statistical analysis of the data. Again, although there was a trend towards more tightly bound α_2m with newborn than with adult, the results show no significant difference between the elution profile seen with newborn plasma versus with adult plasma (p = 0.30, n=5).

A

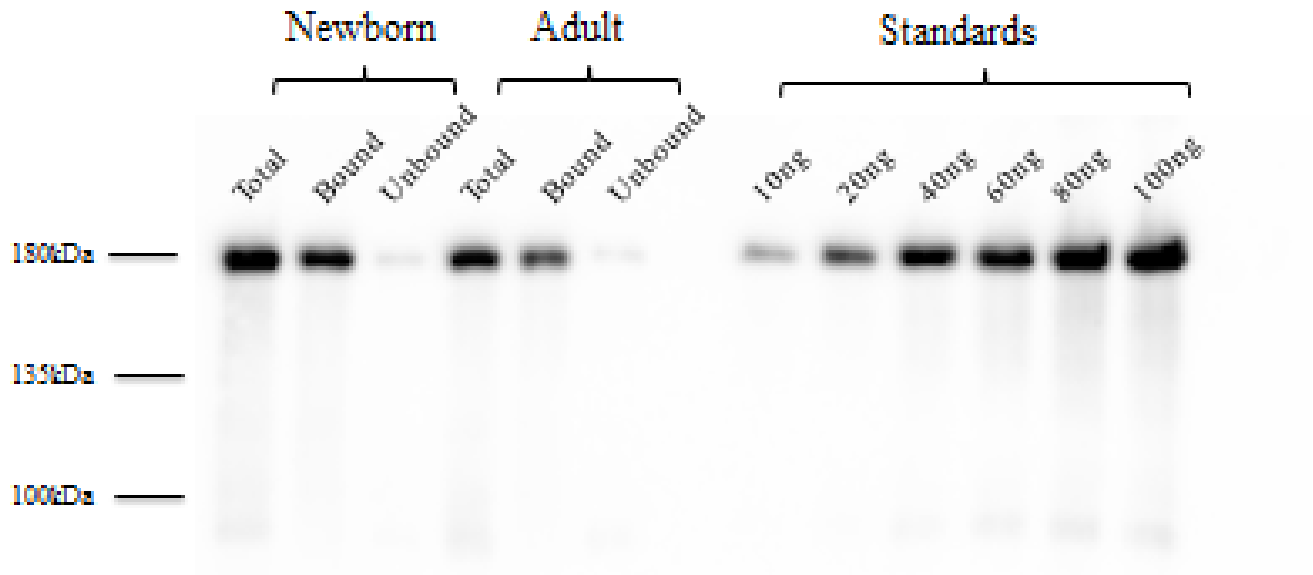

B

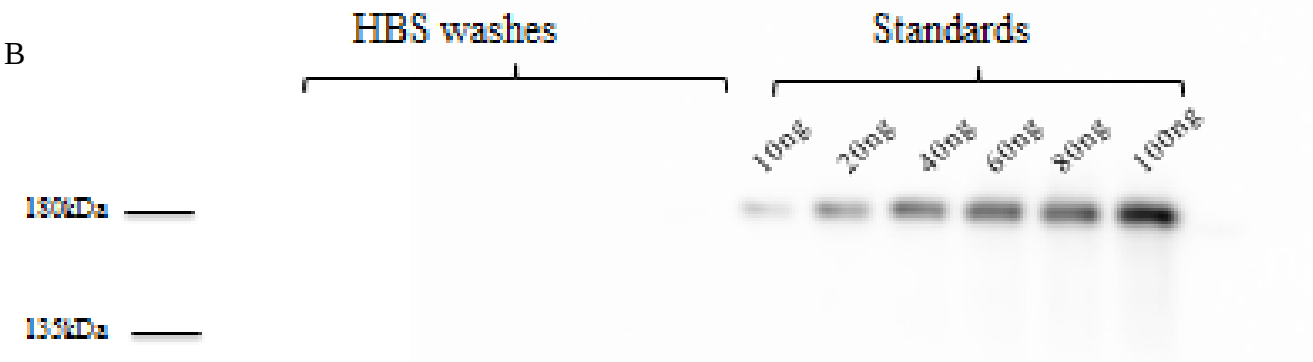

Figure 6: (A) Newborn and adult plasma with and without exposure to agarose-bound RCA_{120}. The unbound fraction was separated from the bound fraction by centrifugation, followed by repeated washing with HBS, shown in (B). Bound α_2m was eluted from RCA_{120} with SDS reducing sample buffer. Shown is a representative western blot of the total α_2m loaded as well as the bound and unbound fractions. Standards ranging from 10-100ng were loaded on both gels and used for quantification of the data.

C

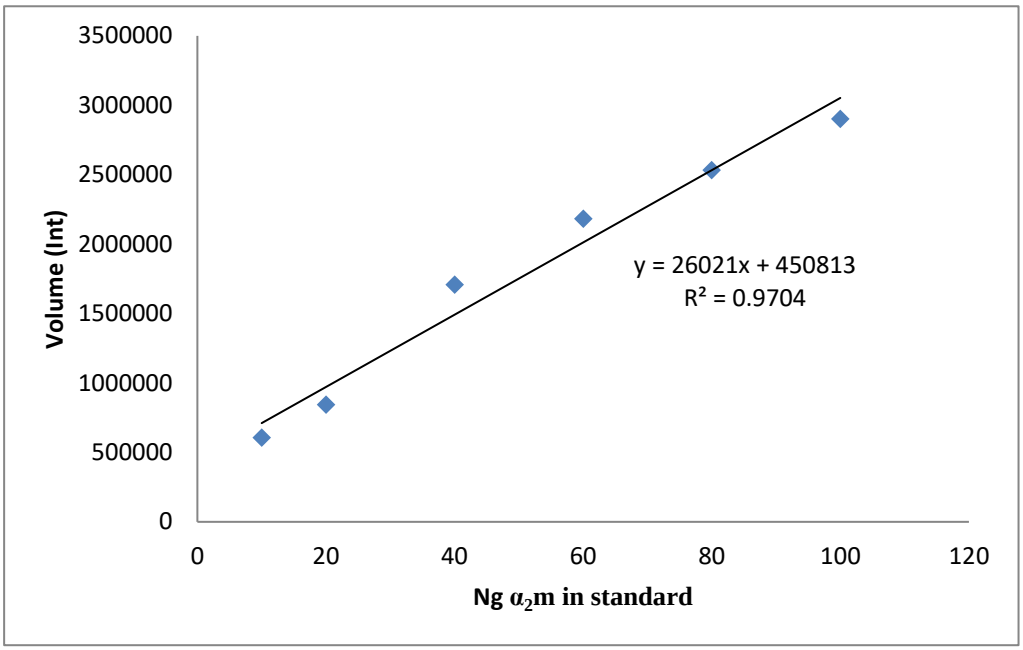

D

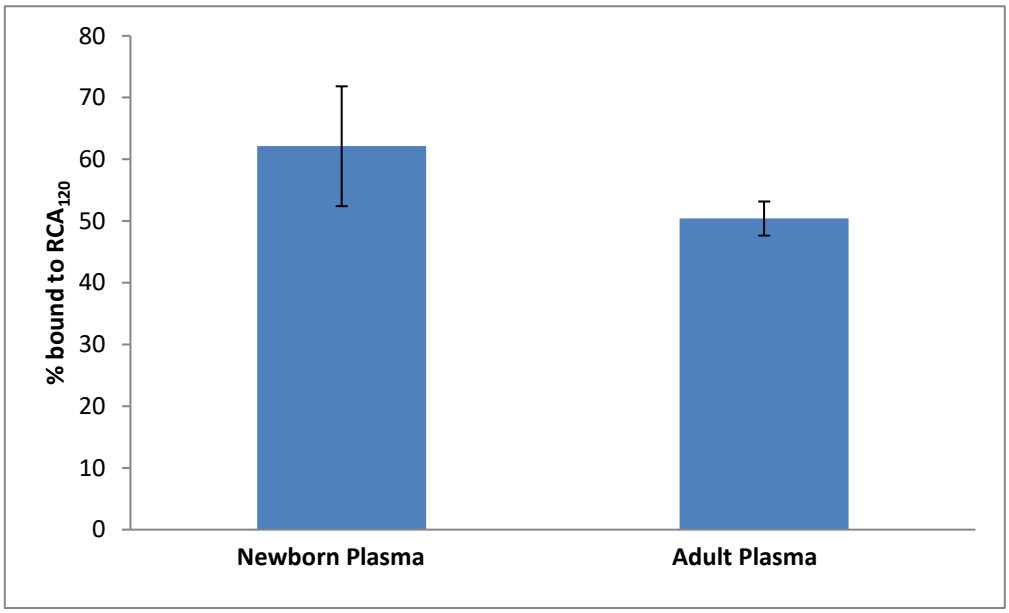

Figure 6 cont'd: (C) Standard curve obtained from densitometry data of standards in (A). (D) Percentage of newborn and adult α_2m bound to RCA_{120}. The amount of α_2m present in each fraction was quantified as described above and expressed as a percentage of the total amount. Results are expressed as mean (n=3) ± SEM.

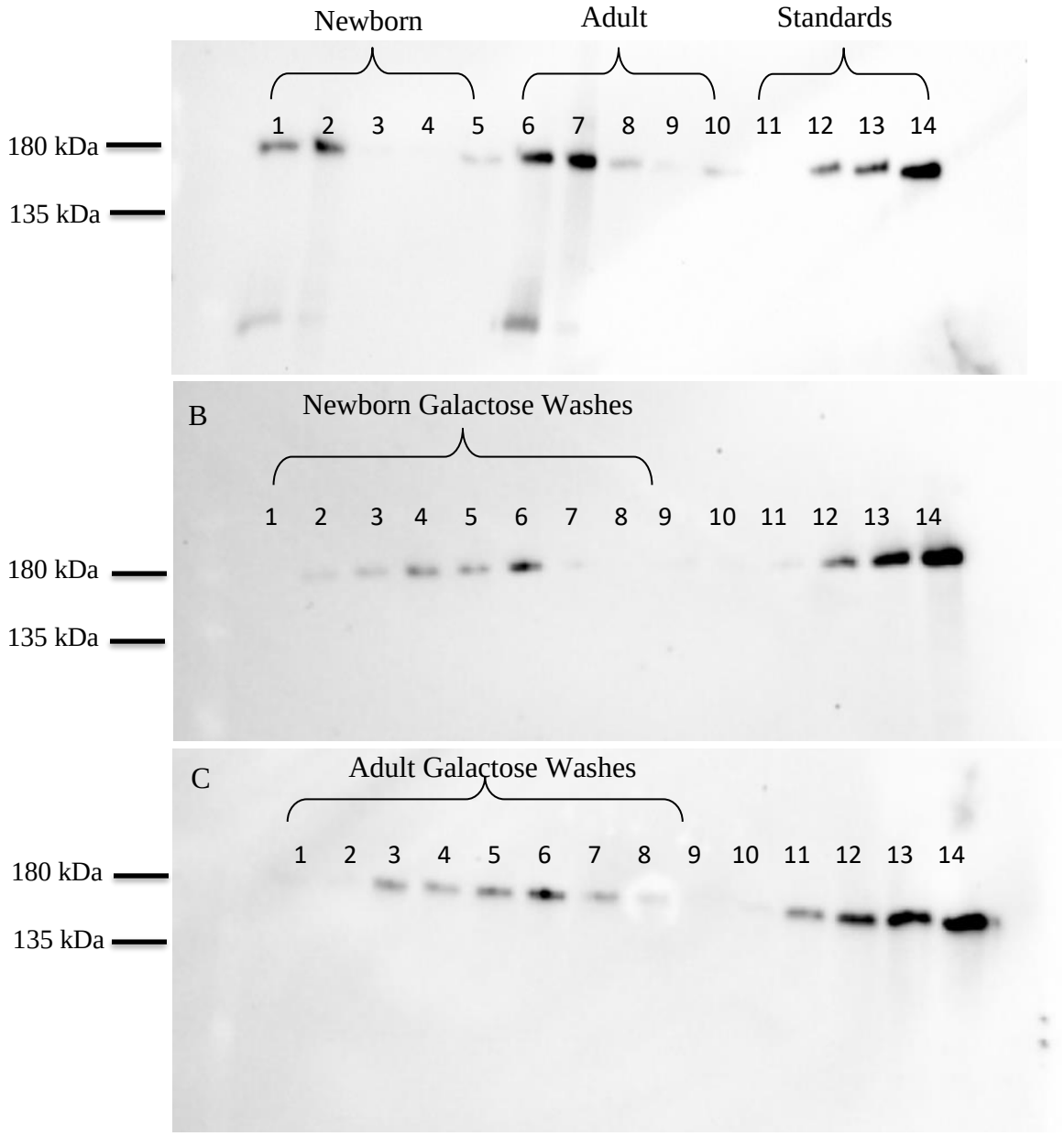

Figure 7: Newborn and adult α_2m samples following binding and elution from RCA_{120} with various concentrations of galactose. (A) Bound and unbound fractions of plasma incubated with RCA_{120}. Lane 1-5 represent newborn plasma samples of the unbound, bound, HBS washes and NaCl wash, respectively. Similarly, lanes 6-10 represent adult samples of the unbound, bound, HBS washes and NaCl wash. Lanes 11 – 14 represent standards from 0.5ng – 10ng. (B) After incubation of RCA_{120} beads with newborn plasma and washing, α_2m bound to beads was eluted with varying concentrations of galactose as follows: Lane 1 – 0.1mM, Lane 2 – 1mM, Lane 3 – 5mM, Lane 4 – 10mM, Lane 5 – 20mM, Lane 6-8 – 200mM and Lane 9 - 1M. (C) RCA_{120} beads incubated with adult plasma were treated as in (B). Samples were electrophoresed on 5% SDS-PAGE followed by western blotting for detection of α_2m in plasma. Shown are representative western blots.

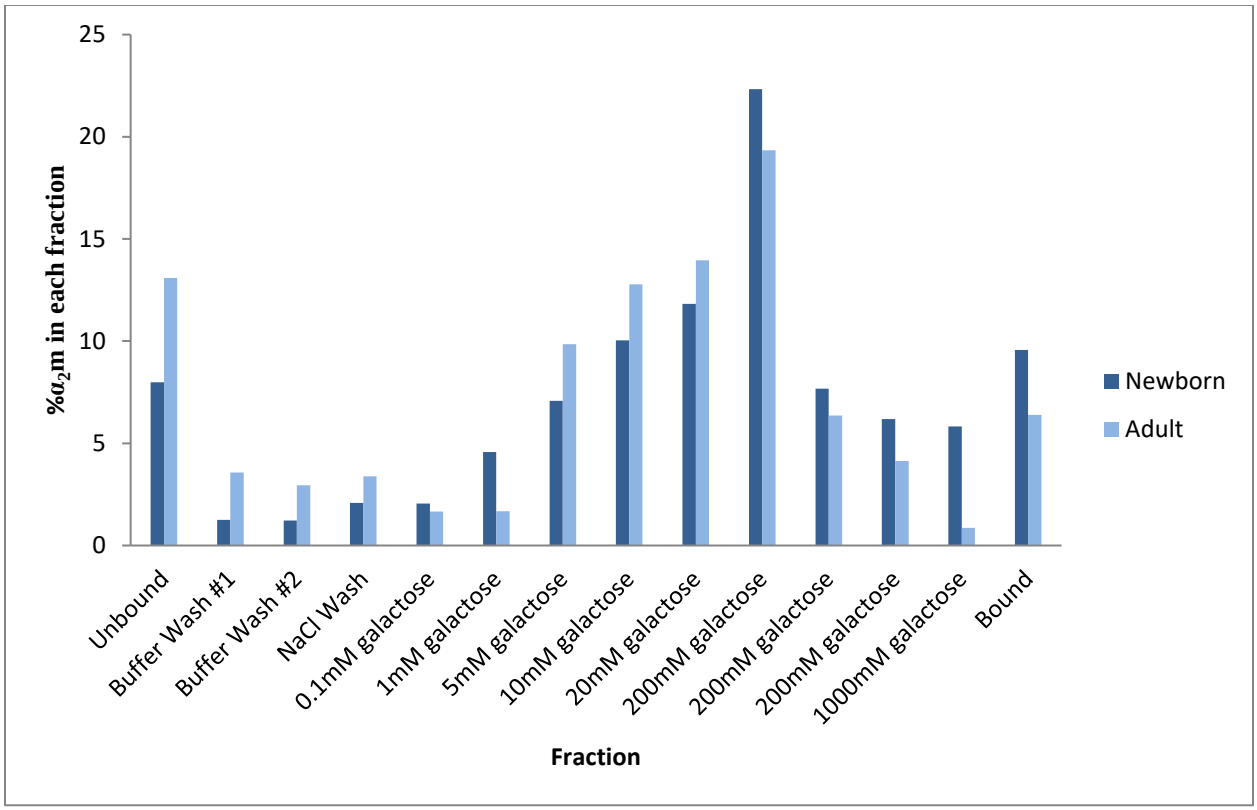

Figure 8: Elution profile of newborn and adult α_2m from agarose-bound RCA_{120}. Data values from Figure 10 were computed as a percentage of total α_2m present in all newborn and adult plasma lanes, respectively. Data shown represents the mean percentage of α_2m in each fraction (n=5) ± SEM.

3.4 2D gel electrophoresis of commercial α_2m, newborn and adult α_2m in plasma

20 ng purified α_2m was run on an IPGphor isoelectric focus system in the first dimension followed by electrophoresis under denaturing conditions on NuPAGE 4-12% Bis-Tris Zoom Gels in the second dimension. Following electrophoresis, the gel was transferred and western blotting was used for specific detection of α_2m. Results from a 20 ng sample of commercially obtained purified α_2m are shown in Figure 9. Results reveal a prominent band around 180kDa that represents the main α_2m monomer. Also present are smaller molecular weight species which appear around 120kDa, 75kDa and 60kDa. It is currently unclear what the source of these bands is, though it is hypothesized that they may be degradation products of α_2m or some impurity in the purified α_2m sample itself.

2D electrophoresis was also conducted on newborn and adult plasma samples. Results are shown in Figure 10. In the newborn sample, a similar banding pattern is seen to that which was previously observed in the commercial α_2m sample. However, in adult plasma, there appears to be a single prominent band around 180kDa consistent with the location of the main α_2m band on 1-dimensional electrophoresis. Lower molecular weight bands present in the newborn sample may be degradation products, as hypothesized above. This degradation could be the result of exposure to the pH gradient, temperature or buffers used throughout the process. Interestingly, this result is not observed in adult plasma, possibly indicating the presence of an entity in adult plasma that protects α_2m from such degradation. Additionally, when examining the pI range of the intact α_2m monomer band for both newborn and adult, there appears to be a difference in the pI range of the two molecules. In the newborn gel, this band spans a pI range of about 5.4-6.1, whereas in adult the corresponding band spans a pI range of about 5.8-6.4. The lower pI range

seen in the newborn sample could indicate greater sialic acid content per α_2m molecule (on average), and this agrees with the finding seen in our previous neuraminidase results.

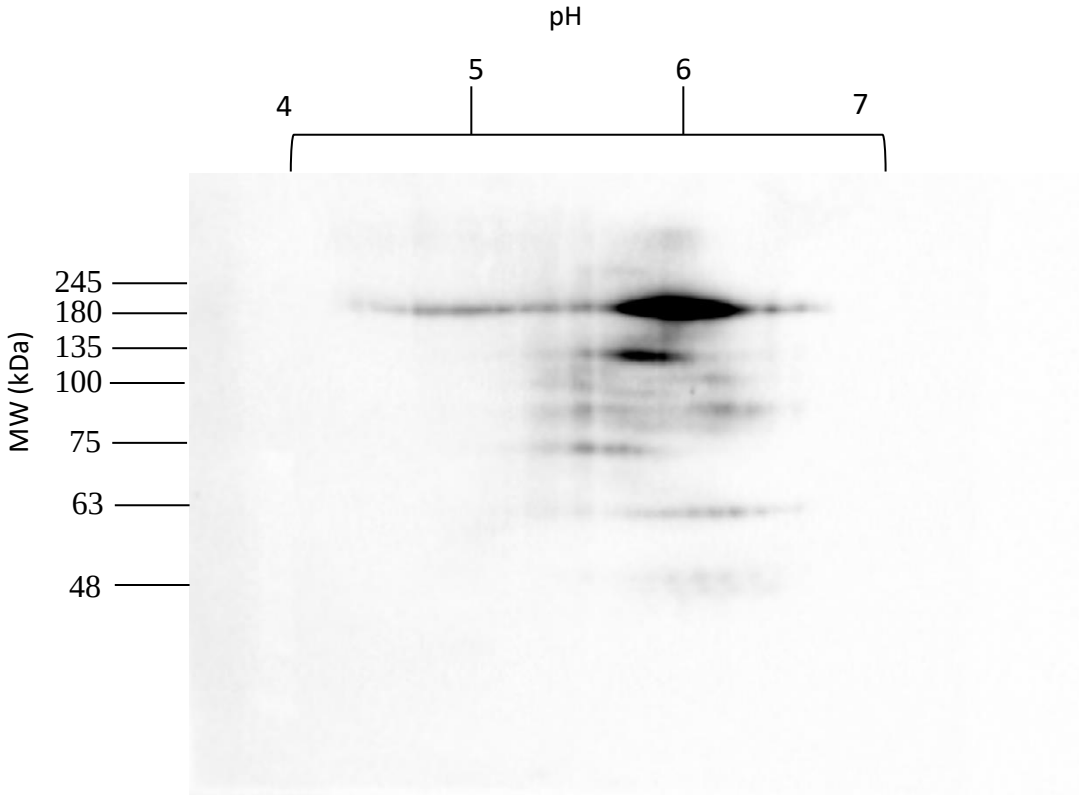

Figure 9: Western blot of 20 ng purified α_2m following 2D gel electrophoresis. α_2m isoforms in the sample were separated by isoelectric point and molecular weight. Electrophoresis occurred on a 4-12% Bis-Tris gel under denaturing conditions.

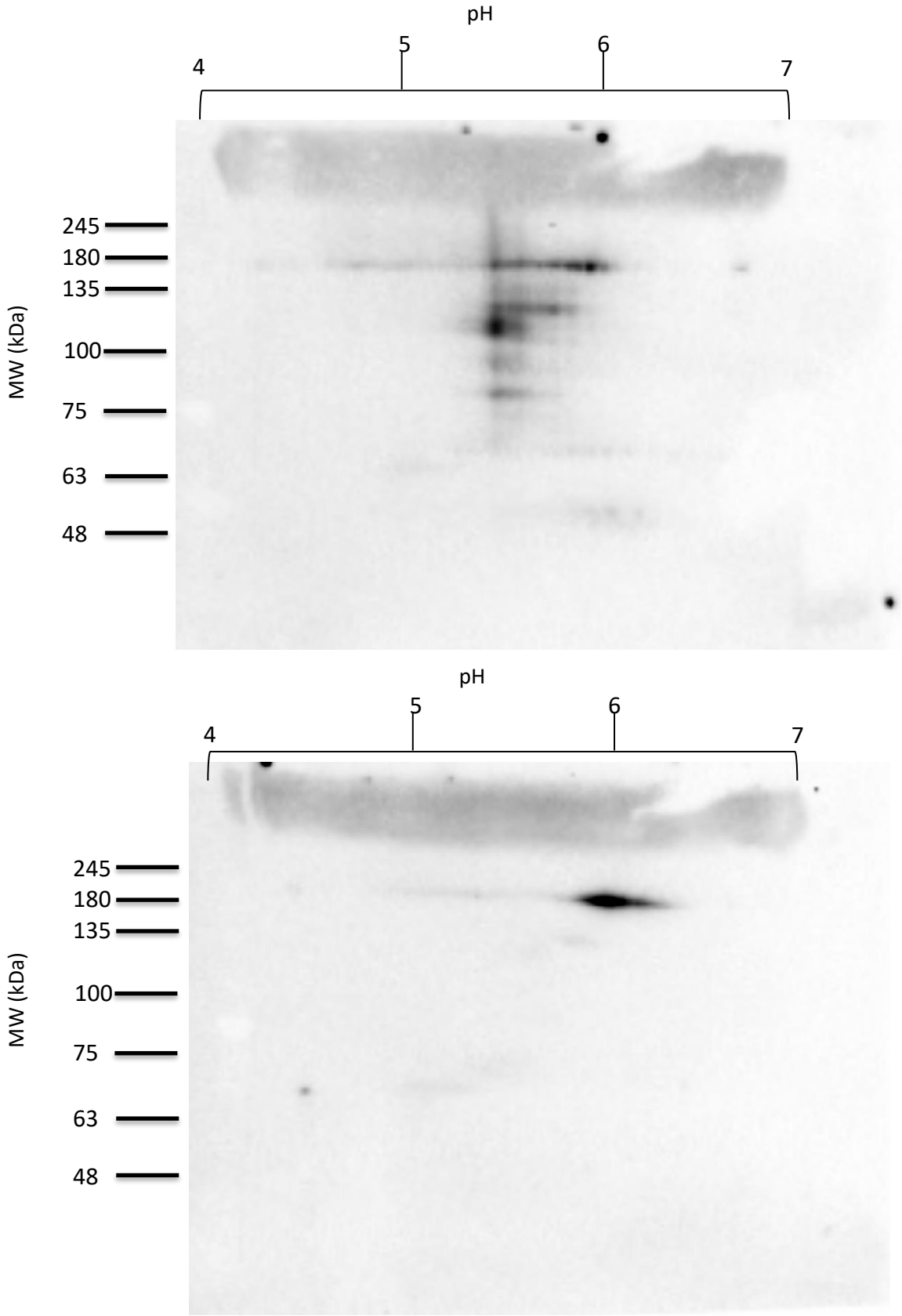

Figure 10: Western blot of α_2m from newborn plasma (top) and adult plasma (bottom) following 2D gel electrophoresis. α_2m isoforms in the sample were separated by isoelectric point and molecular weight. Electrophoresis occurred on a 4-12% Bis-Tris gel under denaturing conditions.

3.5 Testing the effect of 2D buffers on newborn and adult plasma in one-dimensional electrophoresis

In an attempt to determine the cause of degradation seen with α_2m from newborn plasma when run on 2D electrophoresis, buffers were prepared fresh and both newborn and adult plasma samples were exposed to various buffer conditions, as described in the methods, prior to being electrophoresed on 4-15% gradient gels followed by western blotting. By testing all conditions under which newborn and adult plasma are exposed throughout the IEF and equilibration phases of 2D electrophoresis, this experiment was designed reveal which condition produced the degradation of newborn α_2m seen in Figure 10.

Results are shown in Figure 11 (A) and (B). In (A), a 60 second exposure of the gel is shown. In (B), the same image is shown, however the contrast of the image was adjusted in an attempt to reveal other molecular weight bands that were too faint to be visible in the initial image. In both (A) and (B), Condition A represents a newborn and adult sample (N and A, respectively) that were denatured with SDS sample buffer (made with β-ME). Condition B represents a newborn and adult sample that was denatured with SDS sample buffer (made with β-ME) and boiled for 5 minutes at 100^0C. Condition C represents a newborn and adult sample that was denatured with SDS sample buffer containing 60 mM DTT. Condition D represents a newborn and adult sample that was denatured in rehydration buffer and 10% glycerol (added to allow the sample to move through the gel effectively). Condition E represents a newborn and adult sample that was denatured in rehydration buffer and left on the bench for 18 hours. Prior to loading on the gel, equilibration buffer made with DTT was added. Condition F represents a newborn and adult sample that was denatured in rehydration buffer and equilibration buffer, without being left on the bench for an extended period of time. Condition G represents a

newborn and adult sample that was denatured in rehydration buffer and equilibration buffer made with iodoacetamide. Condition H represents a newborn and adult sample that was denatured in rehydration buffer and IPG buffer followed by incubation on the bench for 18 hours. Prior to being loaded onto the gel, equilibration buffer (made with DTT) was added.

The results show that there was α_2m degradation upon heating in SDS sample buffer, as expected (condition B). In addition, one major degradation product was seen in newborn and adult samples in conditions A and C. This result shows that degradation of α_2m in newborn and adult plasma occurs similarly in samples treated with SDS sample buffer containing β-ME and DTT (used in 2D electrophoresis). In condition E, both newborn and adult samples were placed in rehydration buffer and left on the bench for 18 hours. The time frame was chosen as it represents the standard amount of time required for isoelectric focusing to be completed. Following contrast adjustment in condition E, two lower molecular weight bands are revealed in both newborn and adult samples. Interestingly, this trend is the shared between newborn and adult α_2m, and not only seen in the newborn sample, as anticipated. Some faint lower molecular weight bands are seen in conditions F-H, and the pattern is consistent throughout the three samples.

From these results, we can conclude that the buffers used in 2D electrophoresis are capable of producing some degradation of α_2m which can be seen in 1D electrophoresis. However, the degradation tendencies of newborn and adult α_2m in plasma are the same and therefore do not explain the difference in banding for newborn versus adult samples seen in the above 2D results. Further investigation is required in order to determine the exact cause of the differences regarding lower molecular weight bands observed in newborn but not adult α_2m on 2D electrophoresis.

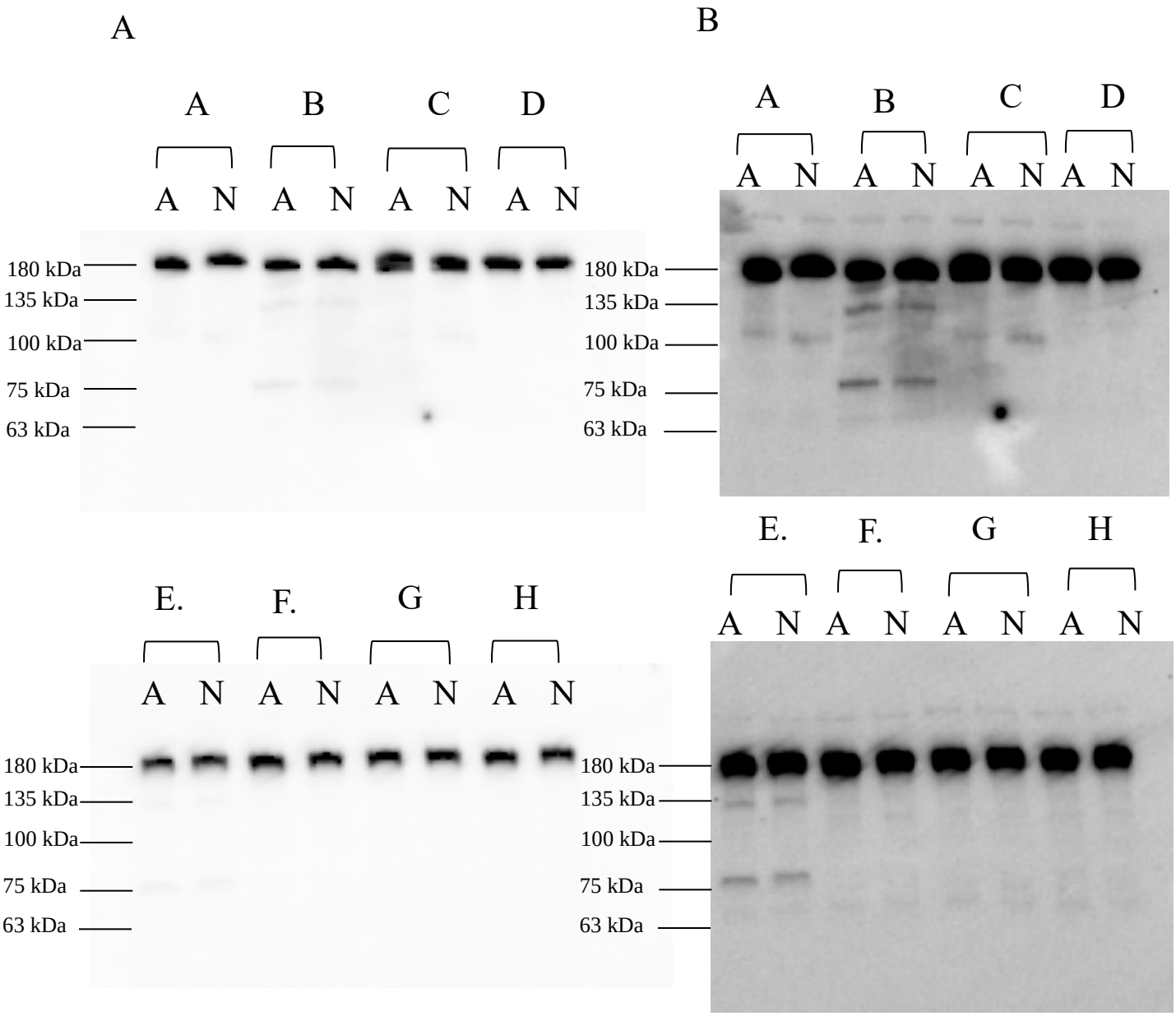

Figure 11: Western blot of newborn and adult plasma samples exposed to 2D buffer conditions and electrophoresed on denaturing gels. Within each reaction condition (A – H), 'A' symbolizes an adult plasma sample and an 'N' symbolizes a newborn plasma sample. Contrast was adjusted using ImageLab software of the initial 60 second exposure image (A) to visualize lower molecular weight bands (B).

3.6 Pre-clearance of IgG from human newborn and adult plasma in preparation for immunoprecipitation

Agarose-bound Protein G was used to remove human IgG from adult plasma in order to ensure no IgG presence for the remaining purification procedure. Due to its Fc region having a strong affinity for Protein G, IgG contamination could diminish the purity of α_2m. Protein G beads were washed with coupling buffer and HBS prior to the addition of human newborn or adult plasma. Plasma was incubated with Protein G beads and pre-cleared plasma samples were isolated by centrifugation and removal of the supernatant. The pre-clearance procedure was performed twice to ensure complete capture and removal of all human IgG in the plasmas. Subsamples were taken and electrophoresed, followed by Western blotting for IgG (Figure 12). Newborn or adult plasma was included to provide a reference for the location of IgG bands on SDS-PAGE.

Figured 12 (A) and (B) show that after one pre-clearance procedure there was very little IgG remaining in both newborn and adult plasma. After the second pre-clearance procedure in each plasma sample, the IgG was virtually undetectable by western blot.

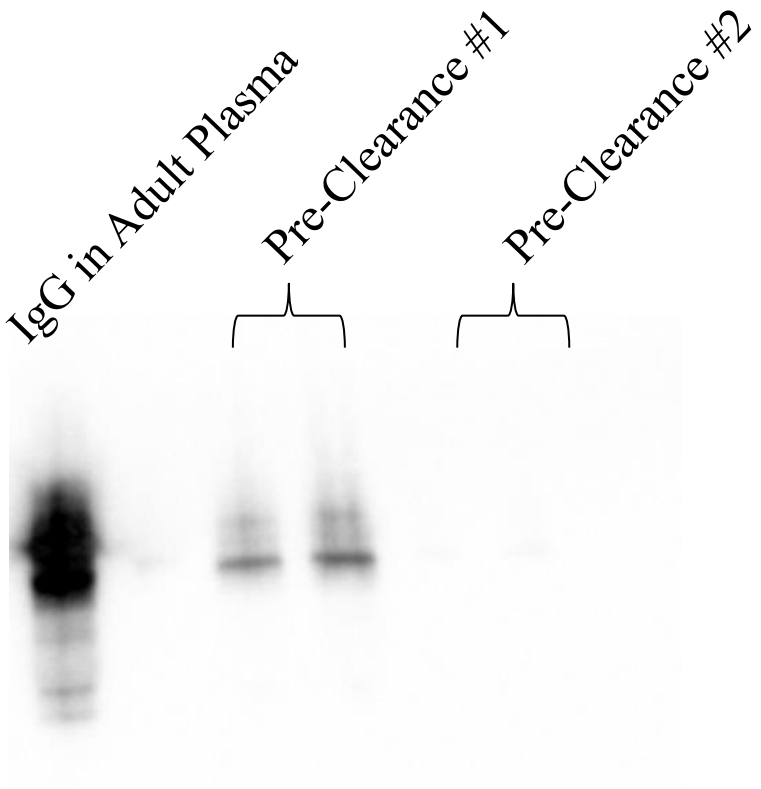

Figure 12 (A): Representative western blot of the removal of IgG from adult plasma with Protein G beads, samples were electrophoresed in duplicates. Adult plasma was incubated with Protein G beads twice for 1 hour at 4^0C followed by centrifugation to remove the pre-cleared plasma fraction. Pre-cleared plasma was retained and is represented in the pre-cleared #1 & #2 lanes. In addition, adult plasma was included on the gel to serve as a reference for the amount of IgG that had been removed from each pre-cleared plasma sample.

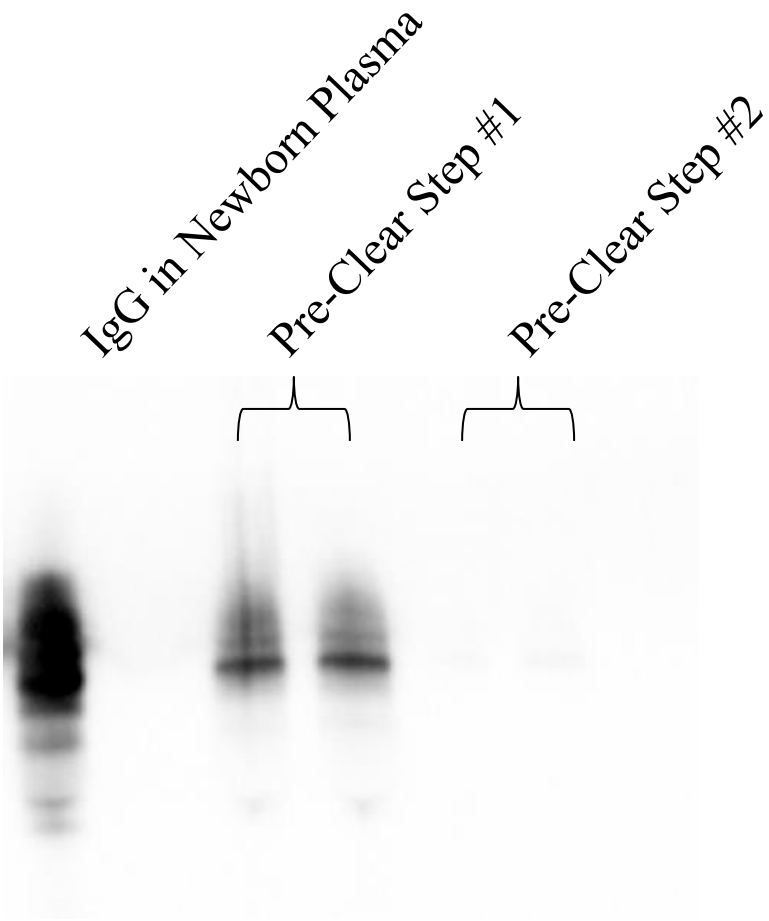

Figure 12 (B): Representative western blot of the removal of IgG from newborn plasma with Protein G beads, samples were electrophoresed in duplicates. Newborn plasma was incubated with Protein G beads twice for 1 hour at 4^0C followed by centrifugation to remove the pre-cleared plasma factions. Pre-cleared plasma was retained and is represented in the pre-cleared step #1 & #2 lanes. Newborn plasma was electrophoresed on the gel to serve as a reference for the amount of IgG that had been removed from each pre-cleared plasma sample.

3.7 Binding and cross-linking of α_2m antibody to Protein G beads in preparation for immunoprecipitation

In order to obtain purified α_2m, polyclonal antibody was bound and cross-linked to the Protein G beads. To accomplish this, fresh Protein G beads were washed with coupling buffer prior to 1 hour incubation with the antibody solution (described in methods). Following incubation, beads were centrifuged and the supernatant was retained to check for free antibody remaining in the fluid phase. Additional washes with coupling buffer were performed and the antibody-bound beads were then incubated for 1 hour with a cross-linking solution (DSS in DMF) to irreversibly bind the antibody to the beads. Cross-linking is critical in order to ensure the antibody will not be eluted with α_2m during the immunoprecipitation process. Following incubation, the antibody-bound beads were washed and incubated in the presence of ethanolamine, a blocking buffer. This incubation ensured that any sites not bound by antibody would be blocked to avoid non-specific binding of proteins in the plasma sample. Following the incubation, the beads were washed with 100mM glycine-HCl (pH 2.8) and HBS, with centrifugation and removal of supernatant occurring after each wash. Samples were electrophoresed on 4-15% gradient gels and silver stained to evaluate the success of the experiment and verify that the antibody was bound and successfully cross-linked to the Protein G beads.

Results are shown in Figure 13 (A) for Protein G beads that were to be used in adult α_2m purification and Figure 13 (B) for beads to be used in newborn α_2m purification. The four gels in each figure represent the four tubes of beads required to accommodate the 1mL volume of plasma being used to purify α_2m. Results reveal a slight presence of antibody following the initial incubation with the Protein G beads. This was consistent throughout the four tubes and

indicates that not all available antibody was bound to the beads. Therefore, the maximal binding capacity of the beads may be less than anticipated. It is also possible that the mixing on the shaker was not enough to allow full incorporation of the antibody into the bead sample. It can be concluded from these silver stains that the α_2m antibody was successfully bound and cross-linked onto the Protein G beads.

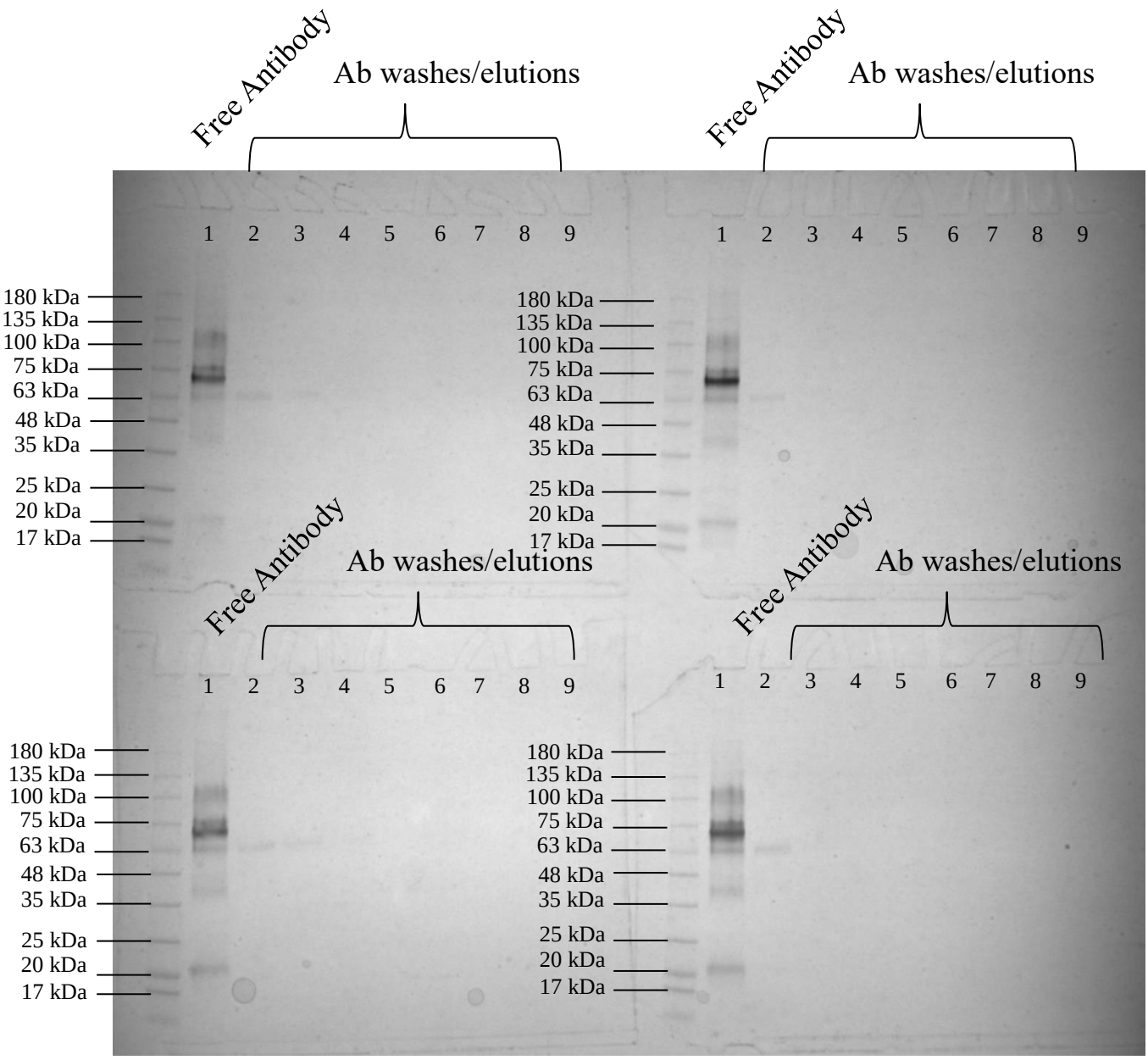

Figure 13(A): Antibody binding to Protein G beads. Protein G beads were incubated with antibody solution for 1 hour. Lane 1 represents an antibody control to be used as a reference for the amount of antibody in all other lanes. Lane 2 represents the supernatant taken immediately following antibody incubation (unbound antibody). Washes with HBS and elutions with 100mM glycine-HCl are represented in lanes 3-9. The samples were electrophoresed on 4-15% gradient gels under denaturing conditions. The 4 gels represent the 4 Eppendorf tubes of antibody-bound beads to be used in the purification of α_2m from adult plasma.

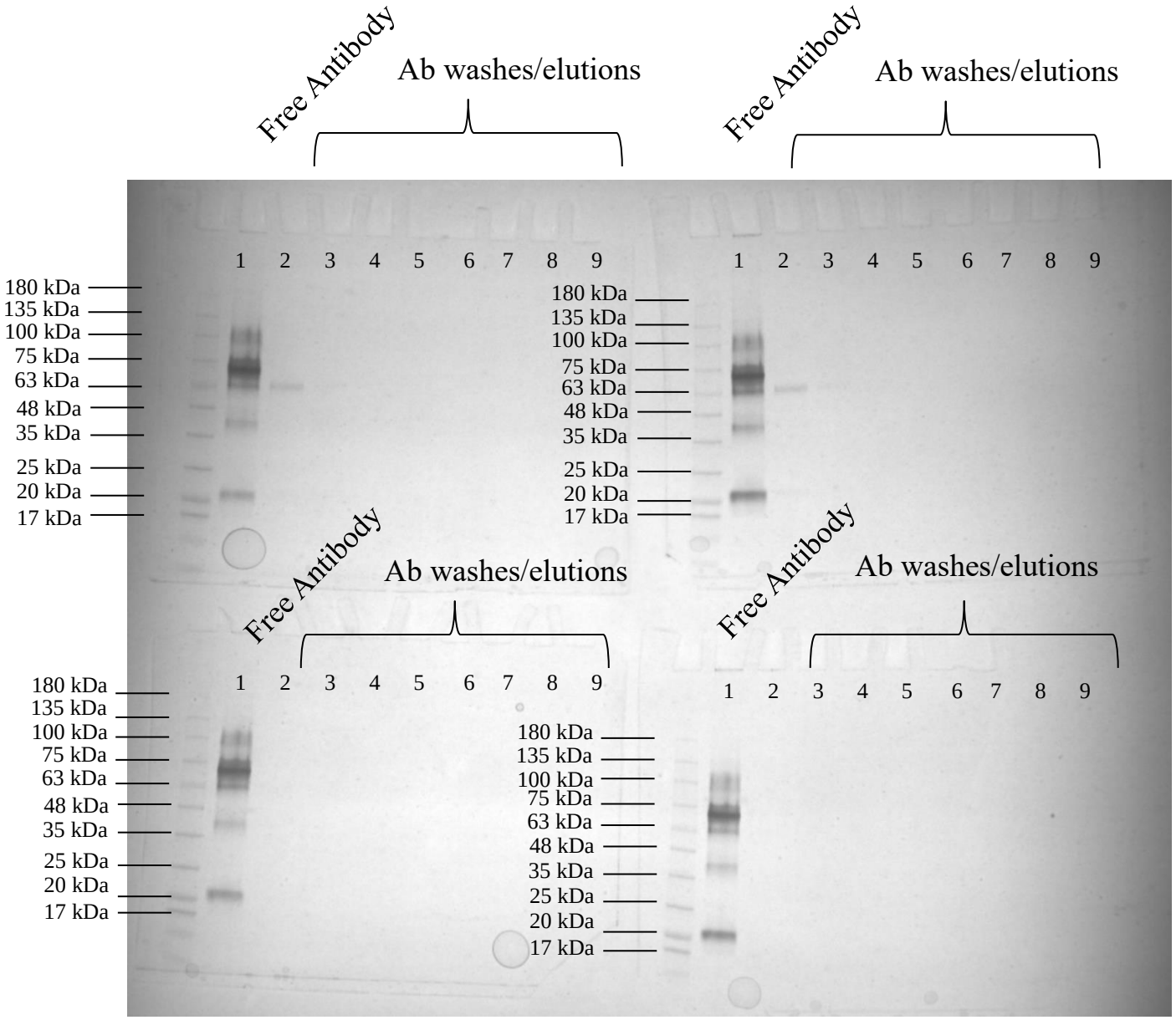

Figure 13(B): Antibody binding to Protein G beads. Protein G beads were incubated with antibody solution for 1 hour. Lane 1 represents an antibody control to be used as a reference for the amount of antibody in all other lanes. Lane 2 represents the supernatant taken immediately following antibody incubation (unbound antibody). Washes with HBS and elutions with 100mM glycine-HCl are represented in lanes 3-9. The samples were electrophoresed on 4-15% gradient gels under denaturing conditions. The 4 gels represent the 4 Eppendorf tubes of antibody-bound beads to be used in the purification of α_2m from newborn plasma.

3.8 Immunoprecipitation of α_2m from newborn and adult plasma

A_2m was extracted from newborn and adult plasma by incubating pre-cleared plasma with the antibody-bound protein G beads in four separate Eppendorf tubes, as described in the methods. For both plasmas, incubation occurred overnight followed by multiple wash steps with HBS. To check for unbound α_2m in the initial flow-through, as well as the HBS washes, samples were taken and electrophoresed on gels followed by silver staining. Results are shown in Figure 14 (A) for adult, and Figure 14 (B) for newborn. There is no presence of α_2m in the flow through or HBS washes (no band occurring at 180 kDa, characteristic of α_2m). This indicates that all α_2m bound to the Protein G beads throughout the overnight incubation and the strength of binding between α_2m and the antibody was high enough to withstand washing with these buffers.

A total of 7 elutions were carried out using 100mM glycine-HCl, however it was decided that only the first four would be used for later FACE analysis. This was decided to avoid excessive storing of samples at room temperature in Glycine-Cl prior to buffer exchange. Therefore, results shown below in figure 15 (A) - (D) represent elutions #1-4 from both adult and newborn purification experiments. Densitometry data obtained following ImageLab analysis of all western blots allowed for standard curves to be generated (figure 15 (E) – (H)) for each gel and the amount of α_2m obtained in each sample to be calculated. Due to the fact that only a fraction of each sample was loaded into each well, quantification data was used to calculate the amount of α_2m in the whole sample. These results are shown in Table 2. Calculations revealed the total amount of adult α_2m eluted with glycine-HCl to be 119 µg (4.5 µg in elution 1, 28.6 µg in elution 2, 39.4 µg in elution 3, 46.6 µg in elution 4), representing a 5.95% yield (based on a concentration of 2 mg/ml α_2m in human adult plasma, previously quantified in our lab).

To verify the purity of the eluted product, samples were taken from each elution (#1-4) and electrophoresed on gels followed by silver staining (Figure 16). In previous purification attempts a contaminant was observed that was the approximate size of HSA, therefore 0.1 µg of HSA was loaded onto each gel to act as a reference for the contaminant in the purified samples. Results show no other sources of contamination.

Newborn α_2m was eluted under the same conditions as adult α_2m and western blot results are shown in Figure 17 (A-D). In Figure 17 (E-H) the standard curves used to quantify the western blot data are shown. Results revealed 124 µg α_2m was purified from newborn plasma in elutions #1-4 (3.7 µg in elution 1, 29.1 µg in elution 2, 54.5 µg in elution 3 and 36.5 µg in elution 4), representing a 6.2% yield (based on a concentration of 4 mg/ml α_2m in human newborn plasma, as previously quantified in our lab). Furthermore, the newborn silver stain results of purity in Figure 18 show α_2m is pure outside of the same contaminating (HSA) band that was observed in the adult plasma experiments. Of course, it is well known that albumin does not contain any glycans which would impact later carbohydrate analysis.

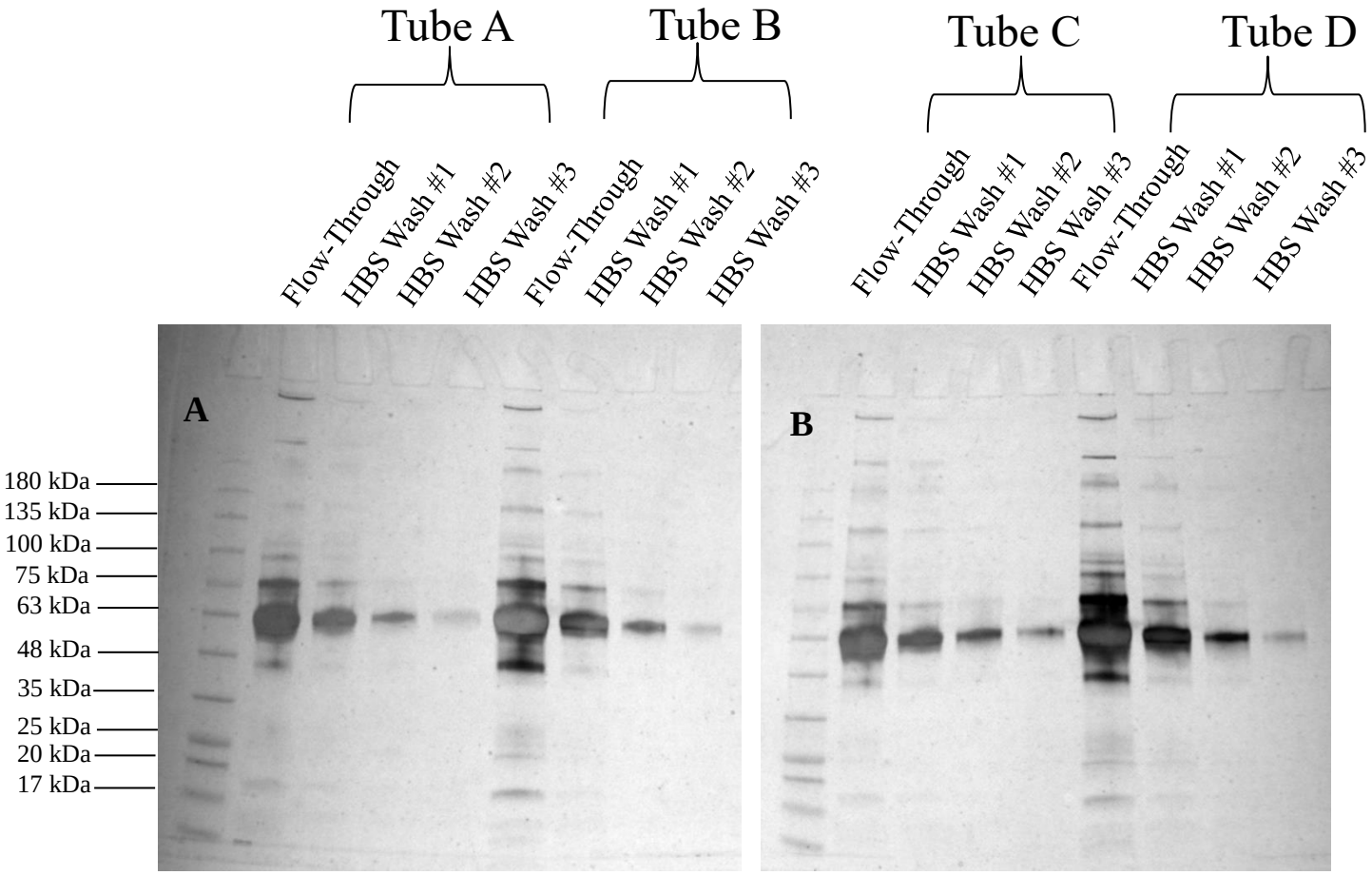

Figure 14 (A): Immunoprecipitation of adult α_2m. Pre-cleared plasma was incubated with antibody-linked Protein G beads overnight at 4^0C. Immediately following incubation, supernatant was removed (flow-through) to check for unbound α_2m. The beads were then washed with HBS prior to α_2m being eluted. Samples from all four reaction tubes are represented in the above silver stains. In (A), lane 1 represents the flow-through from 'tube 'A' and lanes 2-4 represent the initial three HBS washes from the same reaction tube. Lane 5 represents the flow-through from 'tube 'B' and lanes 6-8 represent the initial three HBS washes from the same reaction tube. In (B), lane 1 represents the flow-through from 'tube 'C' and lanes 2-4 represent the initial three HBS washes from the same reaction tube. Lane 5 represents the flow-through from 'tube 'D' and lanes 6-8 represent the initial three HBS washes from the same reaction tube.

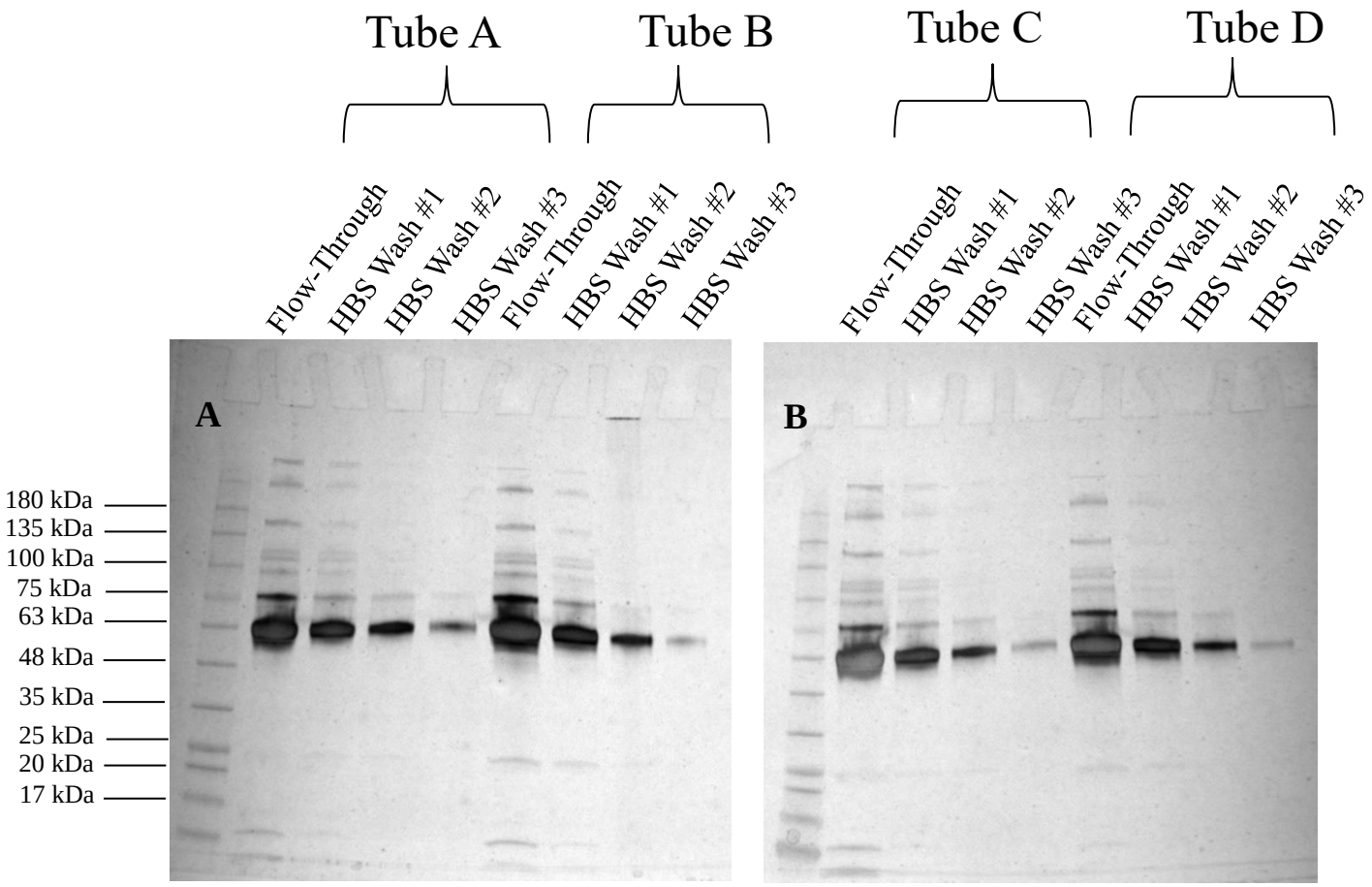

Figure 14 (B): Immunoprecipitation of newborn α_2m. Silver stain of flow-through and HBS washes following overnight incubation of newborn plasma with antibody-bound Protein G beads. Samples from all four reaction tubes are represented. In (A), lane 1 represents the flow-through from 'tube 'A' and lanes 2-4 represent the initial three HBS washes from the same reaction tube. Lane 5 represents the flow-through from 'tube 'B' and lanes 6-8 represent the initial three HBS washes from the same reaction tube. In (B), lane 1 represents the flow-through from 'tube 'C' and lanes 2-4 represent the initial three HBS washes from the same reaction tube. Lane 5 represents the flow-through from 'tube 'D' and lanes 6-8 represent the initial three HBS washes from the same reaction tube.

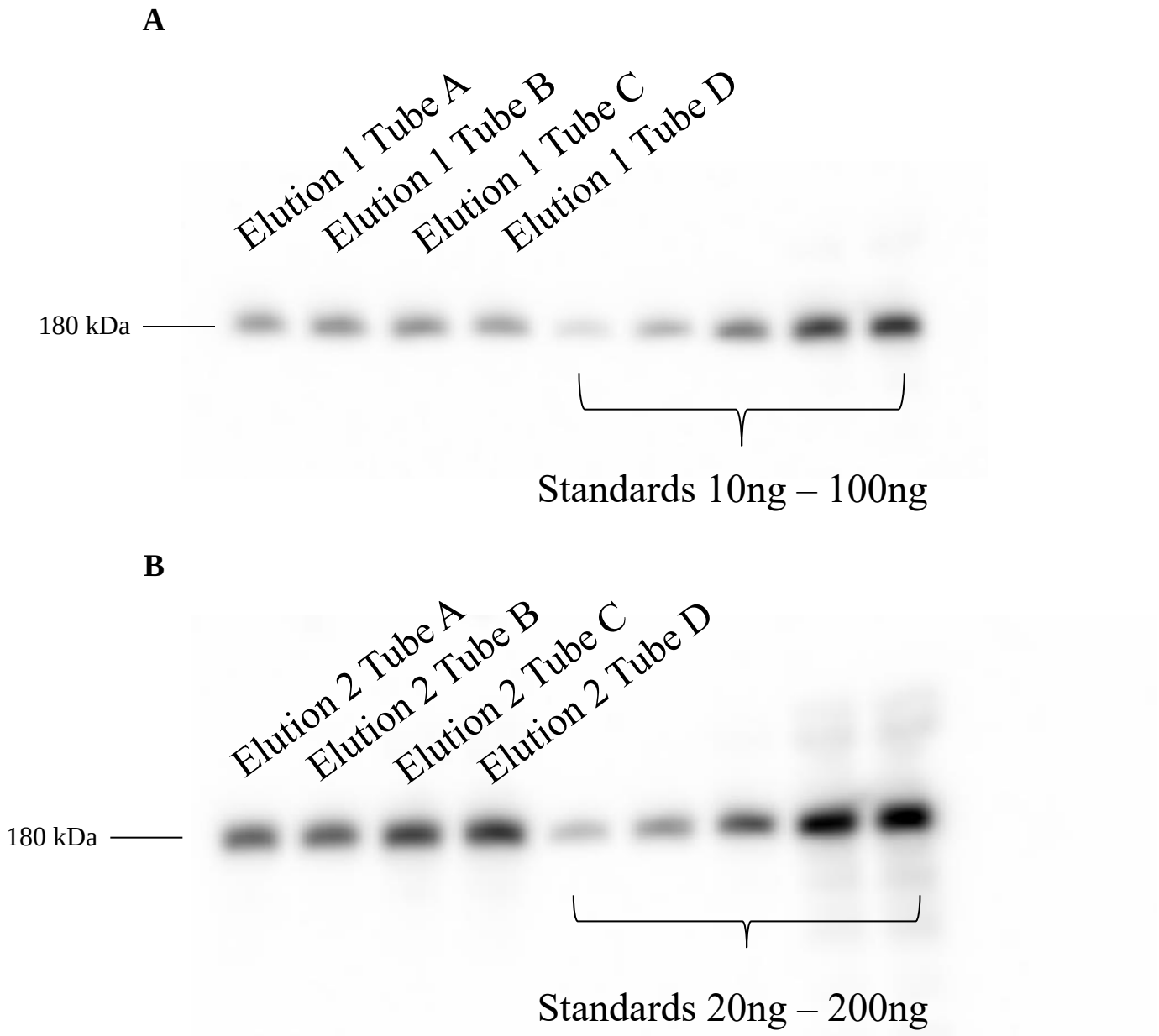

Figure 15: Adult α_2m purified from human plasma. Adult plasma was cleared of IgG prior to being incubated overnight with antibody Protein G beads at 4^0C. Beads were washed with HBS (described above) prior to being eluted with 100mM glycine-Cl pH 2.8. (A) First elution sample from each incubation tube as well as standards ranging from 10-100ng. (B) Second elution sample from each incubation tube as well as standards ranging from 20-200ng. All adult α_2m samples were electrophoresed on 4-15% gradient gels under denaturing conditions followed by western blotting for the detection of α_2m.

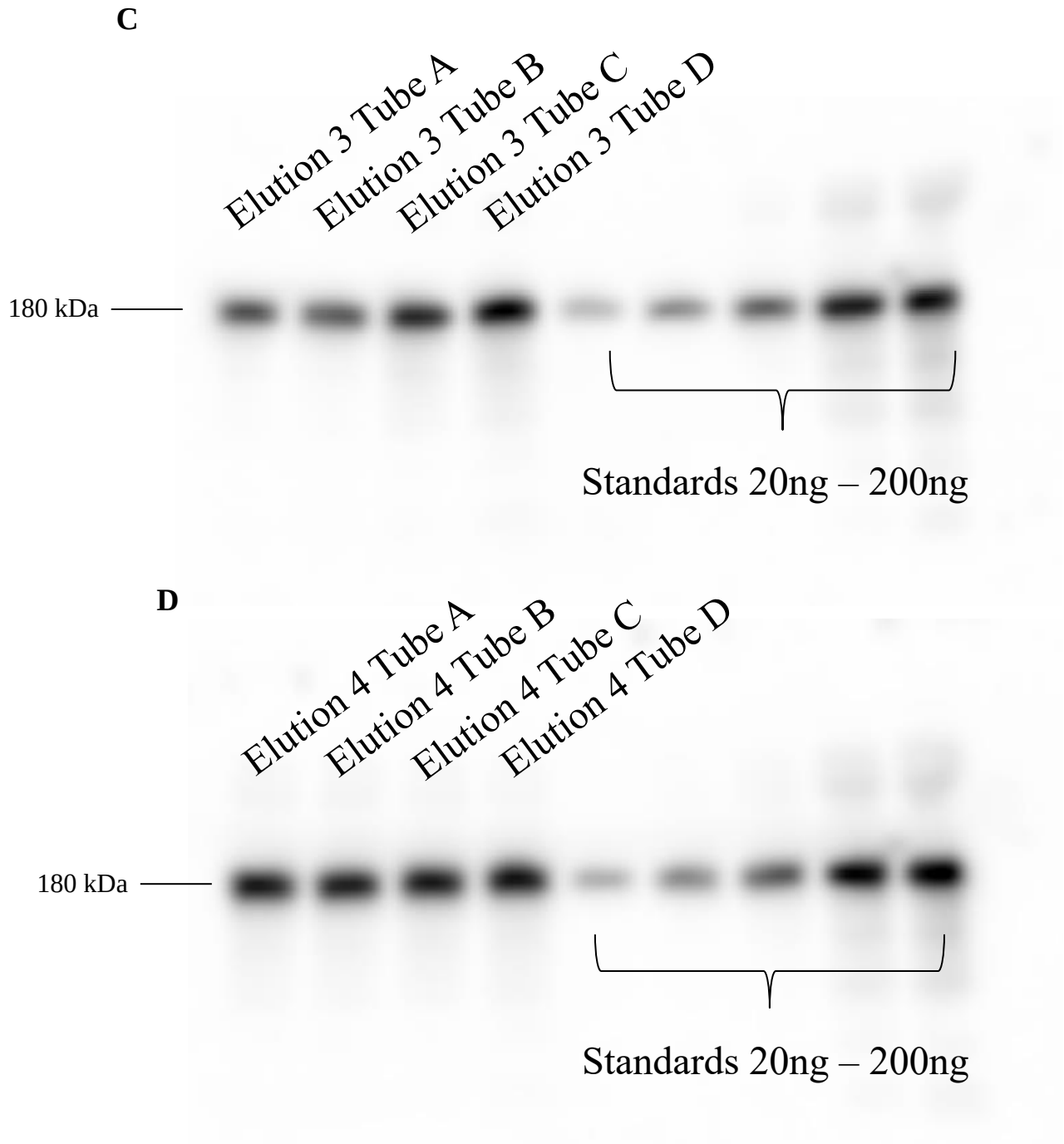

Figure 15 cont'd: (C) Third elution sample from each incubation tube as well as standards ranging from 20-200ng. (D) Fourth elution sample from each incubation tube as well as standards ranging from 20-200ng. All adult α_2m samples were electrophoresed on 4-15% gradient gels under denaturing conditions followed by western blotting for the detection of α_2m.

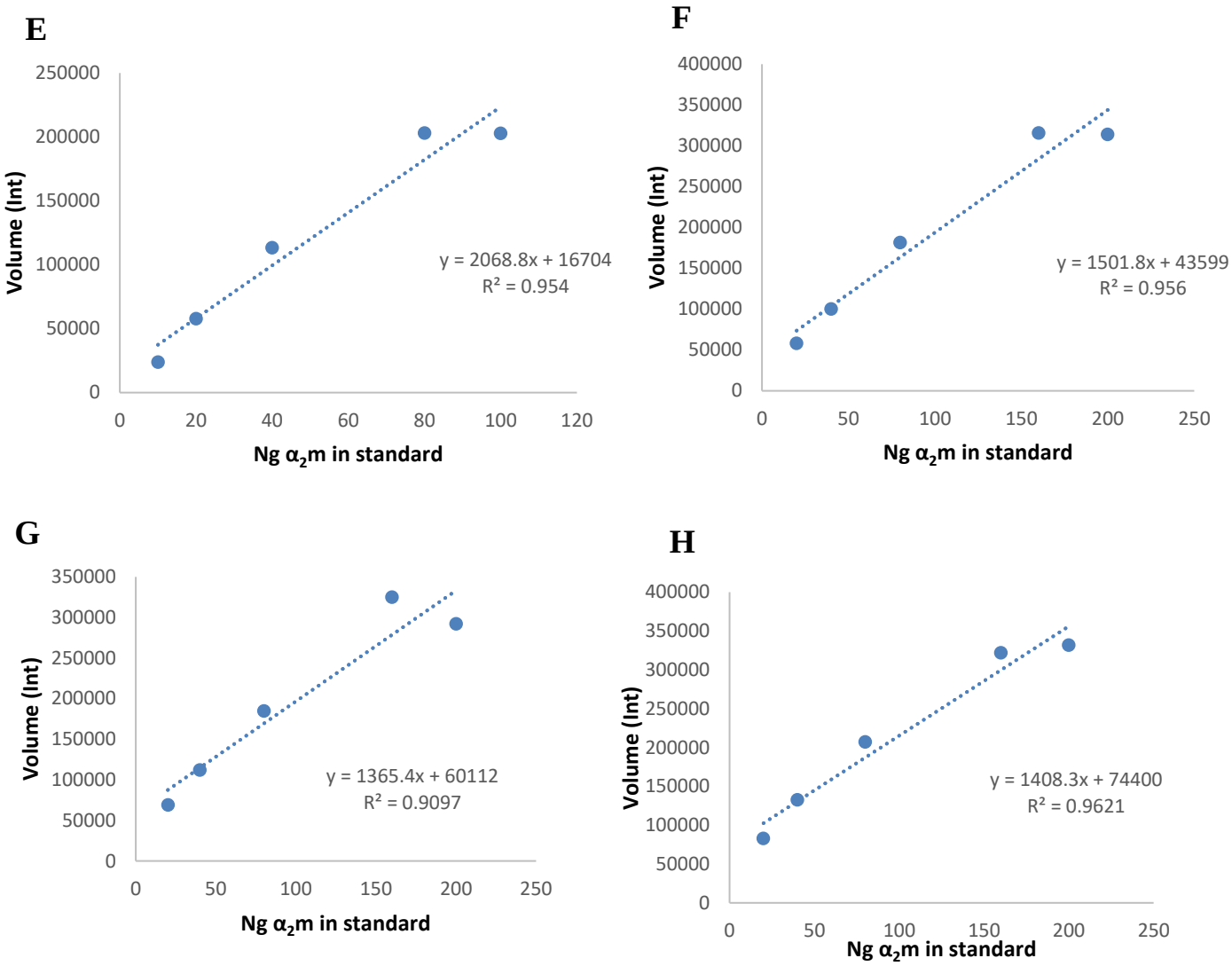

Figure 15 cont'd: (E) Standard curve obtained from densitometry data of standards (10-100ng) in (A). (F) Standard curve obtained from densitometry data of standards (20-200ng) in (B). (G) Standard curve obtained from densitometry data of standards (20-200ng) in (C). (H) Standard curve obtained from densitometry data of standards (20-200ng) in (D). The equation of the line was used to quantify the amount of α_2m in each elution sample.

Sample	Quantity based on densitometry data	Actual quantity (adjusted for total volume in elution)
Elution 1, Tube A	29.83 ng	0.95 µg
Elution 1, Tube B	38.64 ng	1.24 µg
Elution 1, Tube C	40.54 ng	1.30 µg
Elution 1, Tube D	32.10 ng	1.03 µg
Elution 2, Tube A	90.37 ng	5.78 µg
Elution 2, Tube B	90.07 ng	5.76 µg
Elution 2, Tube C	127.18 ng	8.14 µg
Elution 2, Tube D	139.65 ng	8.94 µg
Elution 3, Tube A	101.16 ng	6.47 µg
Elution 3, Tube B	122.86 ng	7.86 µg
Elution 3, Tube C	180.32 ng	11.54 µg
Elution 3, Tube D	210.60 ng	13.48 µg
Elution 4, Tube A	184.82 ng	11.83 µg
Elution 4, Tube B	169.65 ng	10.86 µg
Elution 4, Tube C	180.35 ng	11.54 µg
Elution 4, Tube D	192.53 ng	12.32 µg

Table 2: Using the standard curves from Figure 15 (E) to (H), the quantity of α_2m in each elution fraction obtained during purification was calculated. Quantities were adjusted to represent the elution volume as a whole (instead of representing solely the amount of protein on the gel itself).

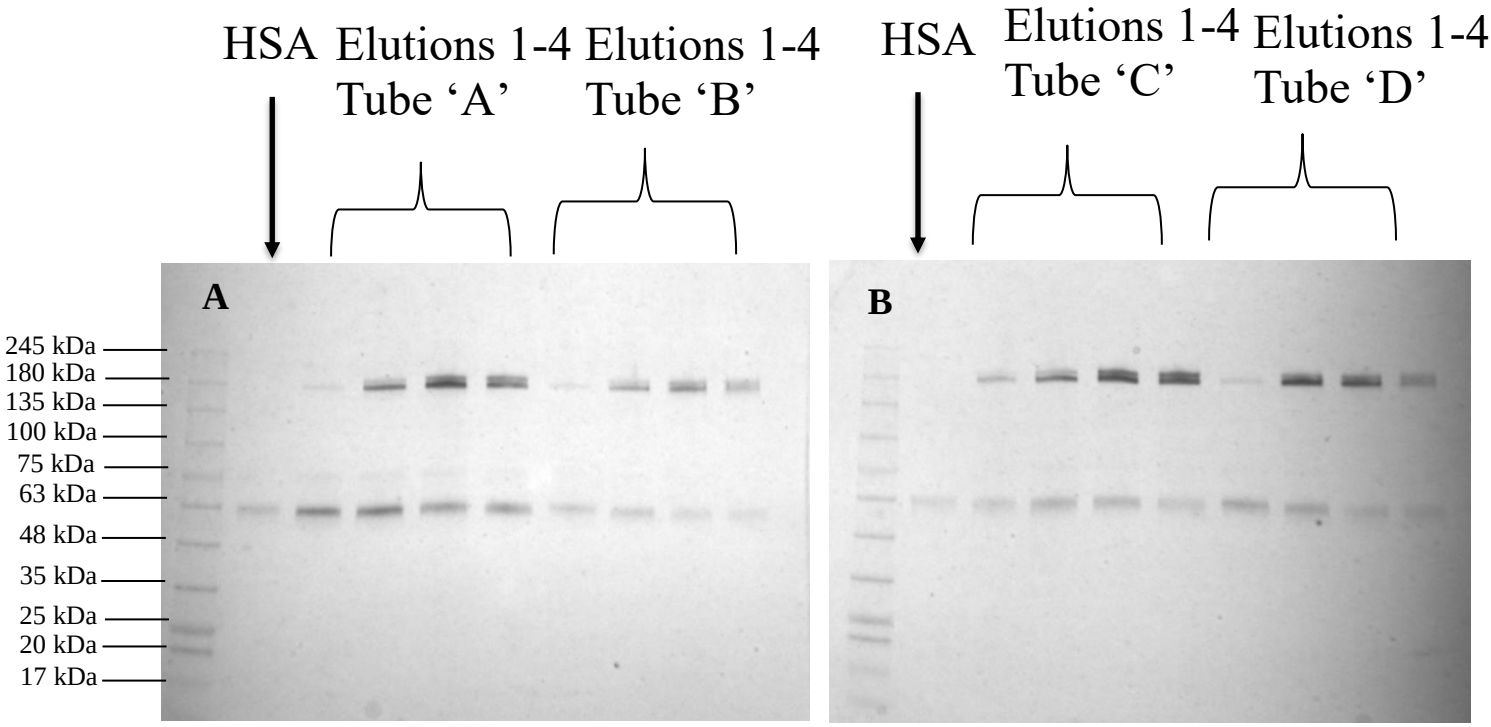

Figure 16: Silver stain of eluted adult α_2m fractions to verify purity. Elution samples were electrophoresed on 4-15% gradient gels under denaturing conditions. As in the above flow-through/HBS figures, each gel represents elutions from two incubation tubes. In (A), lane 1 represents 0.1 µg HSA and lanes 2-5 represent elutions 1-4 (respectively) from tube 'A'. Lanes 6-9 represent elutions 1-4 (respectively) from tube 'B'. In (B)), lane 1 represents 0.1ug HSA and lanes 2-5 represent elutions 1-4 (respectively) from tube 'C'. Lanes 6-9 represent elutions 1-4 (respectively) from tube 'D'.

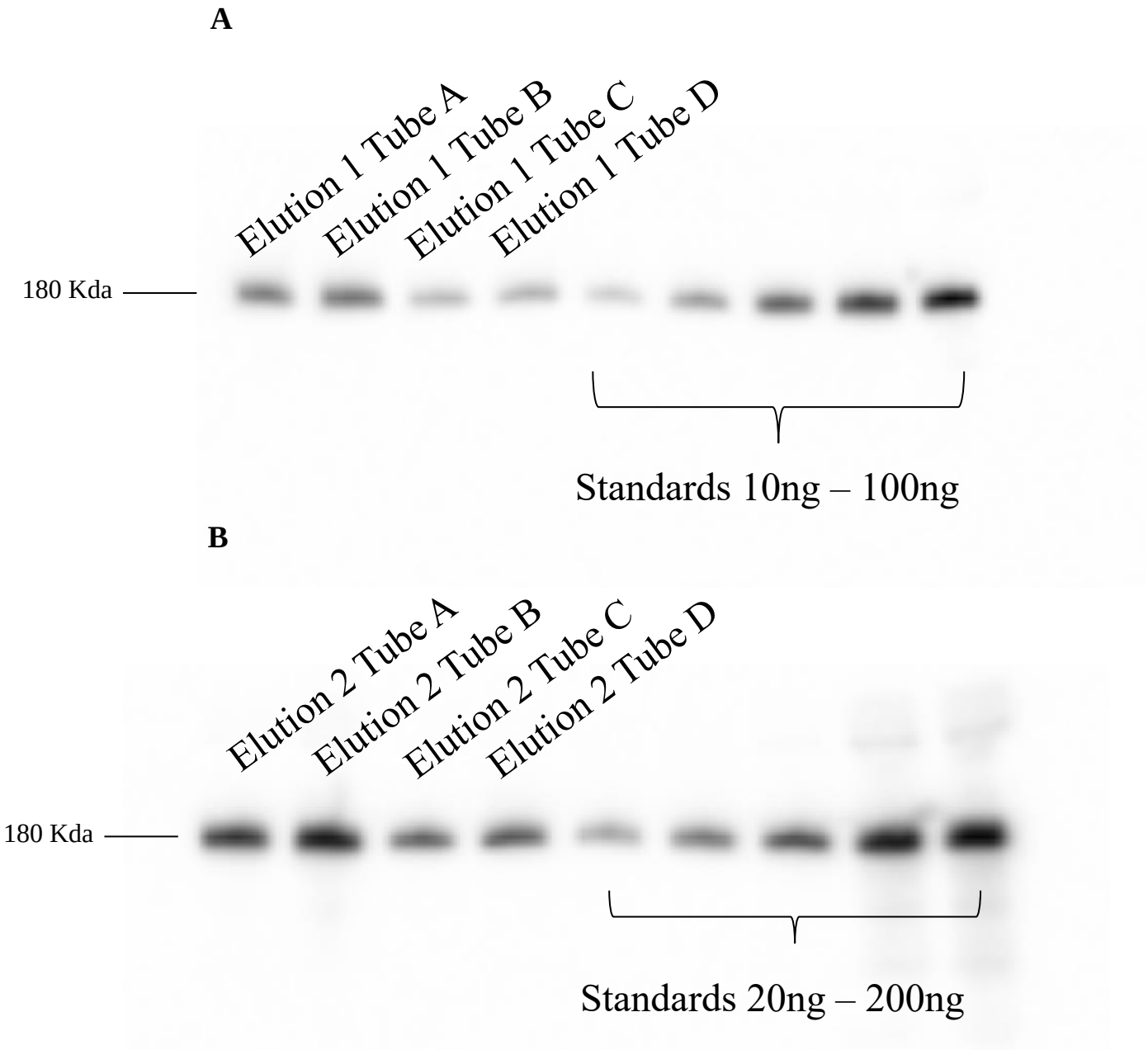

Figure 17: Newborn α_2m purified from human plasma. Newborn plasma was cleared of IgG prior to being incubated overnight with antibody Protein G beads at 4^0C. Beads were washed with HBS prior to being eluted with 100mM glycine-Cl pH 2.8. (A) First elution sample from each incubation tube as well as standards ranging from 10-100ng. (B) Second elution sample from each incubation tube as well as standards ranging from 20-200ng. All Newborn α_2m samples were electrophoresed on 4-15% gradient gels under denaturing conditions followed by western blotting for the detection of α_2m.

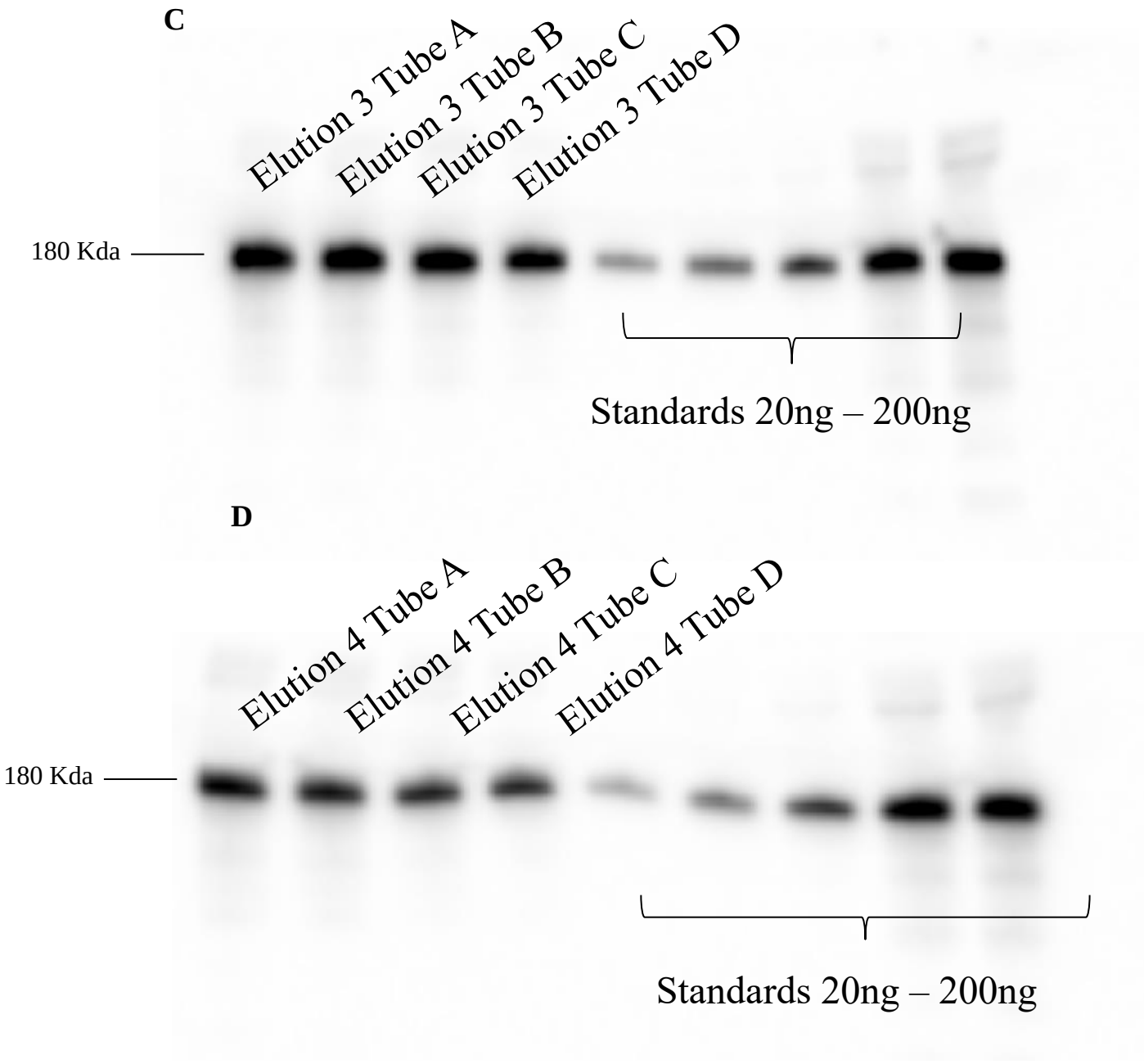

Figure 17 cont'd: (C) Third elution sample from each incubation tube as well as standards ranging from 20-200ng. (D) Fourth elution sample from each incubation tube as well as standards ranging from 20-200ng. All newborn α_2m samples were electrophoresed on 4-15% gradient gels under denaturing conditions followed by western blotting for the detection of α_2m.

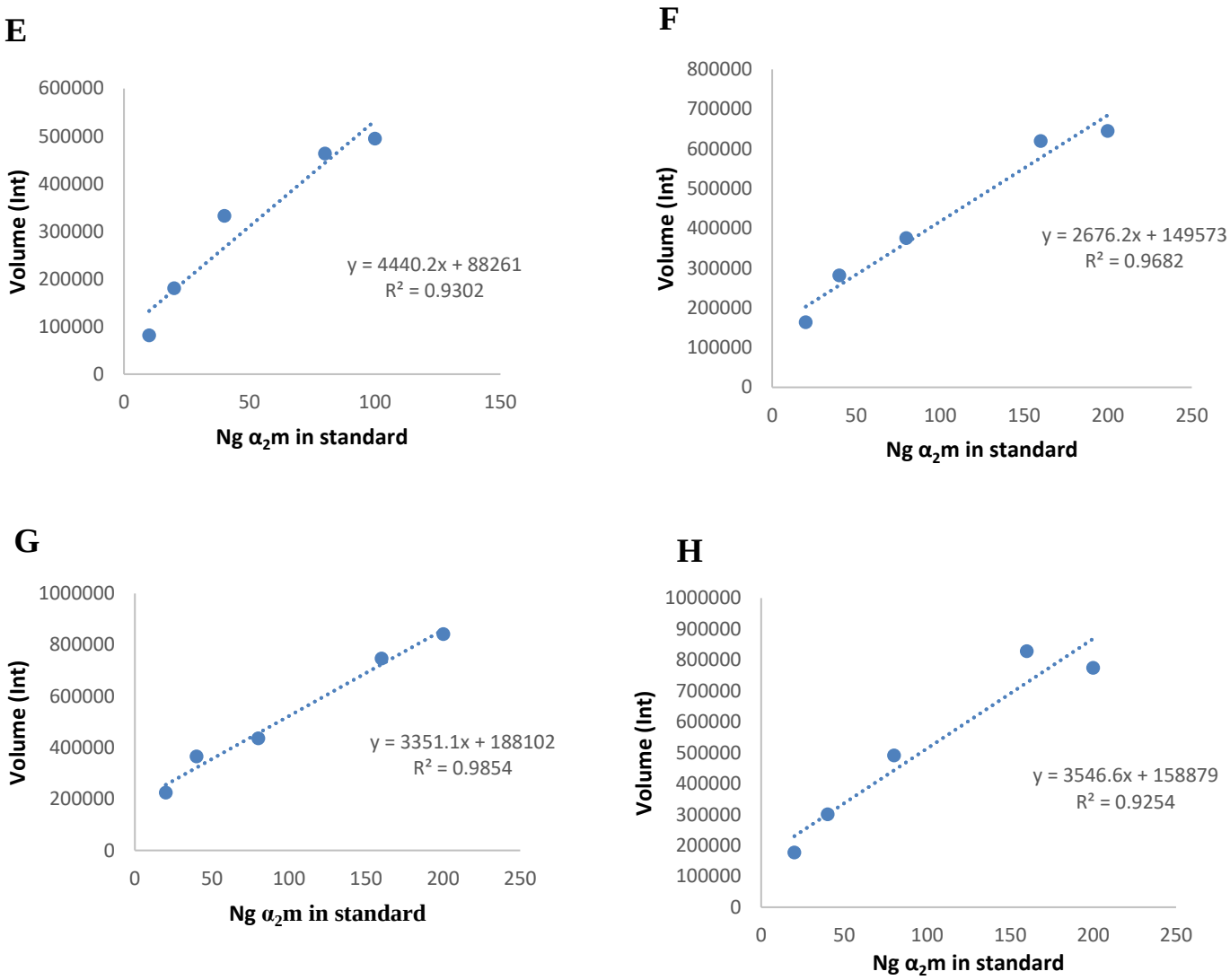

Figure 17 cont'd: (E) Standard curve obtained from densitometry data of standards (10-100ng) in (A). (F) Standard curve obtained from densitometry data of standards (20-200ng) in (B). (G) Standard curve obtained from densitometry data of standards (20-200ng) in (C). (H) Standard curve obtained from densitometry data of standards (20-200ng) in (D). The equation of the line was used to quantify the amount of α_2m in each elution sample.

Sample	Quantity based on densitometry data	Actual quantity (adjusted for total volume in elution)
Elution 1, Tube A	40.46 ng	1.29 µg
Elution 1, Tube B	54.64 ng	1.75 µg
Elution 1, Tube C	8.47 ng	0.27 µg
Elution 1, Tube D	12.36 ng	0.40 µg
Elution 2, Tube A	137.75 ng	8.82 µg
Elution 2, Tube B	176.46 ng	11.29 µg
Elution 2, Tube C	64.63 ng	4.14 µg
Elution 2, Tube D	75.16 ng	4.81 µg
Elution 3, Tube A	225.54 ng	14.42 µg
Elution 3, Tube B	241.9 ng	15.48 µg
Elution 3, Tube C	217.87 ng	13.94 µg
Elution 3, Tube D	166.66 ng	10.67 µg
Elution 4, Tube A	172.6 ng	11.05 µg
Elution 4, Tube B	151.17 ng	9.67 µg
Elution 4, Tube C	131.15 ng	8.39 µg
Elution 4, Tube D	115.17 ng	7.37 µg

Table 3: Using the standard curves from Figure 17 (E) to (H), the quantity of α_2m in each elution fraction obtained during purification was calculated. Quantities were adjusted to represent the elution volume as a whole (instead of representing solely the amount of protein on the gel itself).

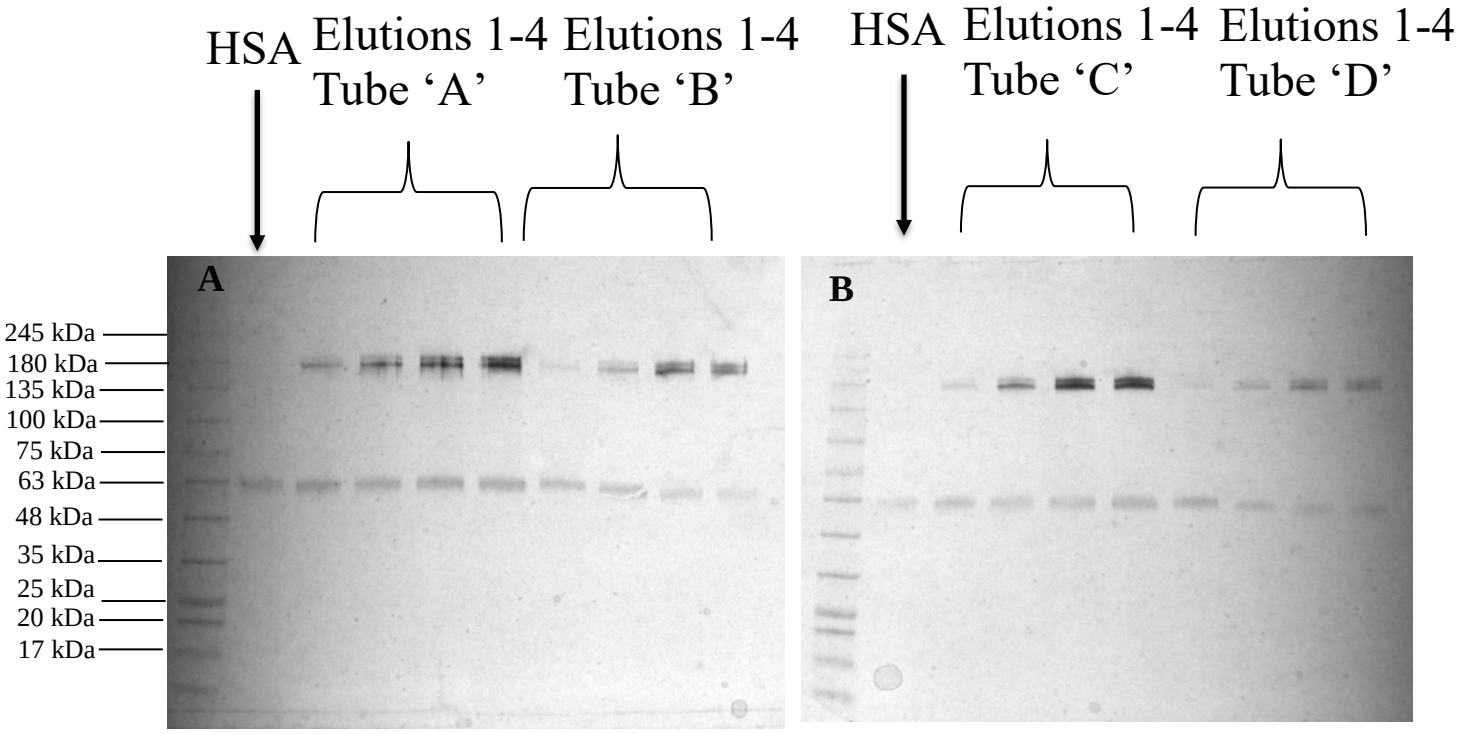

Figure 18: Silver stain of eluted newborn α_2m fractions to verify purity. Elution samples were electrophoresed on 4-15% gradient gels under denaturing conditions. As in the above flow-through/HBS figures, each gel represents elutions from two reaction tubes. In (A), lane 1 represents 0.1 µg HSA and lanes 2-5 represent elutions 1-4 (respectively) from tube 'A'. Lanes 6-9 represent elutions 1-4 (respectively) from tube 'B'. In (B)), lane 1 represents 0.1ug HSA and lanes 2-5 represent elutions 1-4 (respectively) from tube 'C'. Lanes 6-9 represent elutions 1-4 (respectively) from tube 'D'.

3.9 Buffer exchange and concentration of α_2m following elution with glycine-HCl

Immediately following elution of both newborn and adult α_2m from the α_2m antibody cross-linked Protein G beads, elution samples (#1-4 from all tubes) underwent buffer exchange and concentration, as described in the methods. Buffer exchange at this stage was necessary in order to adjust the pH towards neutrality required by PNGaseF. Also, if still present after the PNGaseF reaction, there was a possibility that glycine may later compete with ANDS for conjugation to the terminal GlcNAc of the glycan, thus hindering the fluorescent ANDS labelling required for FACE analysis. Therefore, α_2m samples were buffer exchanged prior to PNGaseF incubation to be in the presence of the 50mM sodium phosphate buffer.

Following the initial buffer exchange in the Amicon Ultra-0.5 devices and prior to the exchanged sample being passed through the Amicon Ultra-2 device (as described in methods), a subsample was taken for western analysis. Obtaining data to quantify the amount of α_2m at this stage in the experiment allowed for improved estimation of protein in the PNGaseF phase of the experiment and beyond. Having previously optimized the percentage yield for both Amicon Ultra-0.5/2 devices (~25% for the 0.5 device and ~95% for the 2 device), it was safe to assume that the amount of protein entering the 2mL device was roughly the same as what would be extracted and present in the downstream FACE processes. In addition, not removing a sample at this stage would allow for the entire volume extracted from the final concentration step to be preserved for use in FACE.

This was done in both newborn and adult purification experiments, and the results are shown in Figure 19. Densitometry data obtained following ImageLab analysis of the western blots allowed for standard curves to be generated for each gel and the amount of α_2m obtained to be calculated (Figure 19 (C) and (D), Table 4). Quantification data was used to calculate the

amount of α_2m in the entire sample volume. These results are shown in Table 4. Results reveal 29.8 µg of adult α_2m and 21.3 µg of newborn α_2m entered the final concentration step. Additionally, this shows a percent yield from the Amicon Ultra-0.5 device to be 25% for adult α_2m and 17% for newborn α_2m.

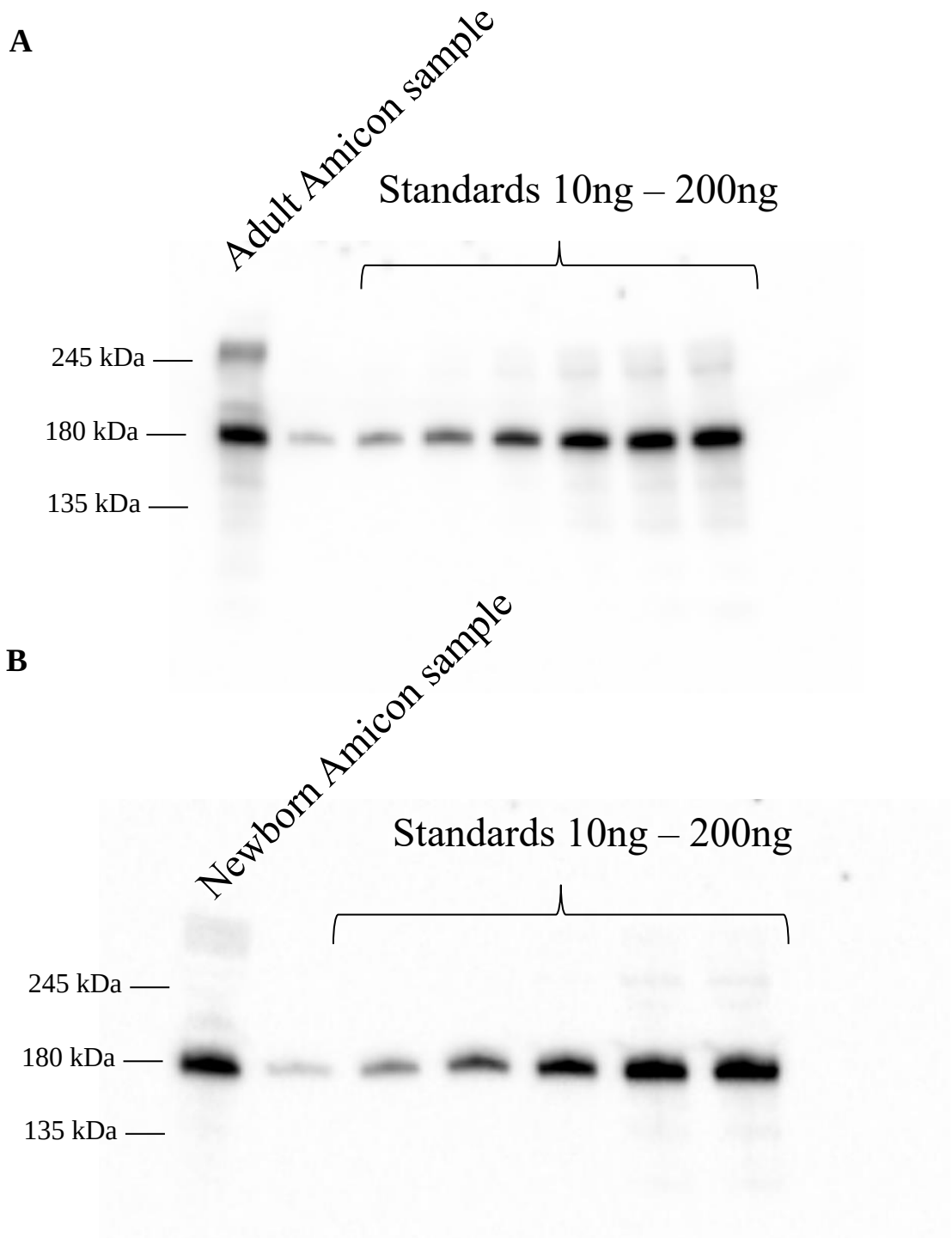

Figure 19: Buffer exchange and concentration of α_2m purified from adult and newborn plasma. Eluted samples in Glycine-HCl underwent buffer exchange. A subsample was taken following exchange from the pooled sample. (A) Western blot of the adult pooled sample, as well as standards ranging from 10ng-200ng. (B) Western blot of the newborn pooled sample, as well as standards ranging from 10ng-200ng. All samples were electrophoresed on 4-15% gradient gels under denaturing conditions prior to western blotting.

C

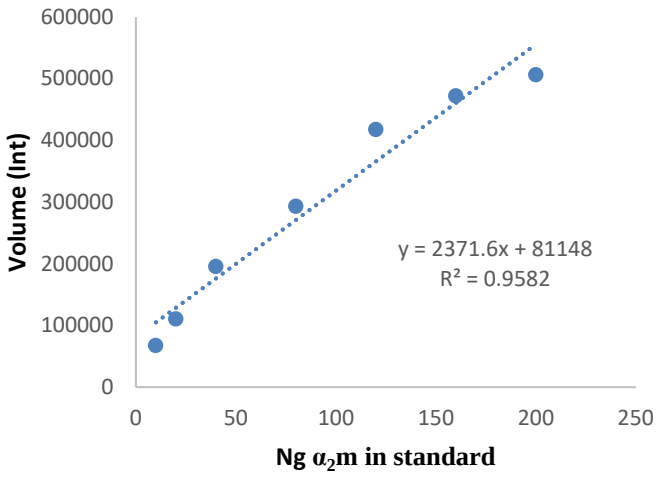

D

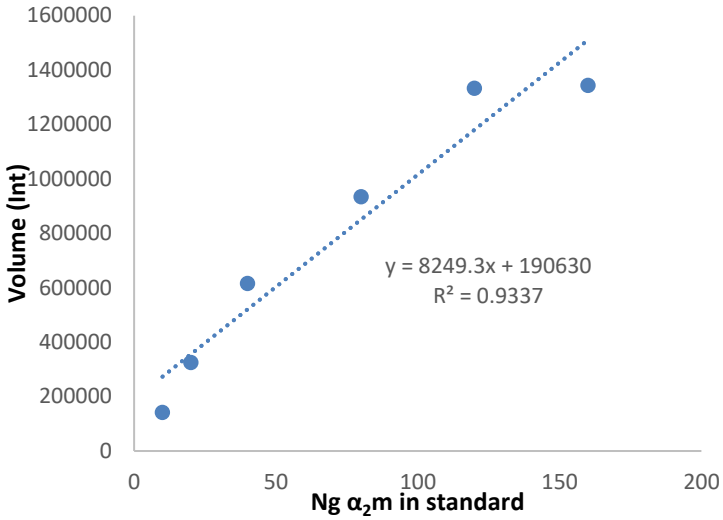

Figure 19 cont'd: (C) Standard curve obtained from densitometry data of standards (10ng-200ng) in (A). (D) Standard curve obtained from densitometry data of standards (10ng-200ng) in (B). The equation of the line was used to quantify the amount of α_2m in each Amicon sample.

Sample	Quantity loaded on the gel based on densitometry data	Actual quantity (adjusted for total volume)
Adult Amicon	150 ng	29.8 µg
Newborn Amicon	113.5 ng	21.3 µg

Table 4: Using the standard curves from Figure 19 (C) and (D), the quantity of α_2m in each buffer exchange sample was calculated. Quantities were adjusted to represent the sample as a whole (instead of representing solely the amount of protein on the gel itself).

3.10 Glycan analysis through FACE of newborn and adult plasma, fetuin and AT

FACE was used to examine glycans from AT, Fetuin, commercial α_2m, and immunoprecipitated newborn and adult α_2m. 25 µg AT, 20 µg Fetuin, 21.3 µg newborn α_2m and 29.8 µg adult α_2m were prepared. Prior to FACE, samples were all denatured and treated with PNGaseF. Results are shown in Figure 20, with change in molecular weight of each band occurring following PNGaseF cleavage of glycans. FACE results are depicted in Figure 21. In the fetuin containing lanes, 2 fluorescent bands are seen. The more intense represents triantennary glycans and the faint band represents a smaller, less branched glycan component that is likely biantennary. In the AT lane, there is a single prominent band representing biantennary glycans. Newborn and adult α_2m both display several bands of varying intensities.

The experiment with both newborn and adult FACE was completed twice. Following conclusion of the second trial, densitometry data was obtained for all fluorescent bands in both newborn and adult lanes of all gels. Analysis was completed as a ratio of intensity between the secondary (second highest intensity peak) and primary (highest intensity peak) peaks on each gel. Data revealed an average secondary:primary band ratio of 0.297 (+/- 0.028) for adult α_2m and 0.557 (+/- 0.060) for newborn α_2m. A t-test of adult vs newborn for data taken from all FACE experiments revealed a p-value of 0.047, indicating that the difference is statistically significant ($p<0.05$). It must be noted that these values were taken from independently purified newborn and adult α_2m, and therefore further experimentation is required to strengthen or weaken this conclusion. Based on these findings, we can conclude that there is a higher proportion of glycans present in the secondary versus the primary band in newborn α_2m. Though it cannot be deduced from FACE what the exact identity of these glycans is, through comparison with glycans from the AT and Fetuin reference standards electrophoresed on each gel, we can

conclude that the primary band seen in both adult and newborn α_2m is likely to be biantennary as it aligns with the AT band previously identified in the literature as fully sialylated biantennary glycans. In addition, the identity of the primary fluorescent band seen in the fetuin lanes has been characterized as triantennary with α (2-3) and α (2-6) linked sialic acid. Therefore, the secondary α_2m band which runs higher in the FACE gel than the primary fetuin band can be labelled as likely a larger and/or more branched species than the triantennary Fetuin glycans.

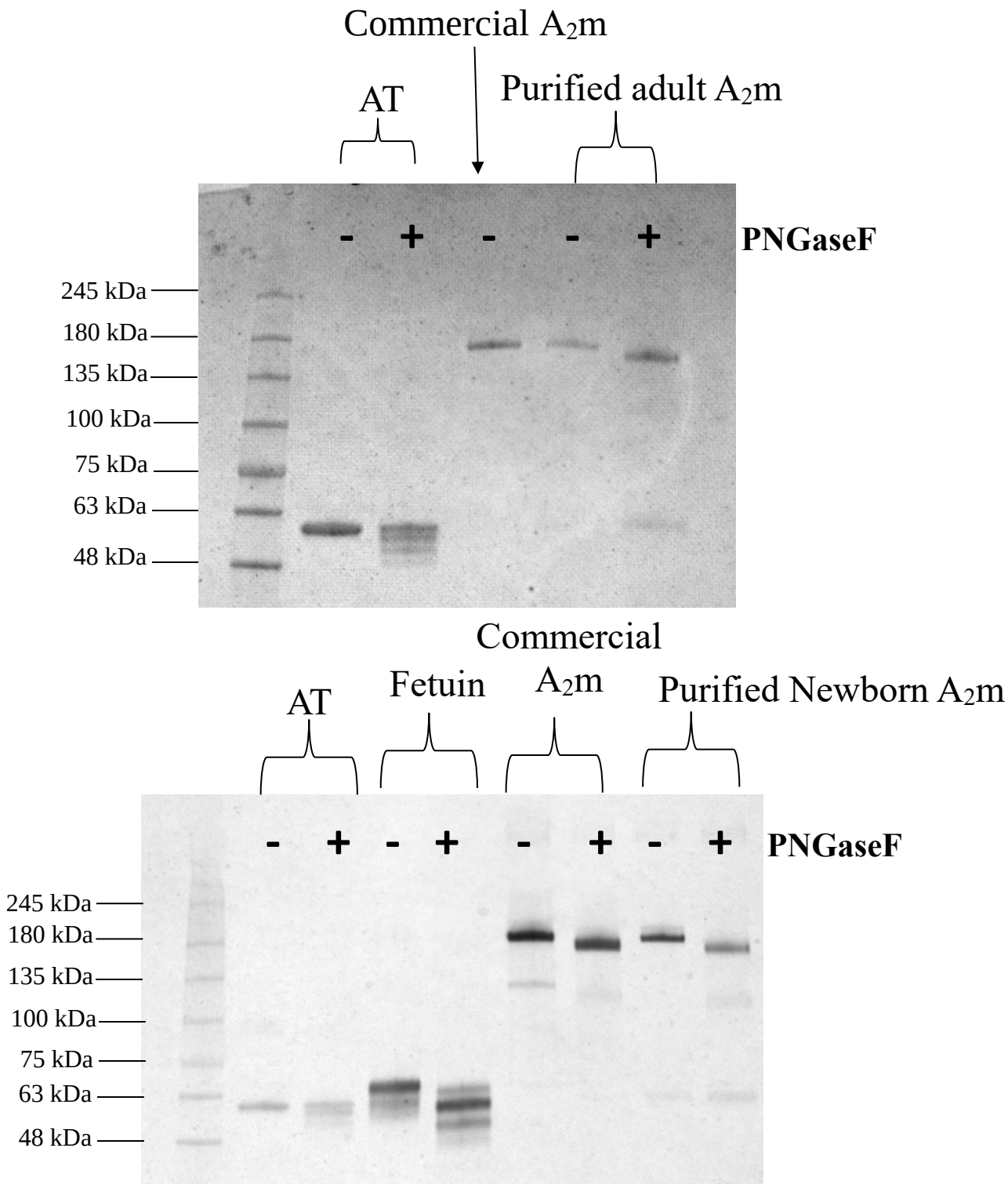

Figure 20: (A) Silver stain of AT, commercial α_2m and adult α_2m +/- exposure to PNGaseF. (B) Silver stain of AT, Fetuin, commercial α_2m and newborn α_2m +/- exposure to PNGaseF. Samples were denatured and either exposed or not exposed to PNGaseF. Following incubation with the enzyme, a subsample was taken and electrophoresed on 4-15% gradient gel. The remainder of the sample was subjected to the FACE protocol.

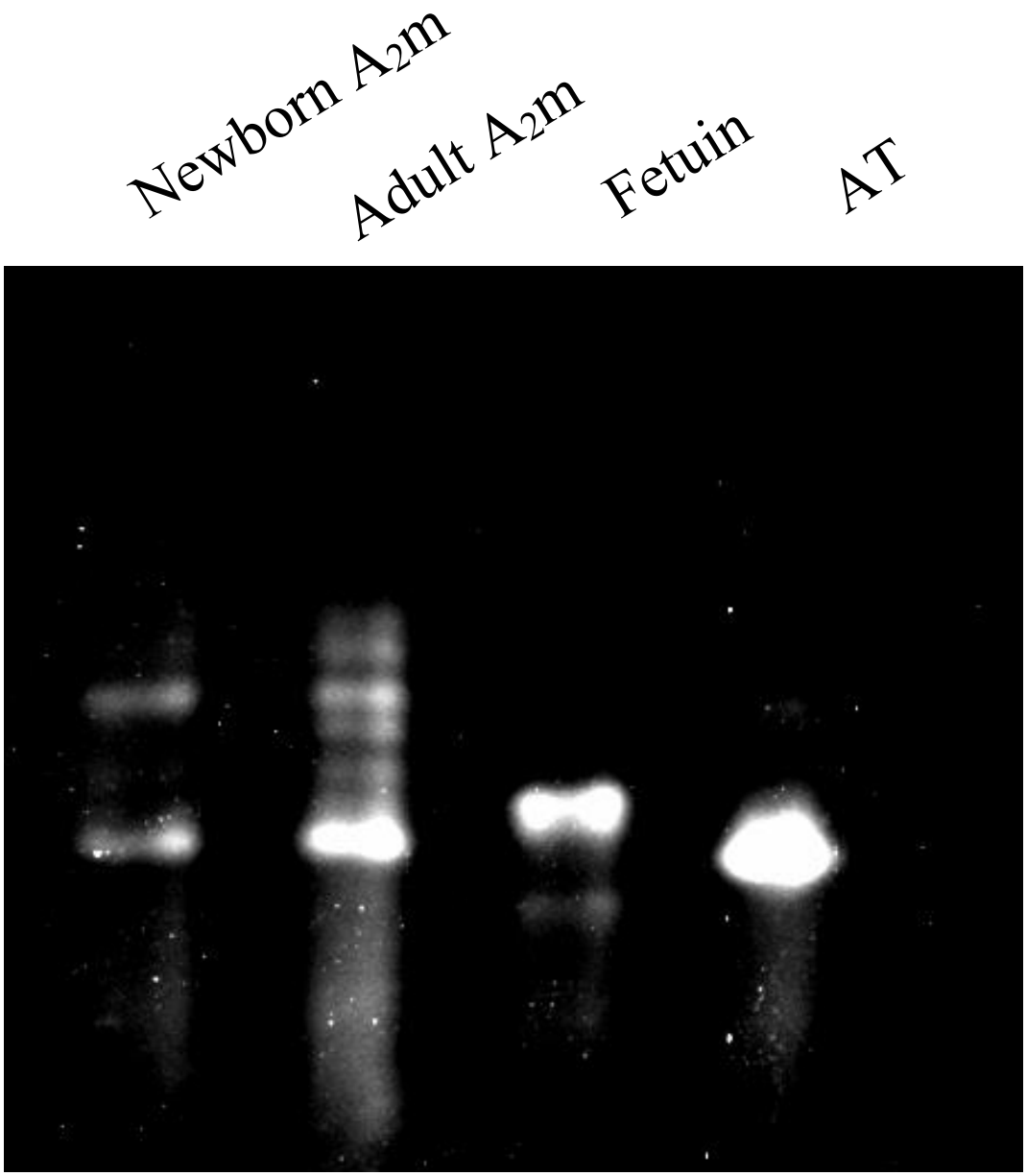

Figure 21: FACE results of Fetuin, AT, newborn α_2m and adult α_2m. Glycans were cleaved with PNGaseF, isolated, labelled with ANDS and electrophoresed on a 20% non-denaturing gel. (A) Lane 1 represents the glycan profile of 21.3 µg newborn α_2m, Lane 2 represents the glycan profile of 29.8 µg adult α_2m, Lane 3 represents the glycan profile of 20 µg Fetuin and Lane 4 represents the glycan profile of 25 µg AT.

3.11 Purification and FACE of commercial α_2m to check for methodological bias

In order to ensure that the purification method was not leading to a preferential selection of certain glycoforms in both newborn and adult α_2m, a commercially prepared α_2m sample was taken through the entire purification protocol and matched with a commercial sample that had not been taken through the purification prior to both samples being electrophoresed on FACE gels.

The experiment to purify the commercial α_2m sample was carried out in the same way as was the newborn and adult purification experiments described in the above methods and results. In short, the experiment began with binding and cross-linking of GAA2M polyclonal antibody to a fresh sample of Protein G beads, in four separate Eppendorf tubes. Once the antibody binding was complete and it was verified that the antibody was irreversibly bound in all tubes by silver stain, 2mg commercial α_2m was incubated overnight with the anti- α_2m beads. Following overnight incubation, the beads were washed with HBS and eluted with 100mM Glycine-Cl pH 2.8. Figure 22 shows western blots and quantification for each elution fraction. It was found that 785.74 µg of α_2m was eluted from the beads in this experiment. This represents a 39.29% yield, as 2mg α_2m went into the initial overnight incubation of commercial α_2m with the anti- α_2m beads. Notably, this is a much higher yield than had been previously obtained in the newborn and adult trials. This information indicated that there may be some effect of pH or other variable occurring in newborn and adult plasma that impacts the ability of α_2m to be eluted from the beads with as much ease as was seen in the commercial sample. There was approximately 6.5 times as much commercial α_2m captured and eluted from the beads than in the previous newborn and adult trials.

Once eluted, samples underwent buffer exchange and concentration in the 0.5- and 2-Amicon Ultra devices, as previously described. Results showing the amount of protein present prior to 2mL Amicon concentration are shown in Figure 23. It was found that there was 258.32 µg α_2m present prior to the final concentration step, indicating a percent yield from the 0.5-Amicon Ultra device of 33%. This was also a greater percent yield from this stage of the experiment than we had previously seen with the newborn and adult trials. Though it is unclear what the exact reason was for protein loss during the buffer exchange portion of the experiment, it can be hypothesized that it is related to the properties of a pure sample vs a plasma sample.

Finally, samples were treated with PNGaseF (Figure 24), ethanol precipitated and dried, prior to being incubated overnight with ANDS and sodium cyanoborohydride in preparation for FACE. Figure 25 displays the FACE image captured at the end of the experiment.

These results, shown in Figure 25, show that the purification-FACE protocol did not select for any specific α_2m isoforms. By re-purifying commercial α_2m and comparing it to an identical sample that had not seen this particular purification process, any possibility of bias could have been detected. Analysis showed identical patterning in terms of band number in each of the two samples, despite a slight difference in the amount of α_2m (and thus, glycans) on the FACE gel. In addition, the ratio of the secondary:primary band was found to be the same, indicated that the overall amounts of each band is the same in the two samples. It remains possible that there is some glycoform selection bias occurring based on the increased recovery of α_2m in this experiment. However, the fact that the recovery of α_2m in the previous newborn and adult trials were nearly identical, strongly suggests that it is likely that no significant bias occurred in purification of newborn α_2m relative to purification of adult α_2m.

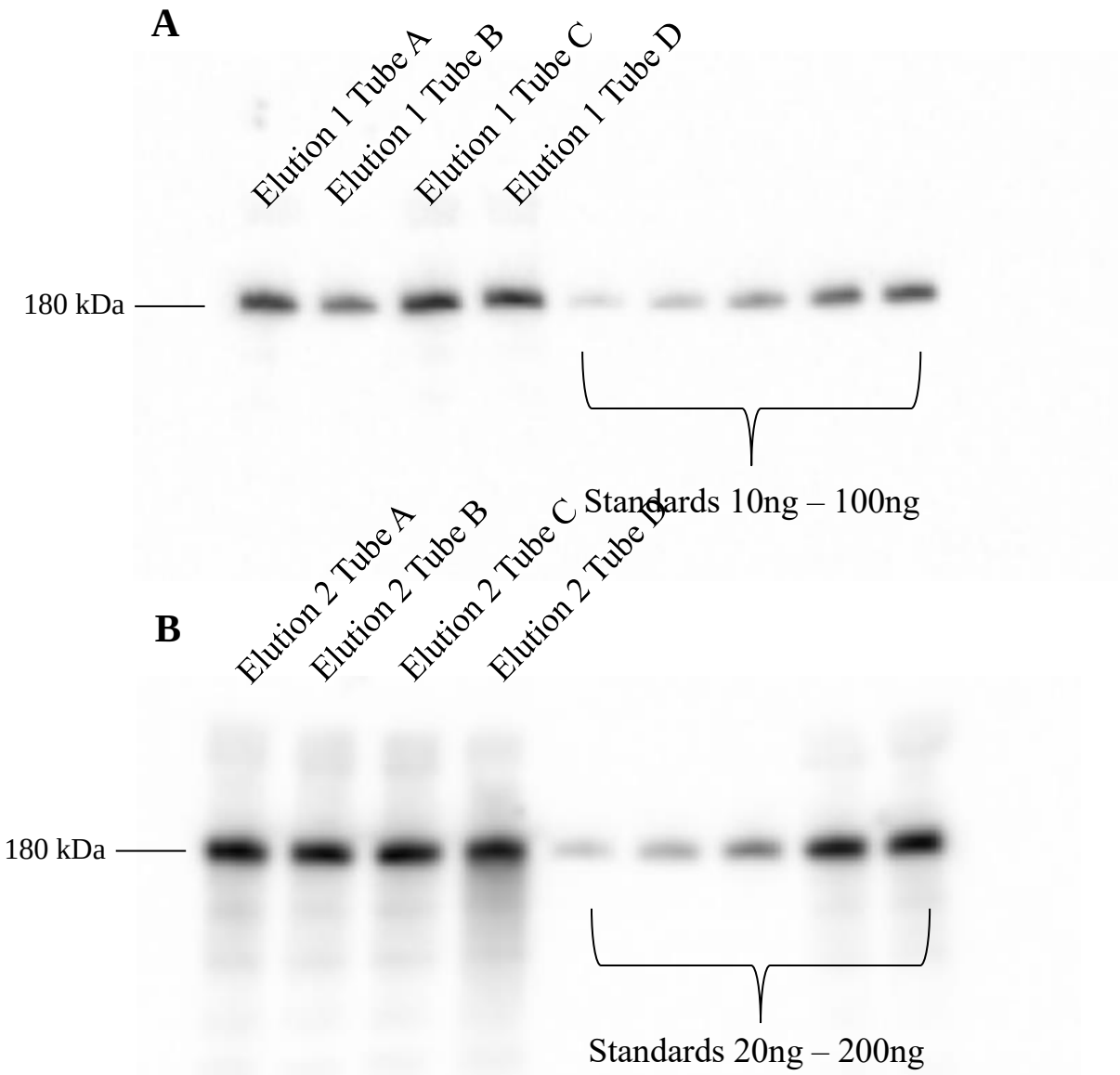

Figure 22: Immunoprecipitation of commercial α_2m. Commercial α_2m was incubated overnight with antibody Protein G beads at 4^0C. Beads were washed with HBS prior to being eluted with 100mM glycine-HCl pH 2.8. (A) First elution sample from each incubation tube as well as standards ranging from 10-100ng. (B) Second elution sample from each incubation tube as well as standards ranging from 20-200ng. All α_2m samples were electrophoresed on 4-15% gradient gels under denaturing conditions followed by western blotting for the detection of α_2m.

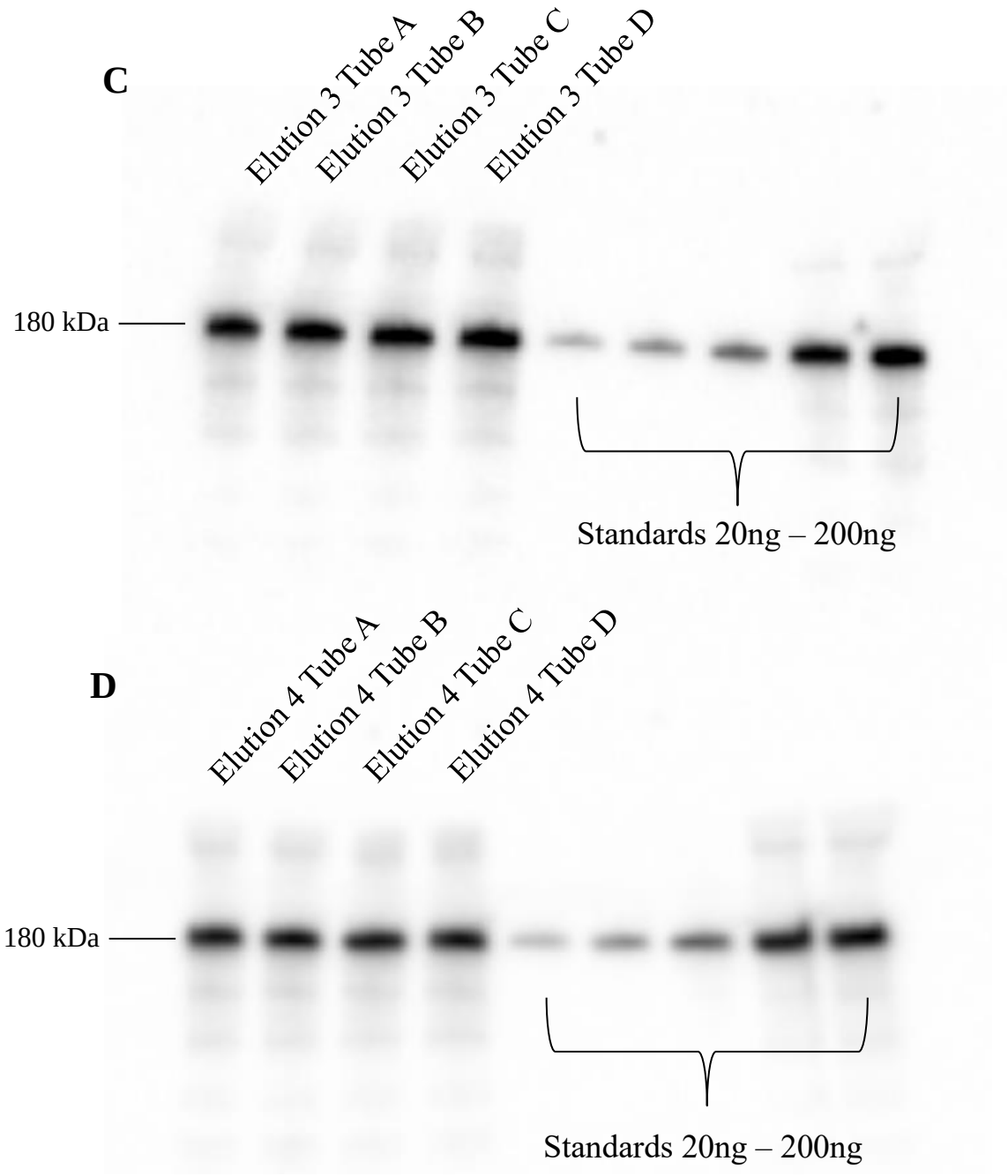

Figure 22 cont'd: (C) Third elution sample from each incubation tube as well as standards ranging from 20-200ng. (D) Fourth elution sample from each incubation tube as well as standards ranging from 20-200ng. All α_2m samples were electrophoresed on 4-15% gradient gels under denaturing conditions followed by western blotting for the detection of α_2m.

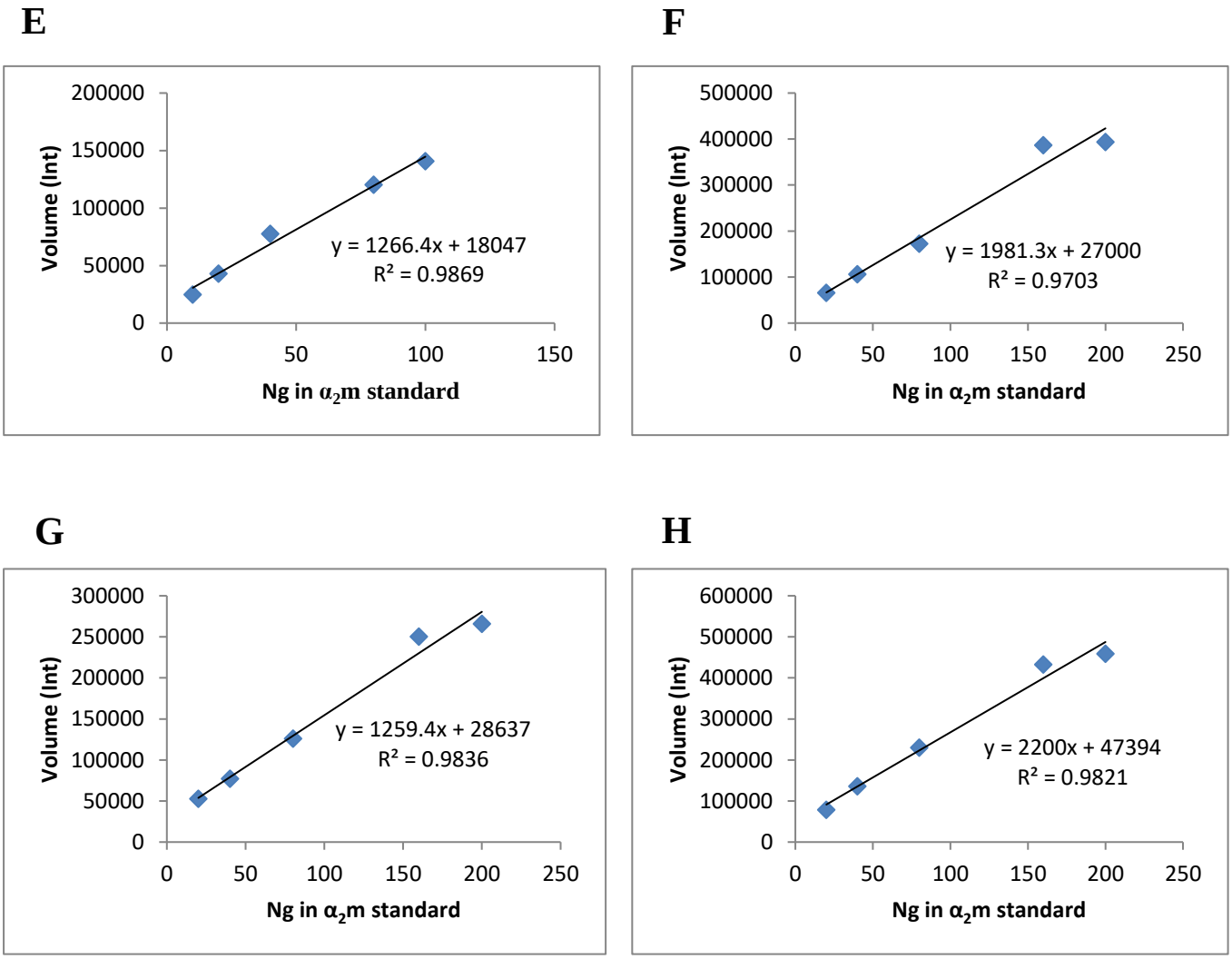

Figure 22 cont'd: (E) Standard curve obtained from densitometry data of standards (10-100ng) in (A). (F) Standard curve obtained from densitometry data of standards (20-200ng) in (B). (G) Standard curve obtained from densitometry data of standards (20-200ng) in (C). (H) Standard curve obtained from densitometry data of standards (20-200ng) in (D). The equation of the line was used to quantify the amount of α_2m in each elution sample.

Sample	Quantity based on densitometry data	Actual quantity (adjusted for total volume in elution)
Elution 1, Tube A	137.61 ng	22.7 µg
Elution 1, Tube B	81.46 ng	13.4 µg
Elution 1, Tube C	153.01 ng	25.3 µg
Elution 1, Tube D	134.93 ng	22.3 µg
Elution 2, Tube A	175.98 ng	58.1 µg
Elution 2, Tube B	174.12 ng	57.5 µg
Elution 2, Tube C	182.63 ng	60.3 µg
Elution 2, Tube D	201.00 ng	66.3 µg
Elution 3, Tube A	174.68 ng	57.6 µg
Elution 3, Tube B	208.82 ng	68.9 µg
Elution 3, Tube C	223.06 ng	73.6 µg
Elution 3, Tube D	222.59 ng	73.4 µg
Elution 4, Tube A	137.36 ng	45.3 µg
Elution 4, Tube B	139.07 ng	45.9 µg
Elution 4, Tube C	146.58 ng	48.4 µg
Elution 4, Tube D	141.55 ng	46.7 µg

Table 5: Using the standard curves from Figure 22 (E) to (H), the quantity of α_2m in each elution fraction obtained during purification was calculated. Quantities were adjusted to represent the elution volume as a whole (instead of representing solely the amount of protein on the gel itself).

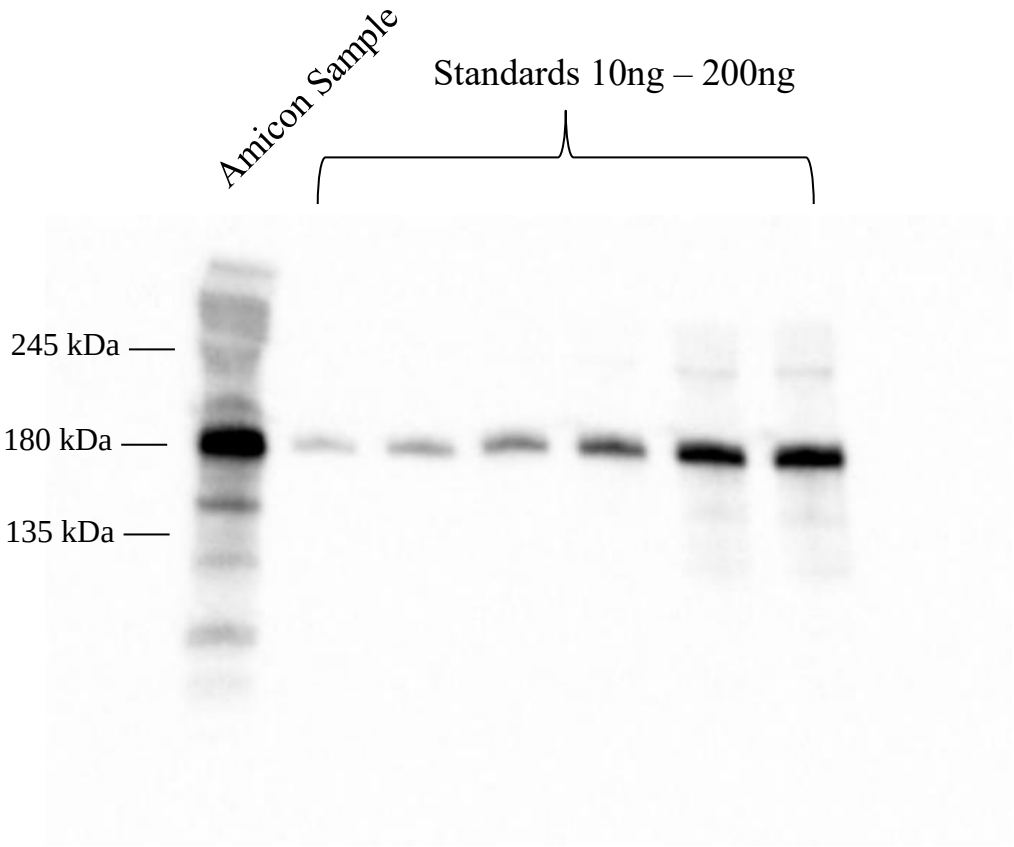

Figure 23: Buffer exchange and concentration of α_2m purified from a commercial sample. Following elution of α_2m from the antibody Protein G beads, samples underwent buffer exchange to replace the 100mM glycine-HCl with 50mM sodium phosphate. Prior to final concentration in the Amicon Ultra-2 device, a subsample was taken for western analysis. Standards ranging from 10-200ng were included to allow for quantification of the concentrated α_2m. All samples were electrophoresed on 4-15% gradient gels under denaturing conditions prior to western blotting.

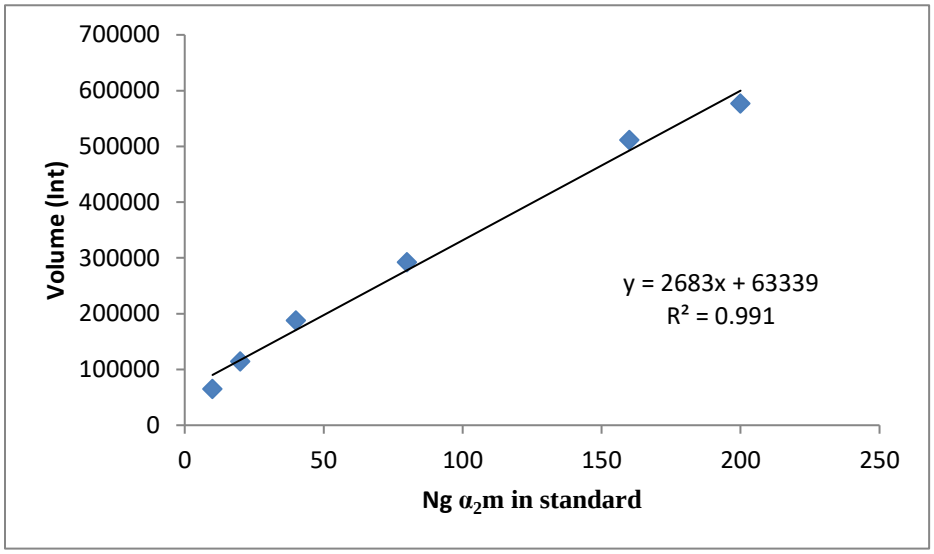

Figure 23 cont'd: Using the densitometry data of the western blot shown above, a standard curve was generated.

Sample	Quantity based on densitometry data	Actual quantity (adjusted for total volume)
Commercial Amicon	234.83 ng	258.32 µg

Table 6: The quantity of commercial α_2m in the buffer exchange sample was calculated and adjusted to represent the sample as a whole (instead of representing solely the amount of protein on the gel itself).

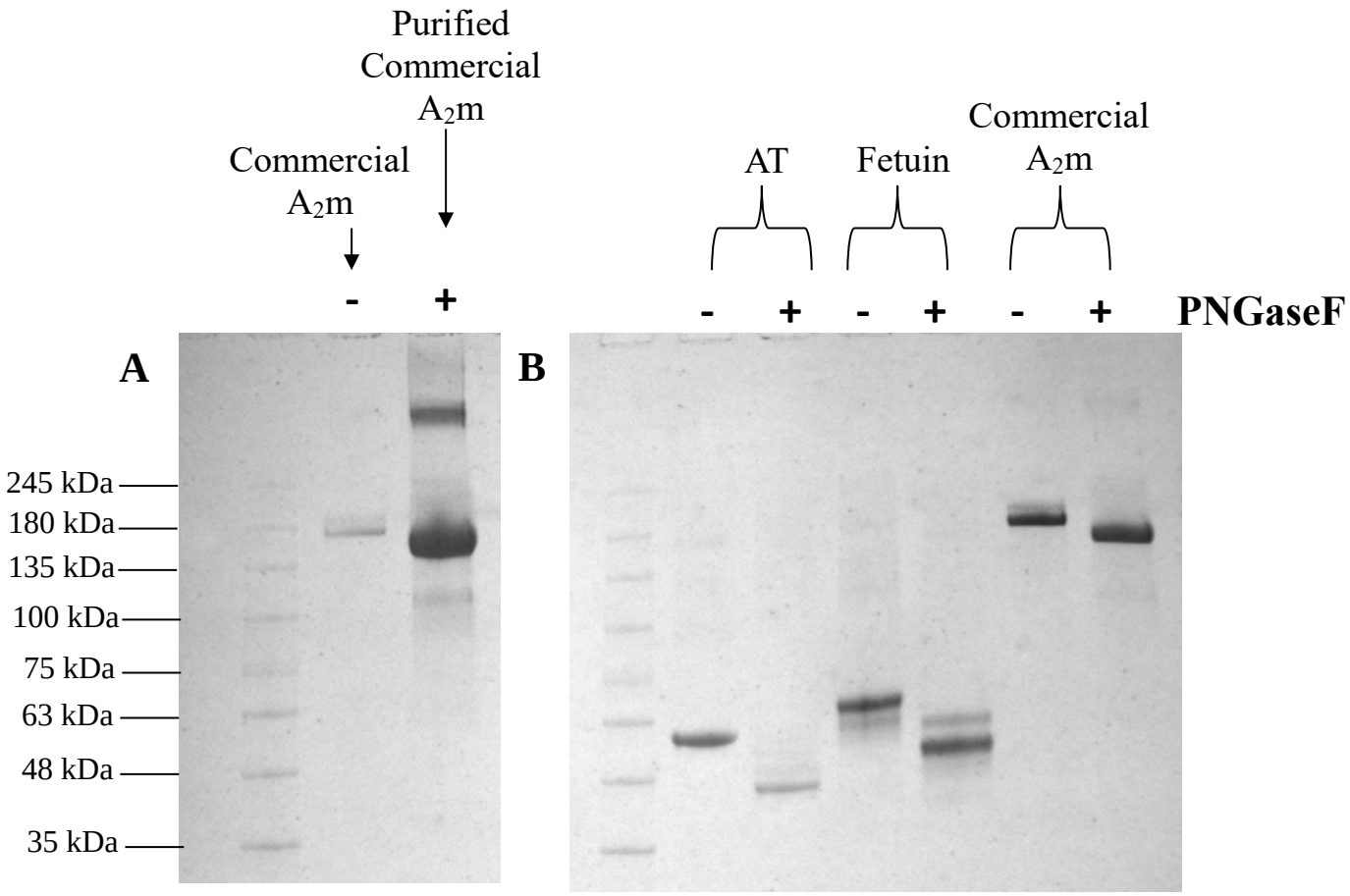

Figure 24: (A) Silver stain of commercial α_2m - exposure to PNGaseF and re-purified commercial α_2m + exposure to PNGaseF. (B) Silver stain of AT, Fetuin and commercial α_2m +/- exposure to PNGaseF. Samples were denatured and either exposed or unexposed to PNGaseF. Following 16 hour incubation with the enzyme, a subsample was taken and electrophoresed on 4-15% gradient gel. The remainder of the sample was subjected to the FACE protocol, described in methods.

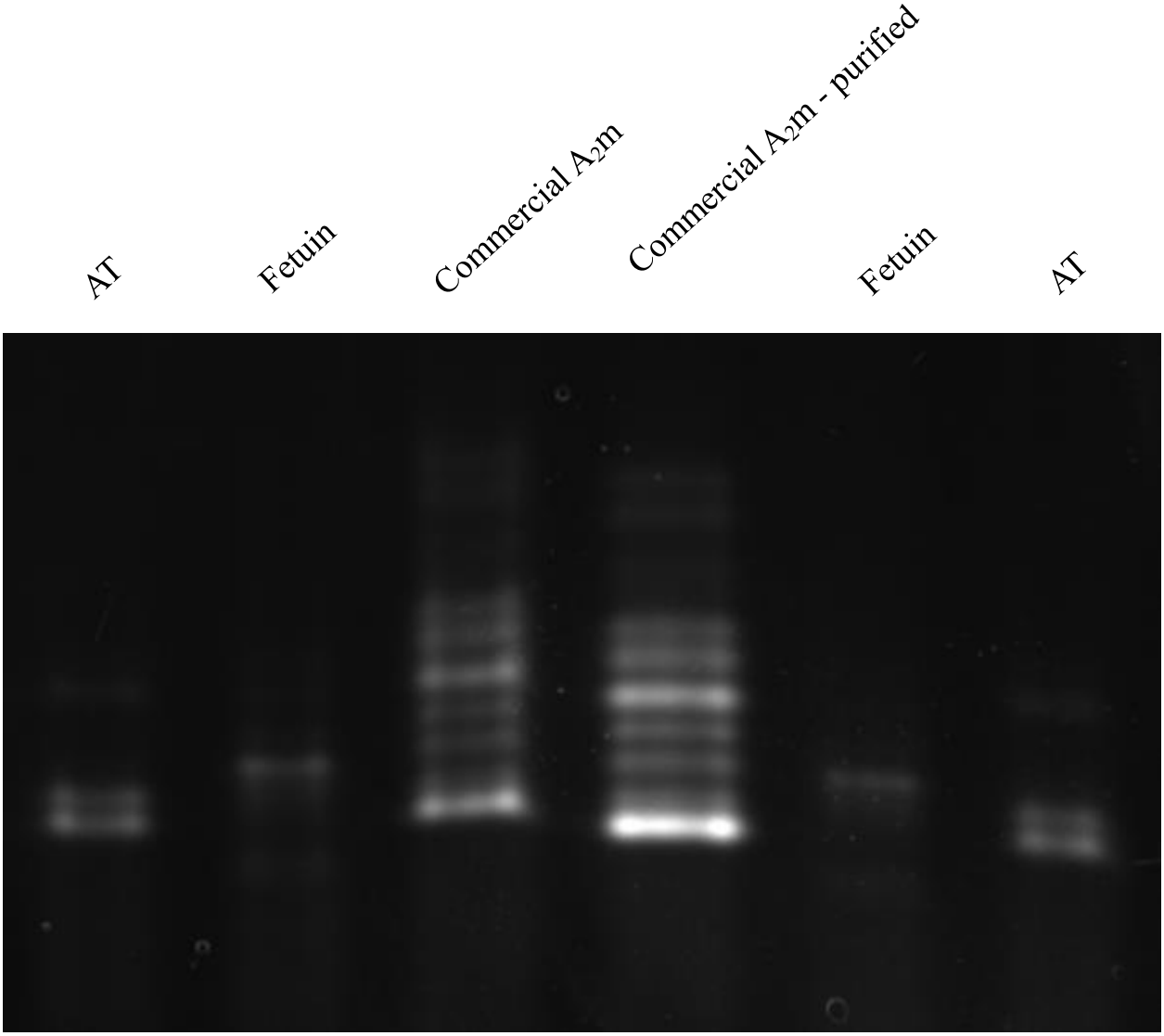

Figure 25: FACE results of Fetuin, AT, commercial α_2m and re-purified commercial α_2m. Glycans were cleaved with PNGaseF, isolated, labelled with ANDS and electrophoresed on a 20% non-denaturing gel. (A) Lane 1 represents the glycan profile of 25 µg AT. Lane 2 represent glycan profile of 20 µg Fetuin, Lane 3 represents the glycan profile of 100 µg commercial α_2m, Lane 4 represents the glycan profile of 250 µg re-purified commercial α_2m, Lane 5 represents the glycan profile of 20 µg Fetuin and Lane 6 represents the glycan profile of 25 µg AT.

4 DISCUSSION

This study began by evaluating the glycosylation of α_2m in newborn and adult plasma samples. In order to conserve the supply of plasma, all methods were first optimized in a system using commercial α_2m. Once methods to be used in plasma were decided upon and prepared, the process of evaluating glycosylation of newborn and adult α_2m in plasma began. Initially, macroheterogeneity was examined by using PNGaseF to cleave N-linked glycans from newborn and adult α_2m in plasma. Although there was a slight trend towards a greater change in molecular weight migration for newborn α_2m on SDS PAGE following PNGaseF treatment, there was no statistically significant difference in the overall molecular weight due to loss of the N-linked glycans attached to newborn and adult α_2m. It is possible that more sensitive techniques may be required to show finer differences in glycoforms between newborn and adult α_2m, given the difficulty in separating high molecular weight species that differ by 1 – 2 kD electrophoretically. Also, further investigation is required to determine the specific sites of glycosylation of newborn and adult α_2m, as we cannot make any conclusions about the overall macroheterogeneity between newborn and adult α_2m from these results. Once this information was obtained regarding the total N-linked glycan content of newborn and adult α_2m, we decided to proceed with investigations towards microheterogeneity in the two proteins. Neuraminidase was used to cleave terminal sialic acid residues off both newborn and adult α_2m. Analysis by western blotting showed a statistically significant difference in the overall change in migration on non-denaturing PAGE following sialic acid cleavage. Newborn α_2m consistently had a greater change in migration following neuraminidase exposure, thus indicating a higher proportion of sialic acids attached on newborn α_2m in comparison to adult.

To complement the sialic acid results, we used agarose-bound Ricinus Communis to investigate the terminal galactose residues on both newborn and adult α_2m. Results from these experiments showed a trend towards newborn α_2m exhibiting a higher percentage of protein bound to the RCA_{120}, however it was not statistically significant, indicating no significant difference in the amount of terminal galactose residues between the two proteins. In addition to binding information, the strength of bond to RCA_{120} was examined using increasing concentrations of galactose for elution. Once more, although there was a trend towards elution of more newborn than adult α_2m as galactose concentration increased, these results showed no statistically significant difference in the elution profile of newborn and adult α_2m, indicating a similar binding strength from terminal galactose residues in the molecules.

In an attempt to develop a more refined assessment of any potential glycoform differences, 2D gel electrophoresis was used to examine the various α_2m species in a commercial α_2m sample, followed by testing of newborn and adult plasma. In the commercial α_2m gel, a long, prominent band is seen as well as several other lower molecular weight species. Lowering the protein load on the gel (not shown) did not have a great deal of impact on this pattern, and the main 180 kDa band remained very dark. A similar pattern of lower molecular weight species is seen in the newborn sample and does not occur in the adult plasma sample. In the newborn sample, there remains a prominent band at 180 kDa, as well as similar lower molecular weight bands that were seen in the previous commercial α_2m gel. However, the prominent band is better resolved to show specific isoforms in varying intensities. Interestingly, the newborn α_2m seemed to span over a lower pI range (about 5.4 – 6.0) than that for the corresponding adult intact α_2m (about 5.8 – 6.2). This lower pI range for cord α_2m is consistent with there being more sialic acid per α_2m molecule on the average. Similar to the commercial α_2m gel, the lower molecular weight

species in newborn α_2m range in size from approximately 50 kDa to 120 kDa. In the adult gel, these lower molecular weight species are not seen. Though there are some faint bands that appear around 70 kDa and 135 kDa, it is not possible to distinguish them as their intensities are faint in comparison to the main α_2m band. Also of note in the newborn and adult comparison is that the separation of discrete subforms seen in the main α_2m band in newborn is not observed in the adult sample. Instead, the adult α_2m band looks more like the one seen in commercial; thick, oval in shape and very dark. To attempt to explain the appearance of low molecular weight species in newborn but not adult samples, we tested the buffer conditions used in 2D gel electrophoresis in a 1D system. It is known that degradation of α_2m occurs upon heating in SDS sample buffer containing β-ME. It is also known that this effect is not seen as severely in an identical sample that was not heated. Therefore, these two conditions were used as controls in the buffer testing experiment. Despite incorporating all possible buffer conditions, the newborn-specific degradation was not observed on 1D electrophoresis. The newborn and adult sample that was left in rehydration buffer at room temperature for 18 hours did exhibit some degradation in both plasmas, indicating that the buffer itself may lead to eventual degradation in both newborn and adult α_2m. Thus, appearance of low molecular weight bands in newborn but not adult α_2m seems to be more related to inherent differences within the starting species in the 2 plasmas. One potential option is that some of these α_2m fragment species pre-exist within the newborn but not adult plasma and are only separated by molecular weight when other molecules in the newborn plasma are separated during isoelectric focusing phase. Alternatively, these α_2m fragments may be generated in newborn (but not adult) samples during separation of species by the first dimension pH gradient. This is a feasible explanation when considering earlier neuraminidase results. Since newborn α_2m contains a higher amount of sialic acid, there will be a greater

presence on the glycan branch termini. The negative charge associated with sialic acid may be interacting with the amide regions of the peptide bonds to stabilize the conformation of the molecule. If this is the case, it is reasonable to consider that upon exposure to the pH gradient, protonation of the sialic acid may cause the peptide to become more labile and thus break down more freely than it would without the increased sialylation, such as in adult α_2m. To further consider this, additional 2D electrophoresis experiments with newborn and adult α_2m should be carried out. Prior to the 2D process, both plasmas should be treated with neuraminidase to cleave all sialic acid. If the lower molecular weight species seen in newborn α_2m are in fact a result of sialic acid presence, this effect should either be eliminated from the newborn plasma result due to protein stability, or enhanced due to an even further reduction in protein stability without sialic acid present.

To evaluate the carbohydrate moieties of newborn and adult α_2m specifically, we proceeded to use immunoprecipitation to purify α_2m from both plasmas for use in fluorescence assisted carbohydrate electrophoresis (FACE). Beginning with the purification, human IgG was depleted from adult plasma using agarose-bound Protein G beads. This step is necessary in order to get rid of IgG as it is an abundant protein which could also bind to Protein G and contaminate future purified product. In addition, polyclonal antibody specific to α_2m was bound to fresh Protein G beads and cross-linked to ensure the binding was irreversible. Employing 0.1M ethanolamine as a blocking buffer prevented any excess cross-linker sites not covalently bound by antibody from reacting later on with proteins in plasma. Without this critical step, anything with an affinity for Protein G or that is reactive with a non-blocked cross linking agent could contaminate the purified product or be lost by permanent binding to the beads, respectively. Lastly, we extracted α_2m from newborn and adult plasma. To accomplish this, plasma pre-

cleared of IgG was mixed with antibody-linked beads and allowed to incubate overnight. A_2m was then eluted from the beads and shown to be of high purity based on silver stained gel results. Of note, the silver stain results did reveal a band of ~63 kDa in all elution fractions. By including a pure sample of HSA on each gel, we were able to confirm the identity of the contaminant. Although having albumin present in the purified product impacts overall purity, since albumin is known to not contain any sites of glycosylation, its presence would not affect FACE results. Moreover, we further confirmed the expected benign nature of this species where, although the α_2m band shifted dramatically as usual, treatment with PNGase F did not cause any change in molecular weight of the putative albumin band indicating that no glycans were present (see Figure 20B lanes containing newborn α_2m with or without pretreatment by PNGase F). Therefore, we decided to proceed with the protocol despite this minor contamination. Overall, the results from this purification protocol demonstrate a low α_2m yield (<10%) and therefore we are retrieving a minimal amount compared to what is being put into the system. This may be explained by several sources of error that we have encountered during the optimization of this protocol. The most prominent source of error was loss of beads throughout the steps of purification. In addition to increasing the centrifuge speed, we exclusively used gel loading pipette tips when working with the Protein G beads, after finding success with this in previous agarose-bound RCA_{120} experiments. Regardless, it is still easy to visualize beads being lost in the tips and supernatants, as well as becoming stuck up the sides of the centrifuge tubes. One option for future work is to carry out binding and elution on small columns of anti- α_2m beads.

Initially, there was speculation that perhaps the low pH of the elution buffer (100mM glycine-HCl pH 2.8) was causing some loss of protein in the purification method, and a slight loss was qualitatively confirmed when comparing α_2m in low pH glycine buffer as well as HBS.

A possible explanation for this could be that some aggregation of protein is occurring in the low pH buffer. In an attempt to pursue this further, several different methods were attempted. First, we attempted to neutralize the low pH incurred with use of glycine-HCl through addition of 1M Tris to the elution fractions. This alteration saw no improvement in the overall yield of α_2m. In addition, we attempted to use 0.02M phosphate (pH 2.8) as an elutant. Immediately following supernatant removal, 0.4M phosphate buffer pH 8.85 was added to neutralize the pH. The optimal pH of the 0.4M phosphate buffer was determined by titration of the 2 buffers until a near neutral pH was obtained. In addition to the attempt to reduce protein loss that seemed to occur with the low pH buffer, using a phosphate buffer instead of glycine would also be beneficial for future FACE experiments when considering the reaction with ANDS. Unfortunately, these alterations did not provide any improvement in yield of the purification procedure. Finally, we tried to use SDS as an elutant to remove α_2m from the Protein G beads. This method did provide an increase in yield; however, the presence of SDS in the eluted product led to other issues. The increased SDS concentration that occurred as a result of the change in elution buffer caused a substantial amount of smearing on the FACE gels. In addition, the micelles formed by SDS in solution made it difficult to remove the SDS (by solvent precipitation, molecular filtration, etc.) prior to proceeding with the FACE method following purification.

Given the above information, we decided to return to the glycine-HCl method of purification. The glycine had to be removed from the elutions prior to FACE and therefore we optimized a method of buffer exchange to be used. Initially, we tested different protein precipitation methods with both Ethanol and Acetone, measured the precipitated pellets and decided that the Ethanol procedure previously used in our lab was ideal for use. In addition, several methods of dialysis, desalting columns and Centricon concentrating columns were tested

in an attempt to exchange the glycine in the eluted samples with phosphate buffer (compatible with FACE). However, all the methods listed above displayed low yield and therefore were deemed problematic for our purposes. Since the purification itself was consistently producing a less than 10% yield of α_2m, it was critical that the buffer exchange process conserved as much protein as possible to not incur additional large-scale losses. Finally, we tested Amicon Ultra 0.5mL devices for the purpose of buffer exchange. Following optimization, it was found that the Amicon Ultra 0.5mL device produced a reliable 25% yield. In addition, we would be able to use a larger device (2mL max capacity) for final concentration, and it displayed a much higher yield of >90%. Multiple repeats deemed these yields reliable and therefore, these devices were used in the remaining experiments.

Once the purified samples had been exchanged and concentrated so that the final volume of pure α_2m product was less than 100 µL, we were able to proceed with FACE. Following overnight incubation of ANDS + $NaBH_3CN$ with the glycan products from both newborn and adult plasma's α_2m, as well as with glycans from AT and fetuin, samples were electrophoresed on native PAGE and imaged for fluorescent banding. In total, 5 samples of α_2m purified from adult plasma were taken for FACE glycan analysis, as well as 2 samples of α_2m purified from newborn plasma (both electrophoresed simultaneously with adult α_2m products). Results show that there is a difference between the glycan band profile seen in newborn and adult α_2m purified from plasma. The purified adult sample appears to show the same banding pattern as a commercial α_2m sample, as expected. The newborn sample shows lower numbers of bands (~4, vs 6-8 in adult), as well as variation in the relative band intensity. To quantify this with the current data, we decided to analyze the highest (primary) and second highest (secondary) intensity bands in both newborn and adult. Visual observations of the results lead us to believe

that there may be a difference between the bands, and therefore we proceeded to gather densitometry data for analysis. The newborn samples consistently showed a higher secondary: primary band ratio. We can conclude from this information that whichever specific glycans are contributing to the two bands, there is significantly more of the slower migrating band in the newborn sample than in the adult. Though we are unable to determine the identity of the glycans in each band from FACE, we can make likely deductions regarding their size. AT's prominent fluorescent band has been characterized as fully sialylated biantennary glycans. Therefore, since the highest intensity band in both newborn and adult move to the same position as the AT band, we can assume this band to be composed of typical biantennary glycans. In addition, the highest intensity band in the fetuin lane has been characterized as triantennary with α (2-3) and α (2-6) linked sialic acids. Though we are unable to obtain specific information about sites of sialylation, the secondary band in both newborn and adult α_2m does not move as far into the gel as the fetuin band. This indicates that the band of second highest intensity in newborn and adult α_2m is larger (more branched) and/or less negatively charged than the primary fetuin band. The 2D electrophoretic experiments did show the 180 kDa bands for newborn plasma α_2m to have a pI ranging towards the more acidic range compared to that for adult, which complements the finding that newborn α_2m contains more sialic acid residues per molecule. It would therefore seem likely that the newborn contains proportionately more of a glycan band that is migrating more slowly, not because it has less negative charge but because it is a larger, more branched triantennary or tetrantennary structure.

To verify that the purification method was not selecting for specific glycoforms, a commercial α_2m sample was taken through our Protein G purification method, matched with a commercial α_2m sample that had not been subjected to the Protein G method, and the

corresponding derivatized glycans electrophoresed on FACE. Results show a banding pattern and ratio of secondary:primary bands which is the same between the two samples, confirming that there is no bias incurred by the methodology and that this purification method can be used for α_2m experiments in the future.

There are differences in the glycosylation footprint of newborn α_2m in comparison to adult. Though no statistically significant change in overall molecular weight was seen following PNGaseF cleavage of N-linked glycans, conclusions cannot be made in regards to specific sites of glycosylation or the identity of the glycans at each site. Our neuraminidase results were the first to show a significant difference between newborn and adult α_2m, with newborn displaying a greater change in relative front on non-denaturing electrophoresis, thus indicating a greater change in charge following sialic acid cleavage. Sialic acid acts as a 'cap' on galactose residues that are components of glycans. Therefore, an increase in the sialic acid content of a glycan should function to extend the half-life of the glycoprotein by preventing the interaction of galactose with the asialoglycoprotein receptor. Additionally, an increase in both sialic acid, (shown in our neuraminidase results) and galactose (shown in our ricin binding results) could alter the conformation of newborn α_2m and potentially mask receptor sites for clearance. FACE results complemented both the sialic acid and ricin binding results by revealing a higher proportion of branched glycans in newborn α_2m as compared to adult. Extra branches attached to the mannose residues could render newborn α_2m less susceptible to uptake by the mannose receptor, and therefore reduce clearance from the plasma. The above possibilities for a reduction in clearance of newborn α_2m compared to adult could be responsible for the increase in concentration in the young population.

Previous studies have examined differences in coagulation proteins between newborns and adults and their impact on protein function. Neonatal plasminogen contains hypersialylation and an increase in mannose[17]. The rise in mannose is indicative of N-linked glycans, therefore this cannot be used as a direct example as α_2m was not shown to contain variation in total N-linked glycan content. However, there was a distinct change in properties of the molecule with the increased glycosylation. Both plasminogen 1 and 2 had a marked increase of sialic acid and mannose in the newborn population. More specifically, in plasminogen 2, there was nearly 20 times the amount of sialic acid (and four times more mannose) in newborns when compared to adults[17]. It was concluded that these increases explained a reduced activity and propensity for activation in newborn plasminogen as compared to adults. Additionally, Protein C has been studied in both age groups. Newborns have been shown to possess greater amounts of alpha-PC (fully glycosylated with 4 sites) than beta-PC (3 of 4 glycosylation sites occupied), and it is hypothesized that this leads to an increase in anticoagulant activity[7]. Considering these findings, it is still unclear what form of impact the rise in sialic acid, branched glycans and perhaps galactose found on newborn α_2m has on the protein activity *in vivo*. However, the literature certainly shows that alterations in glycosylation can lead to changes in protein dynamics and therefore, α_2m is worthy of continuous investigation.

There are many possible paths to pursue as future directions with this project. First, we would like to carry out further 2D electrophoresis experiments to determine the source of degradation seen in newborn and commercial samples that cannot seem to be replicated in adult plasma α_2m samples. At this point, we can determine that the newborn and adult samples behave differently on 2D electrophoresis. This could be due to properties of each sample (discussed above), or differences in protein conformation, however this remains a hypothesis at the time of

writing. To pursue this, we would like to include a commercial, newborn plasma and adult plasma sample on 2D gels at the same time. By running the three samples simultaneously, we would be able to make further comments about the pattern of degradation. Treating newborn and adult plasma samples with neuraminidase would provide insight on the effect in migration of the 180 kDa band seen on 2D electrophoresis due to the amounts of sialic acid in the α_2m species. Once that is complete, we would like to proceed by treating newborn and adult plasma samples with PNGaseF to determine the effect of total N-linked glycan removal on α_2m migration in 2D electrophoresis. Finally, we would like to electrophorese newborn and adult α_2m purified by the above immunoprecipitation method on 2D gels. This would allow us to use both the 2D gel data as well as FACE results to provide conclusions regarding differences in newborn and adult α_2m structures.

Moreover, we would like to further optimize the purification procedure itself. This would include steps to attempt to increase the yield and completely eliminate any albumin to improve overall purity. In addition, possible alterations to greatly increase the amount of protein purified (i.e. with an antibody column) would assist with completing several types of analysis following purification. Earlier in this project, we attempted to optimize a method for use in MALDI-TOF MS in order to obtain data on precise glycan structure, as well as the sites of glycosylation in both newborn and adult α_2m. The presence of polyethylene glycol in previous samples prevented results from being obtained in a purified commercial trial. Therefore, this is something we would like to return to and continue to collaborate with the BioInterfaces Institute at McMaster to complete. Previous research by *Lin et al.* has been conducted on adult α_2m using a mass spectrometry approach with minimal amounts of plasma and therefore, we will be able to use these findings as a guide in our future work.

4 References

1. Andrew, M., Paes, B. & Johnston, M. (1990). Development of the hemostatic system in the neonate and young infant. *The American Journal of Pediatric Hematology/Oncology*. *12*(1): 95 – 104.
2. Andrew, M., Paes, B., Milner, R., Johnston, M., Mitchell, L., Tollefsen, D. M., & Powers, P. (1987). Development of the human coagulation system in the full-term infant. *Blood, 70*(1), 165-172.
3. Andrew, M., Vegh, P., Johnston, M., Bowker, J., Ofosu, F. & Mitchell, L. (1992). Maturation of the hemostatic system during childhood. *Blood. 80*(8): 1998 – 2005
4. Armstrong, P. B., & Quigley, J. P. (1999). α2-macroglobulin: an evolutionarily conserved arm of the innate immune system. *Developmental & Comparative Immunology*, *23*(4), 375-390.
5. Baglin, T. P., Carrell, R. W., Church, F. C., Esmon, C. T., & Huntington, J. A. (2002). Crystal structures of native and thrombin-complexed heparin cofactor II reveal a multistep allosteric mechanism. *Proceedings of the National Academy of Sciences*, *99*(17), 11079-11084.
6. Batty, P., & Smith, J. G. (2010). Haemostasis. *Surgery (Oxford), 28*(11), 530-535.
7. Berry, L. R., Van Walderveen, M. C., Atkinson, H. M., & Chan, A. K. (2013). Comparison of N-linked glycosylation of protein C in newborns and adults. *Carbohydrate research*, *365*, 32-37.
8. Borth, W. (1992). Alpha 2-macroglobulin, a multifunctional binding protein with targeting characteristics. *The FASEB Journal*, *6*(15), 3345-3353.

9. Branson, H. E., Endo, Y., Fagin, A. R., & Schlutz, M. (1984). Heritable α2-Macroglobulin Deficiency in a Patient With Arterial Thrombosis: α2-Macroglobulin Deficiency Irvine. *Journal of the National Medical Association, 76*(11), 1107.
10. Brass, L. F. (2003). Thrombin and platelet activation. *CHEST Journal, 124*(3 suppl), 18S-25S.
11. Carrell, R. W. (1986). alpha 1-Antitrypsin: molecular pathology, leukocytes, and tissue damage. *Journal of Clinical Investigation, 78*(6), 1427.
12. Carrell, R. W., & Lomas, D. A. (2002). Alpha1-antitrypsin deficiency—a model for conformational diseases. *New England Journal of Medicine, 346*(1), 45-53.
13. Carvalho, A., & Ellman, L. (1976). Hereditary antithrombin III deficiency: effect of antithrombin III deficiency on platelet function. *The American journal of medicine, 61*(2), 179-183.
14. Chuansumrit, A., Manco-Johnson, M. J., & Hathaway, W. E. (1989). Heparin cofactor II in adults and infants with thrombosis and DIC. *American journal of hematology, 31*(2), 109-113.
15. Corral, J., Aznar, J., Gonzalez-Conejero, R., Villa, P., Miñano, A., Vayá, A., ... & Vicente, V. (2004). Homozygous Deficiency of Heparin Cofactor II Relevance of P17 Glutamate Residue in Serpins, Relationship With Conformational Diseases, and Role in Thrombosis. *Circulation, 110*(10), 1303-1307.
16. Crystal, R. G. (1990). Alpha 1-antitrypsin deficiency, emphysema, and liver disease. Genetic basis and strategies for therapy. *Journal of Clinical Investigation, 85*(5), 1343-1352.

17. Edelberg, J. M., Enghild, J. J., Pizzo, S. V., & Gonzalez-Gronow, M. (1990). Neonatal plasminogen displays altered cell surface binding and activation kinetics. Correlation with increased glycosylation of the protein. *Journal of Clinical Investigation*, *86*(1), 107-112.
18. Ersdal-Badju, E., Lu, A., Zuo, Y., Picard, V., & Bock, S. C. (1997). Identification of the antithrombin III heparin binding site. *Journal of Biological Chemistry*, *272*(31), 19393-19400.
19. Gailani, D., & Renné, T. (2007). Intrinsic pathway of coagulation and arterial thrombosis. *Arteriosclerosis, thrombosis, and vascular biology*, *27*(12), 2507-2513.
20. Girard, T. J., Warren, L. A., Novotny, W. F., Likert, K. M., Brown, S. G., Miletich, J. P., & Broze, G. J. (1989). Functional significance of the Kunitz-type inhibitory domains of lipoprotein-associated coagulation inhibitor.
21. Gornik, O., & Lauc, G. (2008). Glycosylation of serum proteins in inflammatory diseases. *Disease markers*, *25*(4-5), 267-278. **new add
22. Griffin, J. H., Fernandez, J. A., Gale, A. J., & Mosnier, L. O. (2007). Activated protein C. *Journal of Thrombosis and Haemostasis*, *5*(s1), 73-80.
23. Grinnell, B. W., Walls, J. D., & Gerlitz, B. (1991). Glycosylation of human protein C affects its secretion, processing, functional activities, and activation by thrombin. *Journal of Biological Chemistry*, *266*(15), 9778-9785.
24. He, L., Vicente, C. P., Westrick, R. J., Eitzman, D. T., & Tollefsen, D. M. (2002). Heparin cofactor II inhibits arterial thrombosis after endothelial injury. *The Journal of clinical investigation*, *109*(109 (2)), 213-219.

25. Hoffman, M. (2003). A cell-based model of coagulation and the role of factor VIIa. *Blood reviews*, *17*, S1-S5.

26. Hoffman, M., & Monroe, D. M. (2007). Coagulation 2006: a modern view of hemostasis. *Hematology/oncology clinics of North America*, *21*(1), 1-11.

27. Jaeken, J., & van den Heuvel, L. (2014). Congenital disorders of glycosylation. In *Physician's Guide to the Diagnosis, Treatment, and Follow-Up of Inherited Metabolic Diseases* (pp. 483-512). Springer Berlin Heidelberg

28. Jenkins, N., Parekh, R. B., & James, D. C. (1996). Getting the glycosylation right: implications for the biotechnology industry. *Nature biotechnology*, *14*(8), 975-981.

29. Kalle, M., Papareddy, P., Kasetty, G., Tollefsen, D. M., Malmsten, M., Mörgelin, M., & Schmidtchen, A. (2013). Proteolytic activation transforms heparin cofactor II into a host defense molecule. *The Journal of Immunology*, *190*(12), 6303-6310.

30. Kounnas, M. Z., Church, F. C., Argraves, W. S., & Strickland, D. K. (1996). Cellular Internalization and Degradation of Antithrombin III-Thrombin, Heparin Cofactor II-Thrombin, and-Antitrypsin-Trypsin Complexes Is Mediated by the Low Density Lipoprotein Receptor-related Protein. *Journal of Biological Chemistry*, *271*(11), 6523-6529.

31. Kujovich, J. L. (2005). Hemostatic defects in end stage liver disease. *Critical care clinics*, *21*(3), 563-587.

32. Lane, D. A., & Caso, R. (1989). 9 Antithrombin: Structure, genomic organization, function and inherited deficiency. *Baillière's clinical haematology*, *2*(4), 961-998.

33. Levy, J. H., Dutton, R. P., Hemphill III, J. C., Shander, A., Cooper, D., Paidas, M. J., ... & Lawson, J. H. (2010). Multidisciplinary approach to the challenge of hemostasis. *Anesthesia & Analgesia*, *110*(2), 354-364.

34. Lin, Z., Lo, A., Simeone, D. M., Ruffin, M. T., & Lubman, D. M. (2012). An N-glycosylation analysis of human alpha-2-macroglobulin using an integrated approach. *Journal of proteomics & bioinformatics*, *5*, 127-134.

35. Lundblad, R. L., & White, G. C. (2005). The interaction of thrombin with blood platelets. *Platelets*, *16*(7), 373-385.

36. Maroney, S. A., Ellery, P. E., Wood, J. P., Ferrel, J. P., Martinez, N. D., & Mast, A. E. (2013). Comparison of the inhibitory activities of human tissue factor pathway inhibitor (TFPI) α and TFPIβ. *Journal of Thrombosis and Haemostasis*, *11*(5), 911-918.

37. McMichael, M. (2012). New models of hemostasis. *Topics in companion animal medicine*, *27*(2), 40-45.

38. Mitchell, L., Piovella, F., Ofosu, F., & Andrew, M. (1991). Alpha-2-macroglobulin may provide protection from thromboembolic events in antithrombin III-deficient children. *Blood*, *78*(9), 2299-2304.

39. Monagle, P., Ignjatovic, V., & Savoia, H. (2010). Hemostasis in neonates and children: pitfalls and dilemmas. *Blood reviews*, *24*(2), 63-68.

40. Moustafa, I., Connaris, H., Taylor, M., Zaitsev, V., Wilson, J. C., Kiefel, M. J., ... & Taylor, G. (2004). Sialic acid recognition by Vibrio cholerae neuraminidase. *Journal of Biological Chemistry*, *279*(39), 40819-40826.

41. Paiva, M. M., Soeiro, M. N. C., Barbosa, H. S., Meirelles, M. N. L., Delain, E., & Araújo-Jorge, T. C. (2010). Glycosylation patterns of human alpha2-macroglobulin: Analysis of lectin binding by electron microscopy. *Micron*, *41*(6), 666-673.

42. Panzironi, C., Silvestrini, B., Mo, MY., Lahita, R., Mruk, D. & Cheng, CY. (1997). An increase in the carbohydrate moiety of alpha 2-macroglobulin is associated with systemic lupus erythematosus (SLE). *Biochem Mol Bio Int.* 43(6), 1305-22.

43. Parmar, N., Albisetti, M., Berry, L. R., & Chan, A. K. (2006). The fibrinolytic system in newborns and children. *Clinical laboratory*, *52*(3-4), 115-124.

44. Patnaik, M. M., & Moll, S. (2008). Inherited antithrombin deficiency: a review. *Haemophilia*, *14*(6), 1229-1239.

45. Preston, R. J., Rawley, O., Gleeson, E. M., & O'Donnell, J. S. (2013). Elucidating the role of carbohydrate determinants in regulating hemostasis: insights and opportunities. *Blood*, *121*(19), 3801-3810.

46. Quinsey, N. S., Greedy, A. L., Bottomley, S. P., Whisstock, J. C., & Pike, R. N. (2004). Antithrombin: in control of coagulation. *The international journal of biochemistry & cell biology*, *36*(3), 386-389.

47. Rao, L. V., & Rapaport, S. I. (1988). Activation of factor VII bound to tissue factor: a key early step in the tissue factor pathway of blood coagulation. *Proceedings of the National Academy of Sciences*, *85*(18), 6687-6691.

48. Romisch, J. (2002). Factor VII activating protease (FSAP): a novel protease in hemostasis. *Biological Chemistry*, 383(7-8), 1119-1124.

49. Serres, F., & Blanco, I. (2014). Role of alpha-1 antitrypsin in human health and disease. *Journal of Internal Medicine*.

50. Simioni, P., Kalafatis, M., Millar, D. S., Henderson, S. C., Luni, S., Cooper, D. N., & Girolami, A. (1996). Compound heterozygous protein C deficiency resulting in the presence of only the beta-form of protein C in plasma. *Blood*,*88*(6), 2101-2108.

51. Smith, S. A. (2009). The cell-based model of coagulation. *Journal of veterinary emergency and critical care*, *19*(1), 3-10.

52. Sottrup-Jensen, L. (1989). Alpha-macroglobulins: structure, shape, and mechanism of proteinase complex formation. *J Biol Chem*, *264*(20), 11539-11542.

53. Sottrup-Jensen, L., Stepanik, T. M., Kristensen, T., Wierzbicki, D. M., Jones, C. M., Lønblad, P. B., ... & Petersen, T. E. (1984). . *Journal of Biological Chemistry*, *259*(13), 8318-8327.

54. Spiro, R. G. (2002). Protein glycosylation: nature, distribution, enzymatic formation, and disease implications of glycopeptide bonds. *Glycobiology*, *12*(4), 43R-56R.

55. Stenbjerg, S. (1981). Inherited alpha 2 macroglobulin deficiency. *Thrombosis research*, *22*(4), 491-495.

56. Strauss, T., Sidlik-Muskatel, R., & Kenet, G. (2011, December). Developmental hemostasis: primary hemostasis and evaluation of platelet function in neonates. *Seminars in Fetal and Neonatal Medicine 16*(6), 301-304.

57. Strickland, D. K., & Ranganathan, S. (2003). Diverse role of LDL receptor-related protein in the clearance of proteases and in signaling. *Journal of Thrombosis and Haemostasis*, *1*(7), 1663-1670.

58. Sumer-Bayraktar, Z., Nguyen-Khuong, T., Jayo, R., Chen, D. D., Ali, S., Packer, N. H., & Thaysen-Andersen, M. (2012). Micro-and macroheterogeneity of N-glycosylation

yields size and charge isoforms of human sex hormone binding globulin circulating in serum. *Proteomics*, *12*(22), 3315-3327.

59. Tollefsen, D. M. (2007). Heparin cofactor II modulates the response to vascular injury. *Arteriosclerosis, thrombosis, and vascular biology*, *27*(3), 454-460.
60. Tollefsen, D. M., & Blank, M. K. (1981). Detection of a new heparin-dependent inhibitor of thrombin in human plasma. *Journal of Clinical Investigation*, *68*(3), 589.
61. Tollefsen, D. M., Pestka, C. A., & Monafo, W. J. (1983). Activation of heparin cofactor II by dermatan sulfate. *Journal of Biological Chemistry*, *258*(11), 6713-6716.
62. Varki, A., Cummings, R. D., Esko, J. D., Freeze, H. H., Stanley, P., Bertozzi, C. R., ... & Schauer, R. (2009). Essentials of Glycobiology 2nd edition: Sialic acids.
63. Woods, A. G., Woods, C. W., & Snow, T. M. (2012). Congenital disorders of glycosylation. *Advances in Neonatal Care*, *12*(2), 90-95.
64. Wood, J. P., Bunce, M. W., Maroney, S. A., Tracy, P. B., Camire, R. M., & Mast, A. E. (2013). Tissue factor pathway inhibitor-alpha inhibits prothrombinase during the initiation of blood coagulation. *Proceedings of the National Academy of Sciences*, *110*(44), 17838-17843.
65. Wood, J. P., Ellery, P. E., Maroney, S. A., & Mast, A. E. (2014). Biology of tissue factor pathway inhibitor. *Blood*, *123*(19), 2934-2943.
66. Wood, J. P., Ellery, P. E., Maroney, S. A., & Mast, A. E. (2014). Protein S Is a Cofactor for Platelet and Endothelial Tissue Factor Pathway Inhibitor-α but Not for Cell Surface–Associated Tissue Factor Pathway Inhibitor. *Arteriosclerosis, thrombosis, and vascular biology*, *34*(1), 169-176.